INTRA-SPECTRAL NOISE PROPERTIES OF PULSED HIGH POWER MICROWAVE AMPLIFIERS

A Thesis submitted to the University of London
for the Degree of
Doctor of Philosophy

by

Timothy Penderell Crowfoot B.Sc.[ENG]

March 1974

ABSTRACT

Pulse Doppler radars need to radiate spectrally pure signals to achieve the high levels of clutter cancellation that they are capable of achieving. To produce such signals very stable microwave oscillators and pulsed amplifiers are required and some means of measuring the noise levels produced by these is needed.

A simple additive noise measuring system has been devised for the separate measurement of the A.M. and P.M. noise generated between the spectral lines of the sin x/x spectrum produced by pulsed microwave amplifiers. This system has a sensitivity of 130 dB/Hz below the fundamental spectral line of a pulse train with a duty ratio of 5%, degrading to 96 dB/Hz if the duty ratio drops to 0.1%. With the addition of a feedforward cancellation loop 150 dB/Hz for 5% duty ratio has been achieved. These sensitivities compare with typical radar system requirements of 100-110 dB/Hz at 5% duty.

The noise measuring system has been used to assess the performance of a 5 kW TWT and a 100 kW CFA used as the transmitter in the experimental pulse doppler radar described. The phase noise produced by the TWT itself was 120-130 dB/Hz below one spectral line, while the CFA produced 85-90 dB/Hz. The A.M. noise was about 10 dB lower in each case. These results demonstrate that TWT's could meet most foreseen intraspectral noise requirements for pulse doppler radars, but CFA's would only be suitable for less stringent applications, such as MTI radars.

The stability of the transmitter power supplies is very important if the full potential of the output tube is to be realised. A novel inverter power supply is described which has a chopping frequency locked to the P.R.F. of the system. In this way no power supply modulation is produced between the spectral lines.

CONTENTS

		Page
CHAPTER 1	COHERENT RADAR TECHNIQUES	1
1.1	Introduction	1
1.2	Clutter	1
1.3	The Coherent Radar	4
1.4	Doppler Signal Processing	5
1.5	Summary	14
CHAPTER 2	A REVIEW OF SYSTEM STABILITY REQUIREMENTS AND MEASUREMENT TECHNIQUES	16
2.1	Stability Requirements	16
2.2	Interline Noise	19
2.3	Oscillator Measurement Techniques	21
2.4	Pulsed Amplifier Measurement Techniques	22
CHAPTER 3	NOISE MECHANISMS IN TRANSMITTER TUBES AND POWER SUPPLIES	27
3.1	The Travelling Wave Tube	27
3.2	High Power Travelling Wave Tubes	31
3.3	The Crossed Field Amplifier	32
3.4	Noise in Transmitter Tubes	36

		Page
CHAPTER 4	THE EXPERIMENTAL TRANSMITTER	54
4.1	The Experimental Radar	54
4.2	The Power Amplifiers	60
4.3	Power Supply Stability Requirements	62
4.4	The Design of the 5 kW Transmitter	63
4.5	The Design of the 100 kW Transmitter	64
CHAPTER 5	THE NOISE MEASURING SYSTEM	68
5.1	Additive Noise Measuring System	70
5.2	Development of the Noise Measuring System	77
5.3	Improvements to the Basic Noise Measuring System	85
5.4	Summary	89
CHAPTER 6	RESULTS OF NOISE MEASUREMENTS	90
6.1	Noise Measurements with the 5 kW TWT Transmitter	91
6.2	Noise Measurements on the 100 kW CFA Transmitter	96
6.3	Discussion of Results	100
CONCLUSIONS		105
APPENDIX 1	Analysis of the Effect of Jitter in Pulse Timing and Pulse Length	A1.1-4
APPENDIX 2	Phase Modulation due to Vibration in Waveguide Components	A2.1-7

		Page
APPENDIX 3	Data Sheets on the TWT and CFA	A3.1-4
APPENDIX 4	The Phase Sensitive Detector	A4.1-6
APPENDIX 5	LIST OF SYMBOLS	(1 Page)
APPENDIX 6	CHOICE OF COMPONTS	(8 Pages)
REFERENCES		(4 pages)
ACKNOWLEDGEMENTS		(1 page)

CHAPTER 1

COHERENT RADAR TECHNIQUES

1.1 Introduction

In this chapter the uses of coherent radar will be described with the emphasis on doppler signal processing which is used to distinguish moving targets from a background of clutter. The success of this technique relies upon the achievement of high orders of stability in both the master oscillator and the amplifiers in the radar transmitter. The design of such stable transmitters and the measurement techniques developed to determine the low levels of noise generated by them are difficult problems and form the bulk of the work described in later chapters of this thesis. This chapter is intended to provide the background against which this work can be viewed.

1.2 Clutter

The performance of all radar systems is limited by the environment in which they must operate. One of the most common and troublesome shortcomings is caused by clutter. Clutter, as its name implies, is an echo received by the radar from a reflector that the radar does not want

to detect. An example of this would be reflections from the land to a radar designed to detect aircraft. The scale of the problem can be appreciated if a comparison is made between the echoing areas of typical areas of land, for example hills or large buildings, and an aircraft. The aeroplane may have an echoing area of 10 m^2 while the terrain over which it is flying may have an echoing area of 10,000 m^2. The radar echo from the land is thus 1000 times larger than that from the aircraft and completely swamps it. This type of clutter is called 'land clutter'. A picture of a typical radar display is shown in Figure 1.1. The display is of a plan position indicator or PPI which presents a radar map of the area round the site of the radar. Figure 1.1 shows the clutter seen by a 25 cm radar situated to the north of Portsmouth. North is towards the top of the display and the clutter in this area comes from the South Downs. The clutter to the south is the Isle of Wight. It can be appreciated that tracking aircraft through these clutter areas is a very difficult task.

Land is not the only source of clutter, radar signals can also be reflected by rain and by waves on the sea. These sources of clutter are called rain and sea clutter respectively. Because of its effect upon the performance of radar systems clutter has been studied widely and much is now known about the characteristics of the various types of clutter. Clutter like any other signal is subjected to statistical variation in amplitude with time and much of the work on clutter has been the measurement of this variation for different types of land, sea and rain clutter and at the different frequencies commonly used for radar. For instance great differences are seen in the behaviour of different types of land clutter, for example between wooded areas, hill and urban areas. The properties of clutter also vary markedly with frequency. This is especially

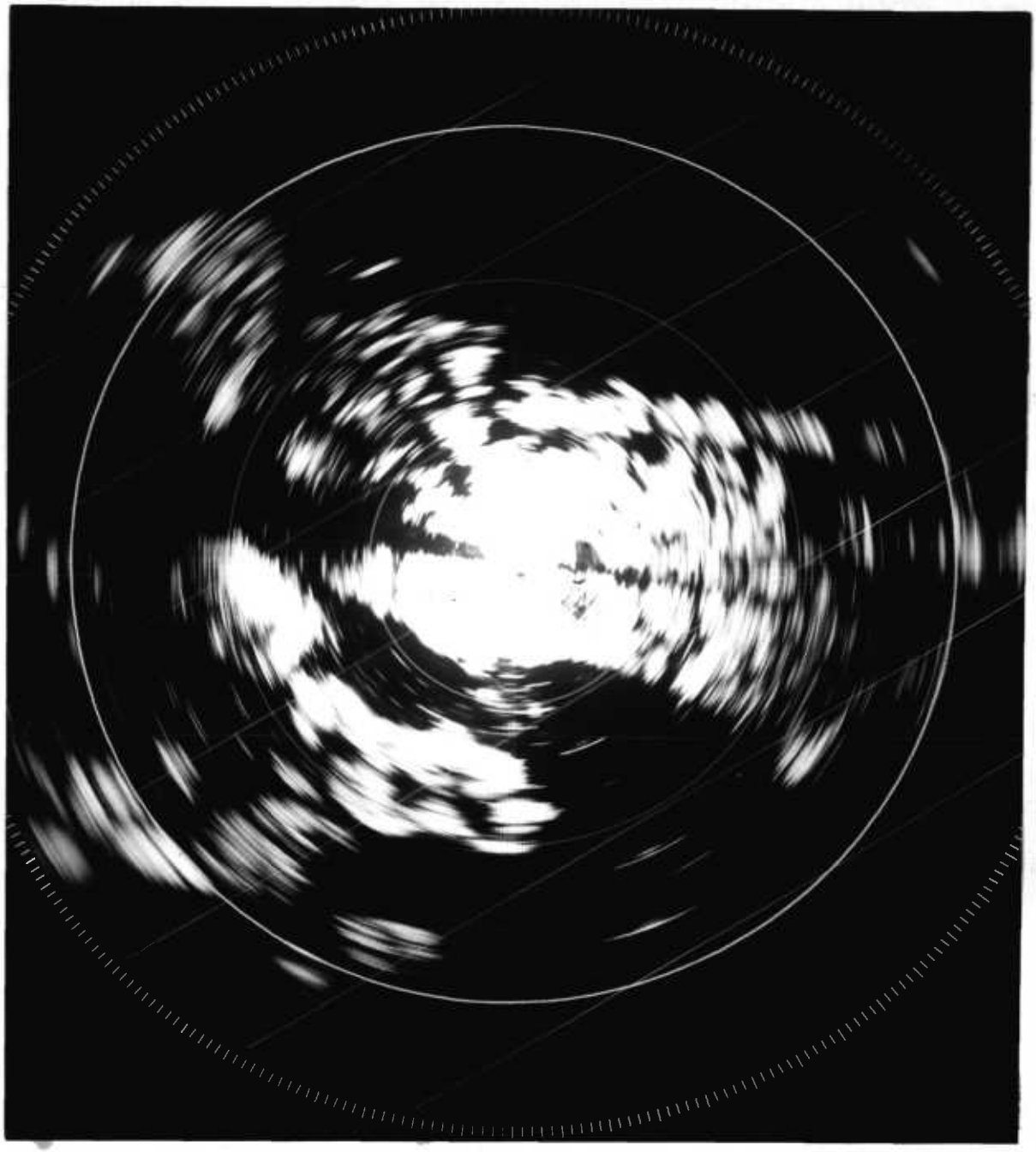


FIG. 1-1
PPI PLOT FROM A 25cm RADAR

10 MILE RANGE RING.
NORTH AT TOP OF DISPLAY

true of rain clutter which is much more severe at higher radar frequencies as the wavelength of the radar signal approaches the size of the individual rain drops. The properties of clutter have been described in some detail by Skolnik [1].

An experienced radar operator is often capable of detecting and tracking targets through quite dense areas of clutter. He accomplishes this by estimating the speed and direction of targets when he can detect them in gaps in the clutter. Past experience then enables him to predict the likely point of emergence from clutter areas that the target may then enter. Although the human operator has been found to excell in this task he can only do so when there are only very few targets to be tracked. For situations where there are many different targets and also targets such as fast missiles a human operator can become overloaded. In these circumstances automatic detection and tracking systems are necessary. Unfortunately these systems are not good at discriminating between targets and the clutter background. To make automatic detection and tracking systems effective some means of reducing the effects of clutter must be used. The simplest is to shape the radar beam so that the radar does not look at the land but only at the aircraft. This technique reduces the magnitude of the clutter echoes but can never completely eliminate them since it is not possible to make a perfectly shaped aerial radiation pattern. The most widely used clutter cancellation systems use the doppler shift in frequency of an echo from a target moving relative to the radar system.

The shift in frequency of an echo from a moving target is given by:-

$$f_D = \frac{2\,V_R}{\lambda} \qquad [1.1]$$

Where f_D is the doppler frequency shift

λ is the transmitted wavelength

and V_R is the radial component of the relative velocity of the target.

In the case of shipborne air surveillance radars, clutter echoes usually only have low doppler frequency shifts caused by ship motion, waves and the effects of wind on trees and clouds. By using some form of filtering in the radar receiver it is possible to distinguish even a small moving target when it is buried in clutter of a far greater echoing area. The degree to which the clutter is suppressed is called the clutter cancellation.

To take advantage of the doppler effect in this way the radar system must be coherent or semi-coherent.

1.3 The Coherent Radar

Although the principles of coherent radar systems were developed well before the end of World War II they have only been put into practice in the last ten to fifteen years. This has been for a variety of reasons. Firstly, at the time coherent techniques were first considered no high power microwave amplifiers had been developed. The magnetron had only recently been brought into use and the travelling wave tube and power amplifier klystrons were only just being conceived. Secondly, the requirements for the performance advantages that coherent systems confer did not become pressing until the middle of the 1950's. At this time guided missile systems, doppler navigation, anti-clutter techniques for air surveillance radars and ballistic missile tracking systems were under active consideration and the problems presented by these systems could best be solved by the use of coherent or semi-coherent radars. Such systems have become much more common in the last ten years, especially

since the start of the US space programme and following the great increase in air traffic.

A coherent system uses the information provided by the phase relationship between the received signal and the transmitted signal. Simple non-coherent pulsed radars cannot take advantage of this phase information and consequently suffer if the target echo is buried in clutter echoes. The ability of the coherent radar system to measure the relative phase of target and clutter echoes enables the doppler frequency shift caused by the movement of the target to be extracted and used for multiple echo discrimination. For example a Moving Target Indication (MTI) surveillance radar will only display a target if its doppler shift has a sufficiently large value. This advantage of the coherent radar system is probably the most important.

The second advantage of the coherent radar is its ability to measure the doppler frequency shift of an echo from a moving target and hence to determine the target's relative velocity. This feature has been used widely, common examples are the radars used by the police to check vehicle speeds and the radars used to aid the docking of super-tankers.

1.4 Doppler Signal Processing

The simplest type of doppler processing was discovered by operators of World War II surveillance radars. They noticed that echoes from moving targets that were at the same range as stronger clutter echoes often caused fluttering of the signal seen on an A-scan (a plot of signal amplitude versus range). This effect which became known as the 'butterfly effect' was caused by the doppler shifted moving target echo beating with the echo from the stationary clutter. This technique is

known as non-coherent MTI since the phase reference is derived externally, from the clutter. The system is limited because moving targets can only be identified as such in the presence of clutter echoes.

a. Coherent MTI

The next development was coherent MTI where the phase reference of the transmitted pulse is remembered within the system by either an oscillator phase locked to a magnetron transmitter or by the use of a coherent amplifier chain driven by a master oscillator. These two arrangements are compared in Figures 1.2a and 1.2b. The phase reference in the fully coherent system of Figure 1.2a is maintained by the master oscillator. In the phase locked MTI system the phase of the output pulse of the magnetron which is random, is remembered by phase locking a coherent oscillator (the COHO) to a sample of the transmitted pulse. The COHO is sufficiently stable to maintain the correct phase relationship with the transmitted pulse during one pulse repetition interval but has a sufficiently low Q to allow the frequency pulling required for phase locking. This system allows the magnetron to be retained as the high power source so reducing the cost and size of the system and maintaining a reasonable MTI performance.

Although both these types of MTI would give an indication of a moving target on an A-scan by means of the butterfly effect even in the absence of clutter this type of signal is not suitable for presentation on a PPI display. The signal must be processed further in what is commonly called a delay line canceller shown diagrammatically in Figure 1.3

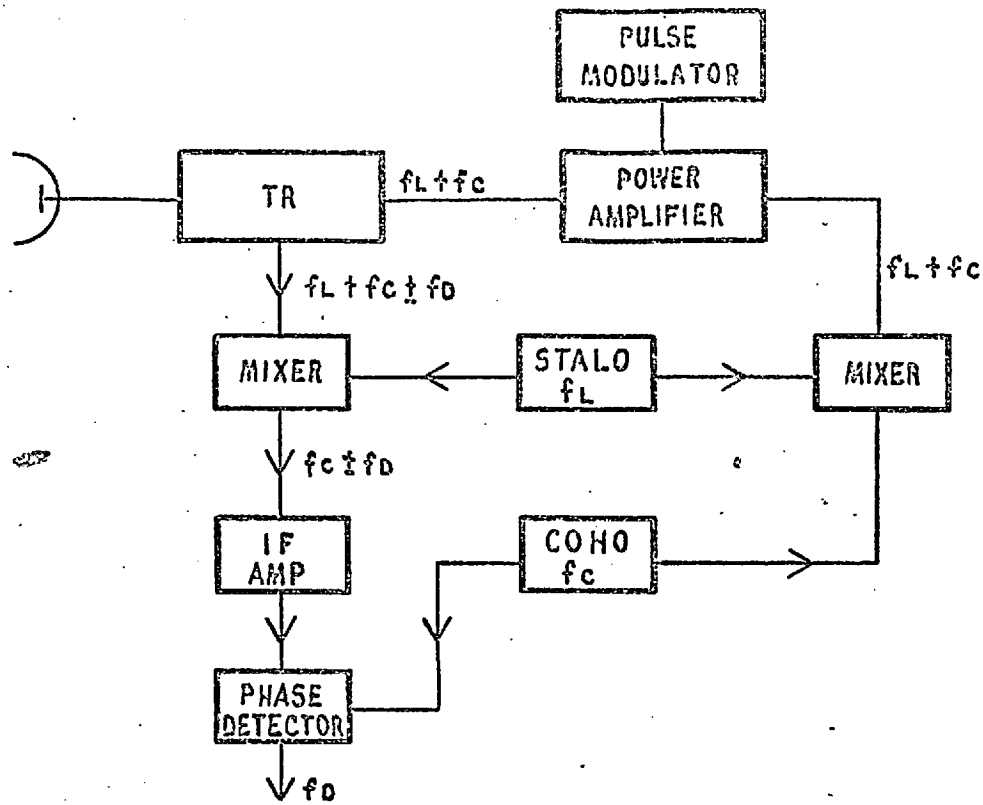


FIG. 1·2 a

MTI RADAR WITH POWER AMPLIFIER TRANSMITTER

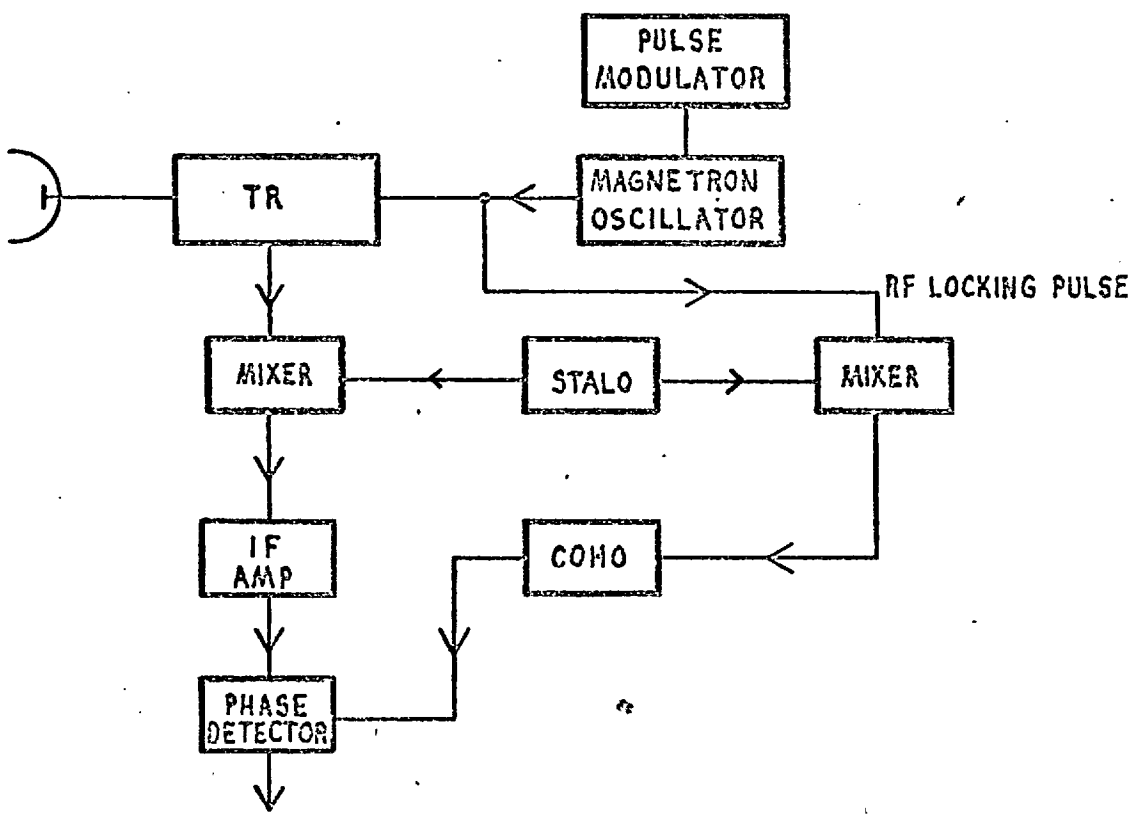


FIG. 1·2 b

MTI RADAR WITH POWER OSCILLATOR TRANSMITTER

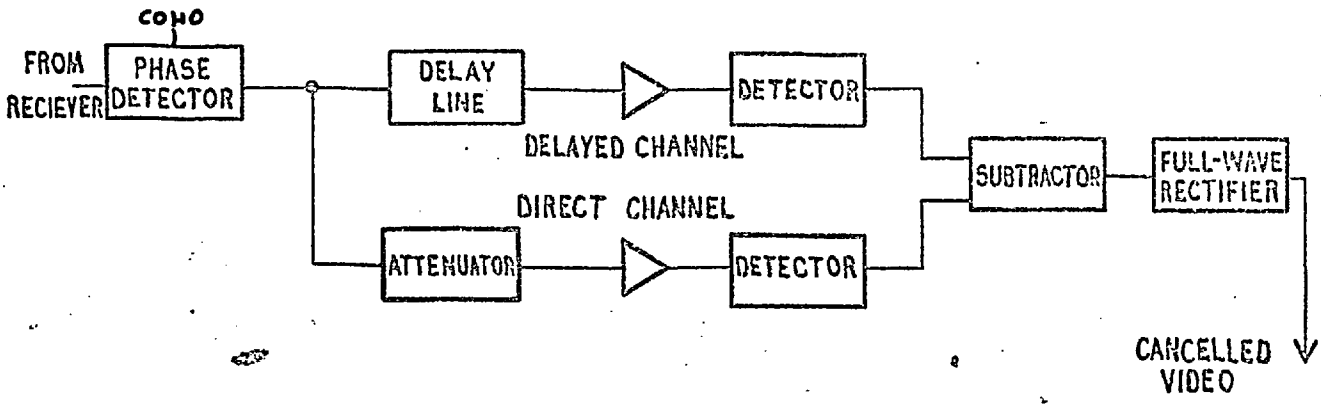
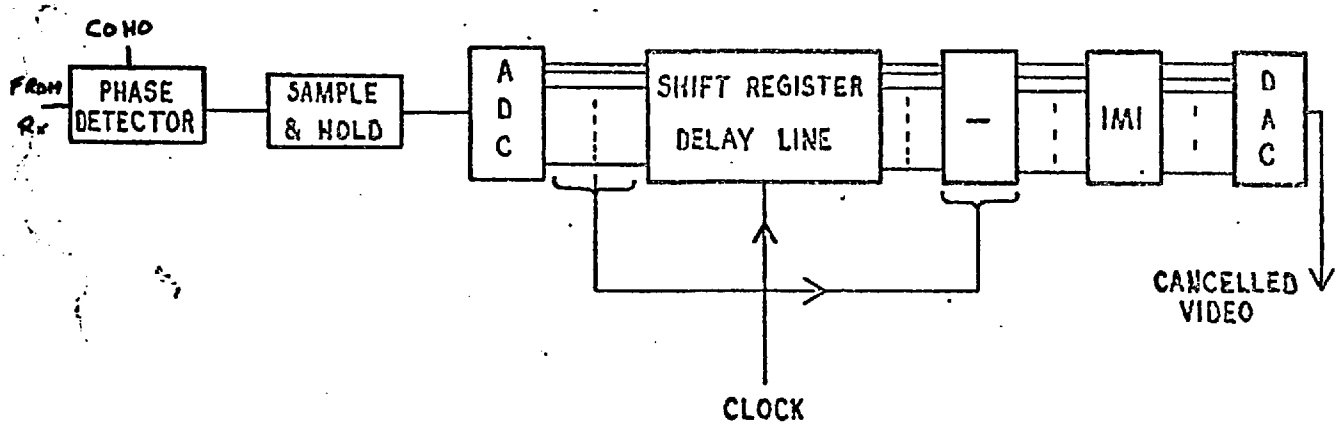


FIG. 1·3

MTI DELAY LINE CANCELLOR



— = SUBRACTOR

IMI = MODULUS TAKER (EQUIVALENT TO FULL WAVE RECTIFIER)

THE INCOMING ANALOGUE SIGNAL IS DIGITISED TO 8 BITS IN MOST SYSTEMS.

FIG. 1·4

DIGITAL MTI CANCELLOR

Successive echoes from fixed clutter sources do not change in phase from pulse to pulse whereas the echoes from moving targets have a changing phase. If successive echoes are compared in a subtractor clutter echoes will be cancelled leaving only the moving target echoes. This is done by delaying successive echoes by a period equal to the pulse repetition interval of the radar and subtracting the delayed echoes from the echoes from the following pulse. The delay must be closely matched to the interpulse interval or incomplete cancellation of the clutter can occur. The delay is at present usually accomplished by using a quartz acoustic delay line.

More recent designs of MTI radar are using digital techniques. Here the video signal is converted to a digital form in an analogue to digital converter and the information on each echo is stored in a shift register. The required delay is achieved by clocking the information through a bank of shift registers. After being delayed for the required time the signal is subtracted from an undelayed sample from the succeeding pulse. After subtraction the digital signals are converted back into analogue form for display on a conventional PPI. A simple digital canceller is shown in Figure 1.4. The digital canceller is very much more expensive than the quartz delay line version but it is very much more flexible. It can tolerate changes in pulse repetition frequency by changing the digital delay and it is possible to easily introduce other features such as feedback which can improve the frequency response of the canceller. The cost can be minimised by only using the digital MTI over a limited range, close to the radar, where clutter is most severe.

The frequency response of the MTI canceller is shown in Figure 1.5. The canceller acts like a comb filter with nulls at multiples of the pulse repetition frequency. The echo pulses will all have a spectrum made up

of lines spaced at the prf of the pulse train and with an envelope obeying a $\frac{\sin x}{x}$ function. Echoes with no doppler shift from clutter sources will have a spectrum of lines each of which will fall into a null of the MTI canceller response. Moving targets which are shifted in frequency will have spectral components which are shifted into the pass-band of the MTI canceller. Unfortunately clutter returns do have some doppler components due to wind movement of trees, clouds and the sea and also due to movement of the radar platform. The effect of this movement is to broaden the clutter spectrum as shown in Figure 1.6. The response of the MTI canceller has been superimposed to show how clutter cancellation can be degraded. The MTI filter characteristics can be improved by adding cancellation stages giving $\sin^2$ and $\sin^3$ responses as shown in Figure 1.7. Feedback around the canceller can give an even better filter characteristic also shown in Figure 1.7. The additional complexity and cost of such circuits can only be justified if a very high level of performance is necessary.

Equation 1.1 states that the doppler frequency shift of a moving target is given by:-

$$f_D = \frac{2 V_r}{\lambda}$$

A study of the filter characteristics of the MTI canceller reveals that the radar will be blind to targets with a velocity such that f_D is equal to the pulse repetition frequency of the radar. Such a velocity is called a 'blind speed' of the radar and these will occur at all doppler shifted frequencies associated with multiples of the prf. The magnitude of the blind speed is determined by the frequency of operation of the radar and the prf, which in turn is set by the maximum unambiguous range required of the radar.

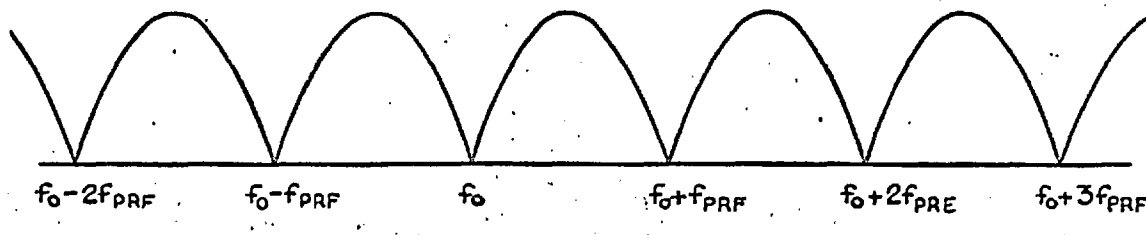


FIG. 1·5 FREQUENCY RESPONSE OF SINGLE MTI CANCELLOR

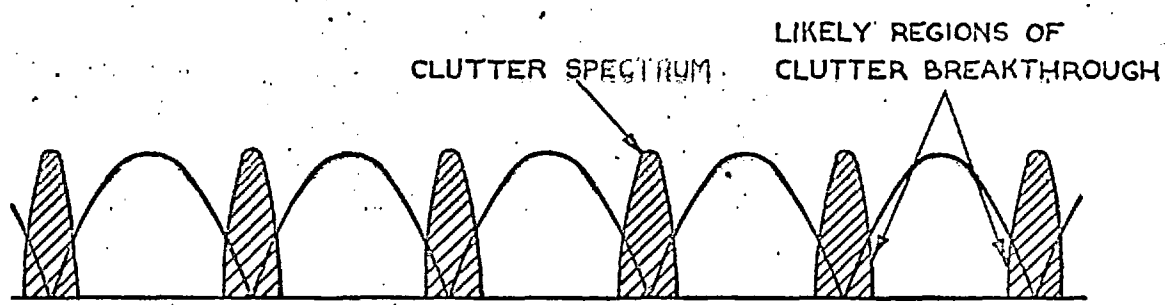


FIG. 1·6 CLUTTER SPECTRUM & MTI RESPONSE

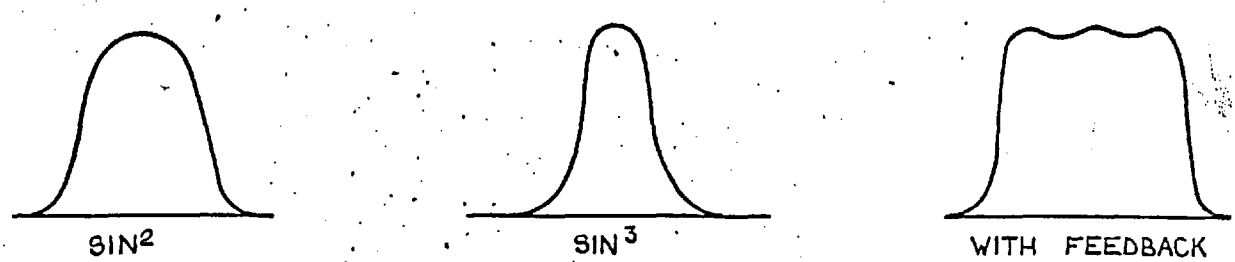


FIG. 1·7 FREQUENCY RESPONSE OF DOUBLE & TRIPLE CANCELLORS & A CANCELLOR WITH FEEDBACK

Figure 1.8 shows a family of curves plotted for different frequencies showing the relationship between the lowest blind speed and the unambiguous range. To see how restricting this effect can be suppose a long range air surveillance radar is required to detect targets moving at up to 2000 mph at a range out to 150 miles. The curves show that if blind ranges are to be avoided then the radiated frequency must be between 50 and 100 MHz. For most applications the aerial size is limited and the angular resolution required places a limit on the lowest frequency that can be used. Consequently most MTI radars must tolerate blind speeds which can be a serious limitation to their operational value. The first blind speed can be raised by staggering the prf and thus the nulls in the frequency response of the canceller are jittered around allowing detection of a target moving at a blind speed on perhaps every second or third pulse. This complicates the delay line since a different delay is required for each prf. This is another area in which the digital MTI system is superior.

It was shown earlier that clutter movement affected the degree of clutter cancellation achievable. A similar degradation can be caused by noise on the transmitted signal as shown in Figure 1.9. The noise modulates the clutter echoes and appears within the filter bandwidth of the MTI canceller causing clutter breakthrough. This effect is not usually serious in MTI radars since the clutter cancellation is seldom more than 30 dB and even magnetron transmitters are sufficiently stable to provide this level of performance. However modern digital cancellers have been demonstrated with clutter cancellation ratios of up to 45 dB and the stability of the transmitter may then be a determining factor in the ultimate performance of such a system. The type of noise that is of importance in such systems is called "Interline Noise" and is the noise

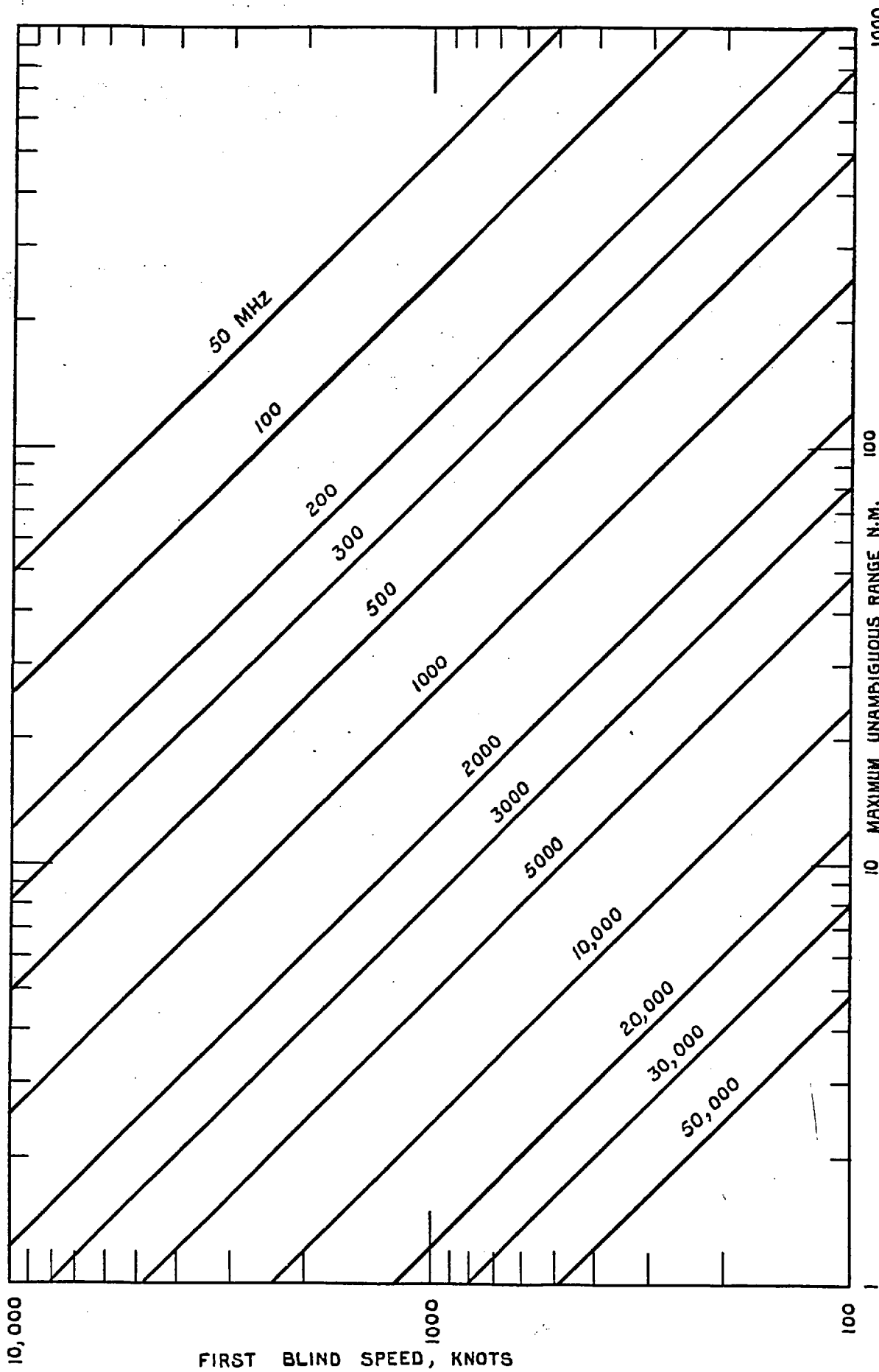


FIG. 1·8

PLOT OF MTI RADAR BLIND SPEED AS A FUNCTION OF MAXIMUM UNAMBIGUOUS RANGE

present between the spectral lines of the transmitted pulse spectrum. The characteristics of this noise will be described in Chapter 3 but it is obvious that the noise midway between the lines is of greater significance due to the weighting of the canceller frequency response which is usually a sine or sine squared function.

Interline noise is of much greater significance in systems using a related anti-clutter technique known as Pulse Doppler.

b. Pulse Doppler Radars

The Pulse Doppler radar is a form of MTI radar generally characterised by operation at a high pulse repetition frequency resulting in ambiguous range information but usually unambiguous doppler information. The transmitter consists of a coherent amplifier chain and the doppler information is extracted by means of range gates and filters. The pulse doppler radar is capable of very much higher levels of clutter cancellation than the MTI radar.

This cancellation is achieved by using a bandpass filter to reject the clutter component of the received signal. The filter can be designed with very sharp skirts and cut-off frequencies approaching the ideal as shown in Figure 1.10. The filter is tailored to fit between the two spectral lines of the pulse spectrum with a lower cut-off frequency higher than the highest expected doppler component of the clutter. In this way excellent clutter cancellation can be obtained, limited only by the filter design and the stability of the system.

Since the filter rejects all the components of the pulse spectrum except for the doppler shifted line between the first and second prf lines

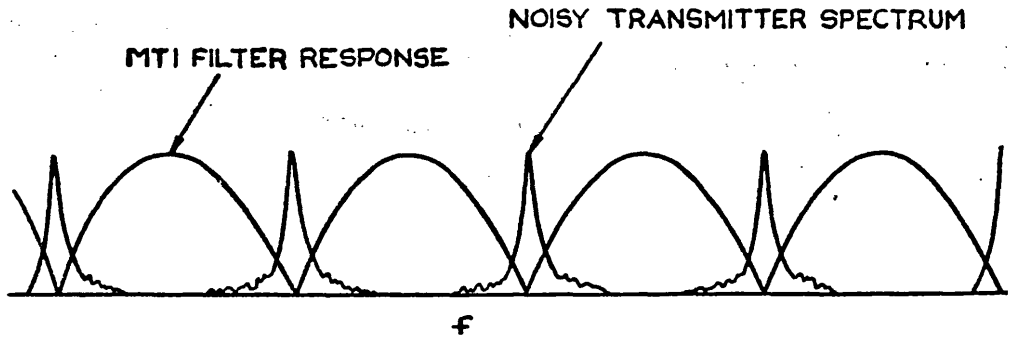


FIG. 1·9 DEGRADATION OF MTI CANCELLATION BY NOISE ON TRANSMITTED SIGNAL

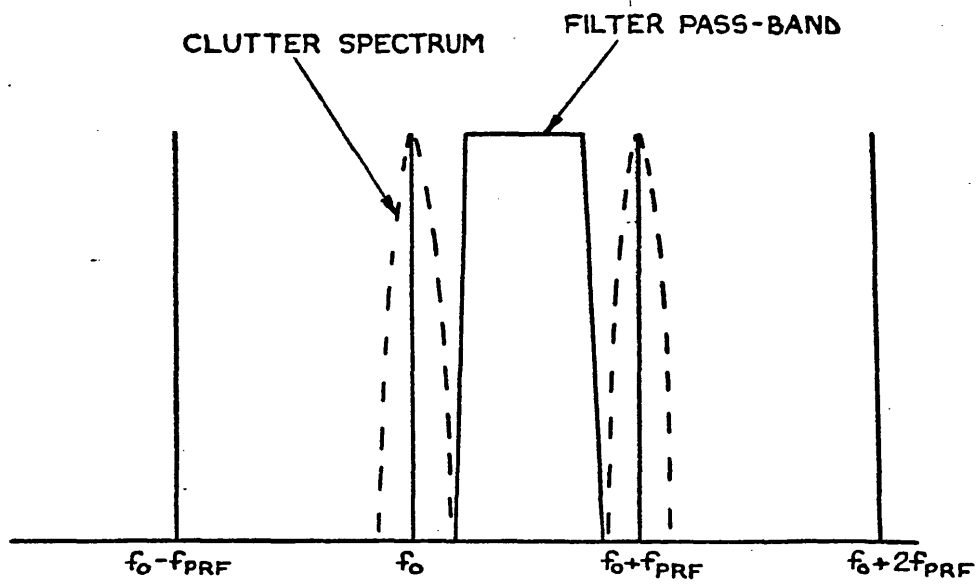


FIG. 1·10 IDEAL CLUTTER FILTER CHARACTERISTIC

the output of the filter approximates to CW and the range information contained in the pulse timing is destroyed. Range information may be retained by using a bank of filters and range gates as shown in Figure 1.11. The range gates are opened in sequence after a pulse has been transmitted and remain open for a period which usually equals the pulse length. The range information is thus quantized, each channel corresponding to a particular range interval. The signals in each channel can now be filtered to remove any clutter echoes since the range information contained in the pulse timing has been extracted. The doppler frequency band is often further subdivided, after clutter rejection, by banks of very narrow band velocity filters which can be used to measure a target's radial velocity. This additional information can aid automatic tracking systems which may be incorporated in the equipment.

The pulse doppler radar suffers from the same constraints as the MTI radar. To get good angular resolution with a restricted aerial size requires operation above a certain frequency. In most cases this means that the radar must operate with blind speeds, blind ranges or both. If advantage is to be taken of measuring a target's radial velocity to help the tracking equipment then it is advantageous to raise the prf to a value such that the velocity measurement of the fastest target to be detected becomes unambiguous. To illustrate this consider a radar operating at 1200 MHz and designed to detect targets moving at up to 900 m/s (mach 3). The maximum doppler shift of a Mk III target (given by $f_D = 2\ V_R/\lambda$) is 7200 Hz. If the prf is less than this value then the target may be detected as a slow moving target. If the prf is equal to 7200 Hz the target will be rejected as clutter and the radar will be blind. The diagrams of Figure 1.12 demonstrate this effect. If in this example the prf were to be fixed at 8 kHz, velocity measurements would be

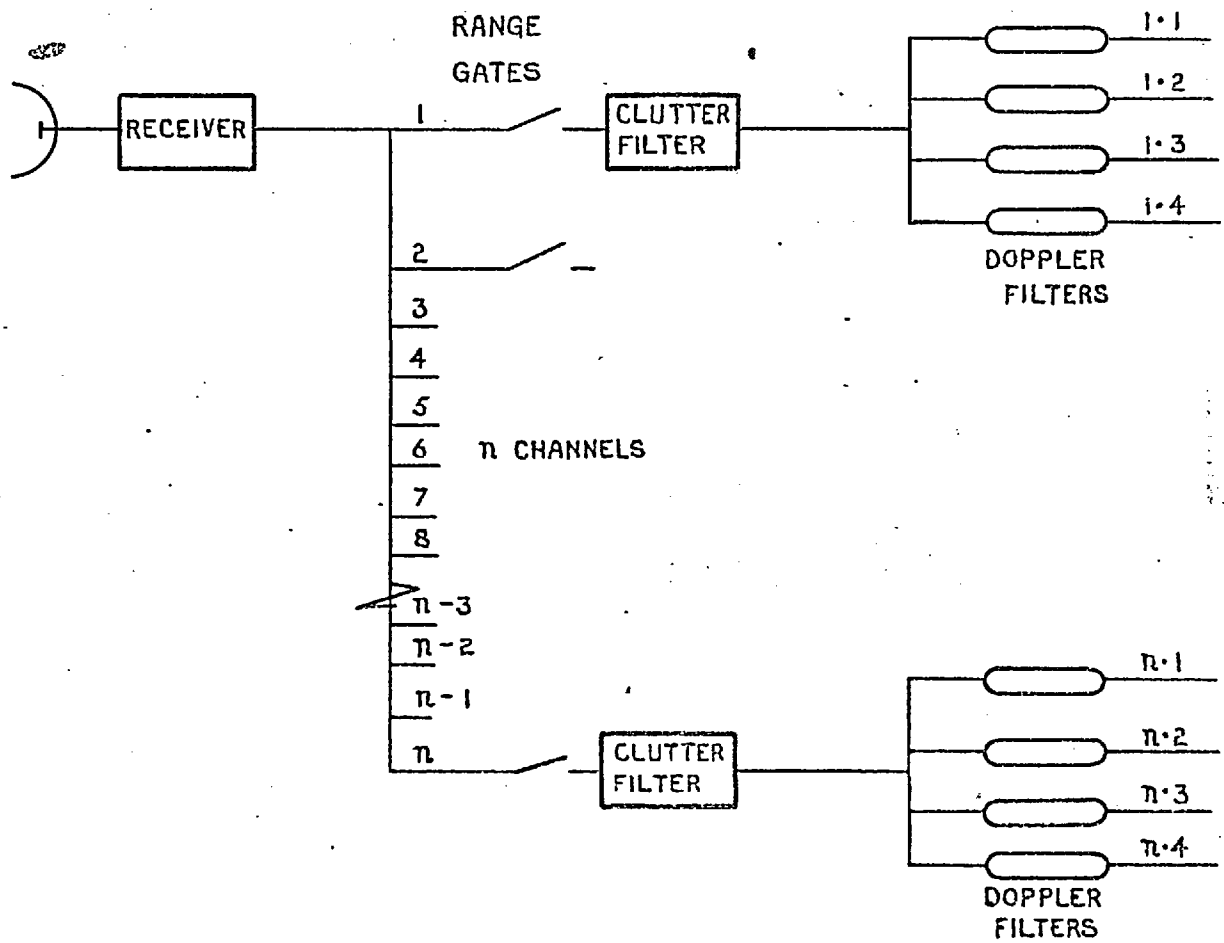
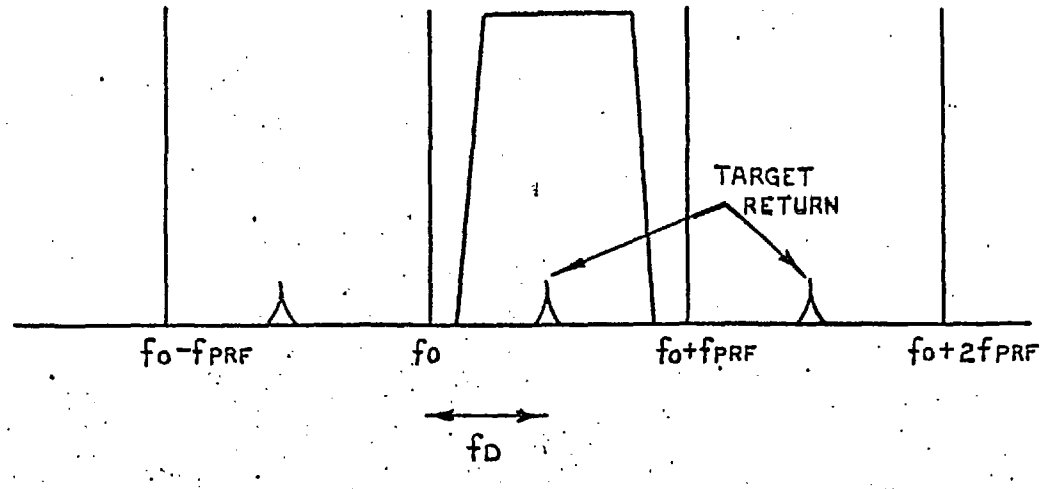
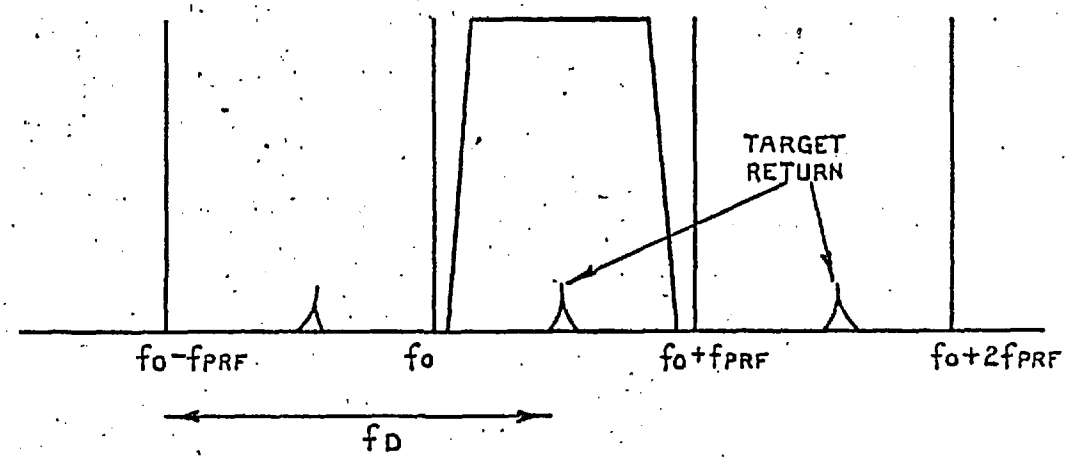


FIG. 1-11

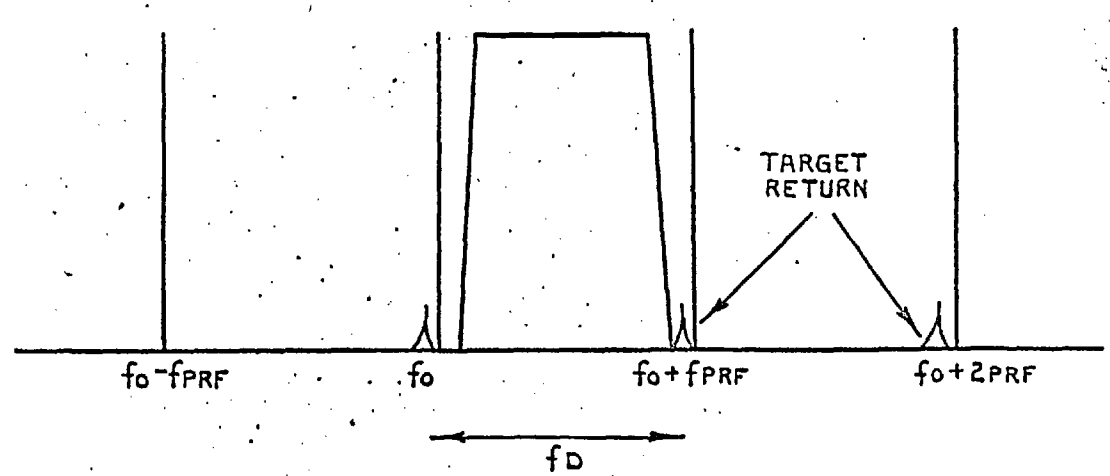
PULSE DOPPLER RADAR RECEIVER



(a) TARGET WITH LOW RADIAL VELOCITY & LOW DOPPLER SHIFT



(b) TARGET WITH VERY HIGH RADIAL VELOCITY DETECTED AMBIGUOUSLY AS A LOW VELOCITY TARGET



(c) TARGET MOVING AT A BLIND VELOCITY NOT DETECTED

FIG. 1·12
VELOCITY AMBIGUITIES WITH PULSE DOPPLER RADARS

unambiguous but the radar would have ambiguities in range and also blind ranges. Range ambiguities occur because for a long range target many pulses may have been transmitted before the first pulse arrives back at the radar. The receiver has no way of telling whether the returned pulse is the first pulse from a long range target or succeeding pulses from closer range targets. The radar will also be blind to those targets whose echoes arrive at the receiver when it is turned off during transmission. These gaps in the coverage of the radar can be filled in and the range ambiguities can be resolved by operation at more than one prf.

The high repetition rate of a pulse doppler radar presents a very confusing picture on a conventional PPI display. All the information from all different ranges is overlaid because of the multiple range ambiguities. Additionally those targets detected in the outer range ambiguities will jitter about in range as the prf is changed. It is not practical to expect even the most experienced of operators to make sense of such a display and in general a radar of this type will be controlled by a computer which will analyse the incoming data and present a synthetic display to the operator. To resolve the range ambiguities the computer can change the prf of the radar and re-measure the range of the target detected. If the target is close to the radar the range will not change and the target is then at a known range. If the range of the target changes then the target is ambiguous in range and the computer can calculate the true range by comparing the change in range produced with the change made in the prf. It is possible that by changing the prf the target will be moved into a blind range in which case a further change in the prf must be made to complete the measurement of its true range. It is possible to compiete these measurements in the time that the aerial beam is pointing at the target although it can also be done by changing the prf from scan to scan.

The multiple range ambiguities also introduce further complication because a greater degree of clutter suppression is required. This need arises because large clutter echoes in the first range ambiguity can arrive at the receiver at the same time as a very small target echo in one of the outer ambiguities. Because of its greater distance from the radar the amplitude of the target is further reduced compared with the clutter echo by the fourth power law which applies to all radar sets. A much greater degree of clutter cancellation is required compared to the MTI radar if adequate levels of performance are to be retained. Whilst a typical MTI canceller radar can offer a clutter cancellation of up to 35 dB, the pulse doppler radar can readily achieve 50-60 dB. It is now considered that systems with 80-90 dB of clutter cancellation could be made and these would virtually eliminate clutter since few clutter peaks exceed 90 dB above the receiver noise level.

The actual clutter cancellation achieved in a pulse doppler radar is determined by the stability of the system and by the characteristics of the clutter rejection filter. Crystal filters can now be made to closely approximate to the ideal characteristic shown in Figure 1.10. Two filters are normally used to provide the bandpass characteristic on either side of the rejection notch. This enables approaching and receding targets to be distinguished. Although crystal filters are widely used the use of active filters and digital filtering techniques are being considered for use in experimental systems.

The problems involved in designing a system which is stable enough to enable the desired levels of clutter cancellation to be achieved are far more intractable. Like the MTI canceller radar any noise on the transmitted signal will modulate the clutter echoes and may cause clutter breakthrough. The stability requirements are very much more severe than

than with the MTI radar because of the much higher levels of clutter cancellation that can be achieved. Moreover the stability must be maintained over a large number of pulses because of the range ambiguities and the integration time required in the receiver to charge the high Q clutter rejection filters.

The stability specification for the system will be determined by the clutter cancellation required, the doppler frequency spectrum of the clutter and the bandwidth of the pre-detection velocity filters. A typical interline noise specification is shown in Figure 1.13 for a radar designed to operate at L Band with 70 dB of clutter cancellation and a velocity filter bandwidth of 1 kHz. At L Band the doppler frequency components of the clutter extend out to about 400 Hz which explains the relaxation in the noise specification close to the carrier frequency where the clutter rejection filter will cut-off. At higher doppler frequencies the noise must be 100 dB/Hz below a prf line so that noise modulation on 70 dB clutter peaks will not break through the 1 kHz bandwidth velocity filters. This type of specification can only be met by a coherent amplifier chain and a very stable master oscillator.

1.5 Summary

The operating characteristics of both the MTI radar and the pulse doppler radar have been compared and it has been shown how these radars can assist the detection and tracking of multiple fast targets in a clutter environment. The penalty to be paid for this level of performance is complexity and the very high levels of stability required to achieve the clutter cancellation desired. To investigate the problems associated with pulse doppler radars an experimental system was constructed. One of

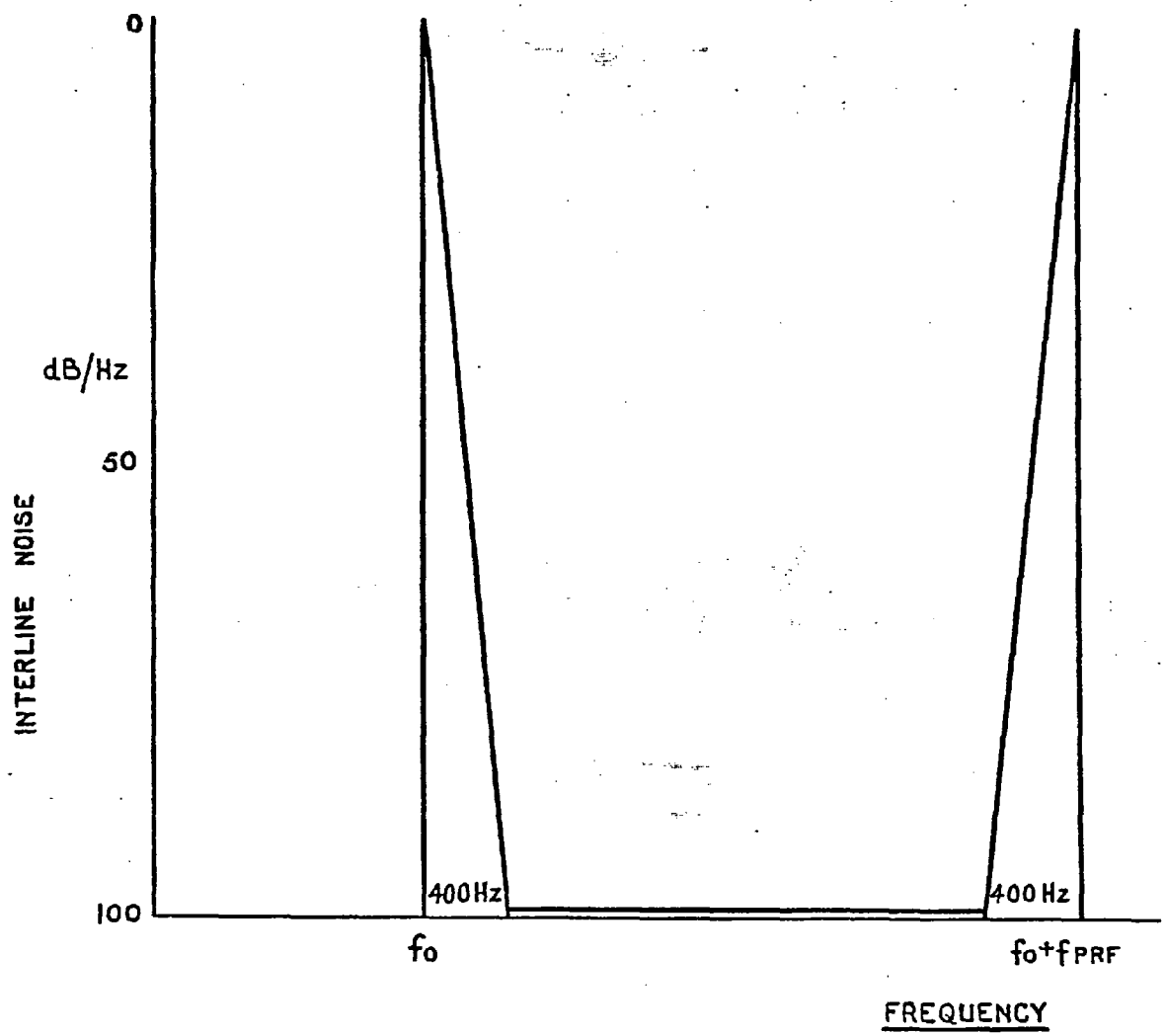


FIG. 1·13
INTERLINE NOISE SPECIFICATION

the most important components of this radar was a very stable coherent power amplifier chain for the transmitter. Not only was this transmitter to be very stable but some measuring system had to be devised to demonstrate its stability so that instabilities in various parts of the entire system could be separately identified. The design of a measuring system to do this forms the bulk of the work described in this thesis. Some background to the problem is given in Chapter 2 which describes the general problem of stability and its relation to radar performance as well as referring to other work in this field. Chapter 3 describes the characteristics of the various types of amplifier tube commonly used in radar transmitters and also examines the various types of noise and instability which can degrade the performance of a system. Chapter 4 outlines the design of the transmitter used in the experimental system and with which all the results of the noise measurements described in Chapter 6 were obtained. A description of the noise measuring system developed in the course of this work is given in Chapter 5.

The measurement technique developed is capable of measuring interline noise down to a level of 150 dB/Hz below the fundamental line of the pulse spectrum. To get the high dynamic range needed a novel method of cancelling the lines of the pulse spectrum was developed since the simple system previously used was limited to 120 dB/Hz.

The noise measuring system was used to measure the noise of a travelling wave tube and a crossed-field amplifier. The interline noise spectrum of the travelling wave tube was dominated by power supply ripple but the noise produced by the tube itself was about 130 dB/Hz below one spectral line. The crossed-field amplifier produced an interline noise level of 85-90 dB/Hz below on spectral line and there was no modulation from the power supply. These results are given in Chapter 6.

CHAPTER 2

A REVIEW OF SYSTEM STABILITY REQUIREMENTS AND MEASUREMENT TECHNIQUES

In Chapter 1 two types of anti-clutter techniques were examined and it was shown that for a pulse doppler radar the stability of the system must be good. The first section of this chapter looks briefly at other types of radar system which need high stability and examples are drawn from the literature. In the next section 'interline noise' is described and finally some of the methods that have been used to measure interline noise are discussed.

2.1 Stability Requirements

A high stability system is not just required to eliminate clutter but is also needed to make accurate measurement of velocity and acceleration of radar targets. This need has arisen because of the increasing use of both ballistic missiles and space vehicles. Radar is also used for airborne doppler navigation where the doppler shifted echo from the sea or land is used to measure the aircraft's velocity. In all these systems the stability of the master oscillator and power amplifier is important although the stability required varies from system to system.

Because of the increasing need for better stability, especially for the control of rockets used in the US space programme a conference was held in 1964. This was a conference on 'Short Term Frequency Stability' and was jointly organised by the IEEE and NASA and took place at the Goddard Space Flight Centre. Several papers were presented comparing the stability requirements of different systems and some of these results are tabulated here. Hadad [2] gave a survey paper comparing the stability required for many of the functions already mentioned. His results are included in Table 2.1. From this table the stability needed to give good clutter rejection is the most stringent. Other papers given by Leason & Johnson [3], Goetz & Skillman [4], Raduziner & Gillespie [5], Caldwell [6] and Sydnor [7] all quoted results that agreed broadly with those of Hadad's in Table 2.1. The results quoted by Goetz and Skillman and reproduced in Figure 2.1 are interesting This figure shows the spectral requirements of a transmitter for a pulse doppler radar and is similar to the specification shown in Figure 1.13.

The papers given by Caldwell and Sydnor were both concerned with the problems of deep space ranging and the stability needed to enable accurate tracking of both space vehicles and planetary bodies. For this purpose the stability required is of a different form since a stable oscillator is used to measure interpulse intervals which can be several minutes for very distant targets such as Venus. In this case the stability measured in parts per 10^x is significant. Sydnor quotes stability requirements of one part in 10^{10} for terrain mapping of the Moon or Venus. If doppler processing is used as well then the spectral content of the transmitted signal is also significant.

There are many ways of specifying the stability of an oscillator and the method used is determined by the application for which the

TABLE 2·1

STABILITY REQUIREMENTS FOR VARIOUS SYSTEMS

SYSTEM	REQUIREMENTS	MAXIMUM ALLOWABLE DEVIATIONS
RADAR GUIDANCE OF BALLISTIC MISSILES	0·05 ft/sec ACCURACY	3Hz/kHz
PRECISION TRAJECTORY MEASUREMENTS	0·05 ft/sec ACCURACY	3Hz/kHz
PHASE MEASUREMENTS	1° ACCURACY	36Hz/kHz
TARGETS IN SEA CLUTTER	-100 dB REJECTION	0·1Hz/kHz
FIXED TARGETS	INFINITE PLANE	0·03Hz/kHz
DIRECT LEAKAGE OR FEEDTHROUGH	0·5 μW FEEDTHROUGH	4Hz/kHz
LUNAR - LANDING VEHICLE	4% AT 25 ft/sec	11·7Hz IN 1Hz BAND

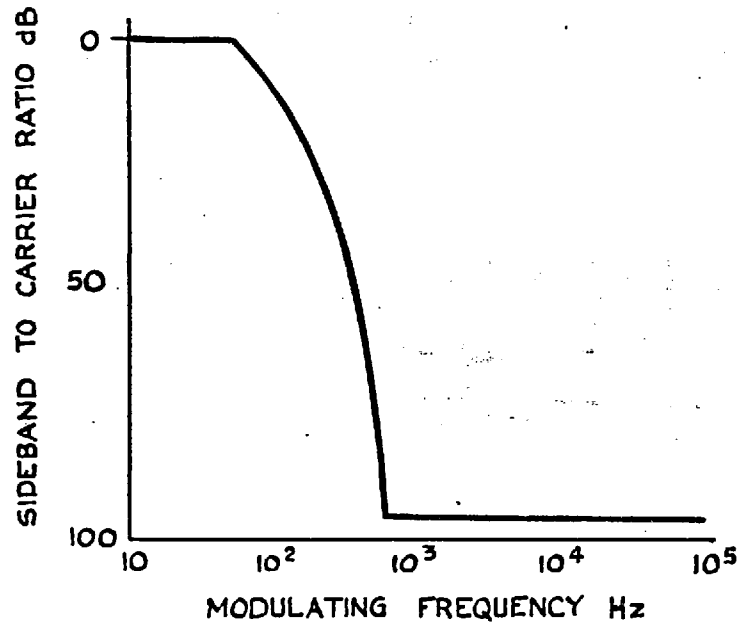


FIG. 2·1 MASTER OSCILLATOR STABILITY REQUIREMENTS

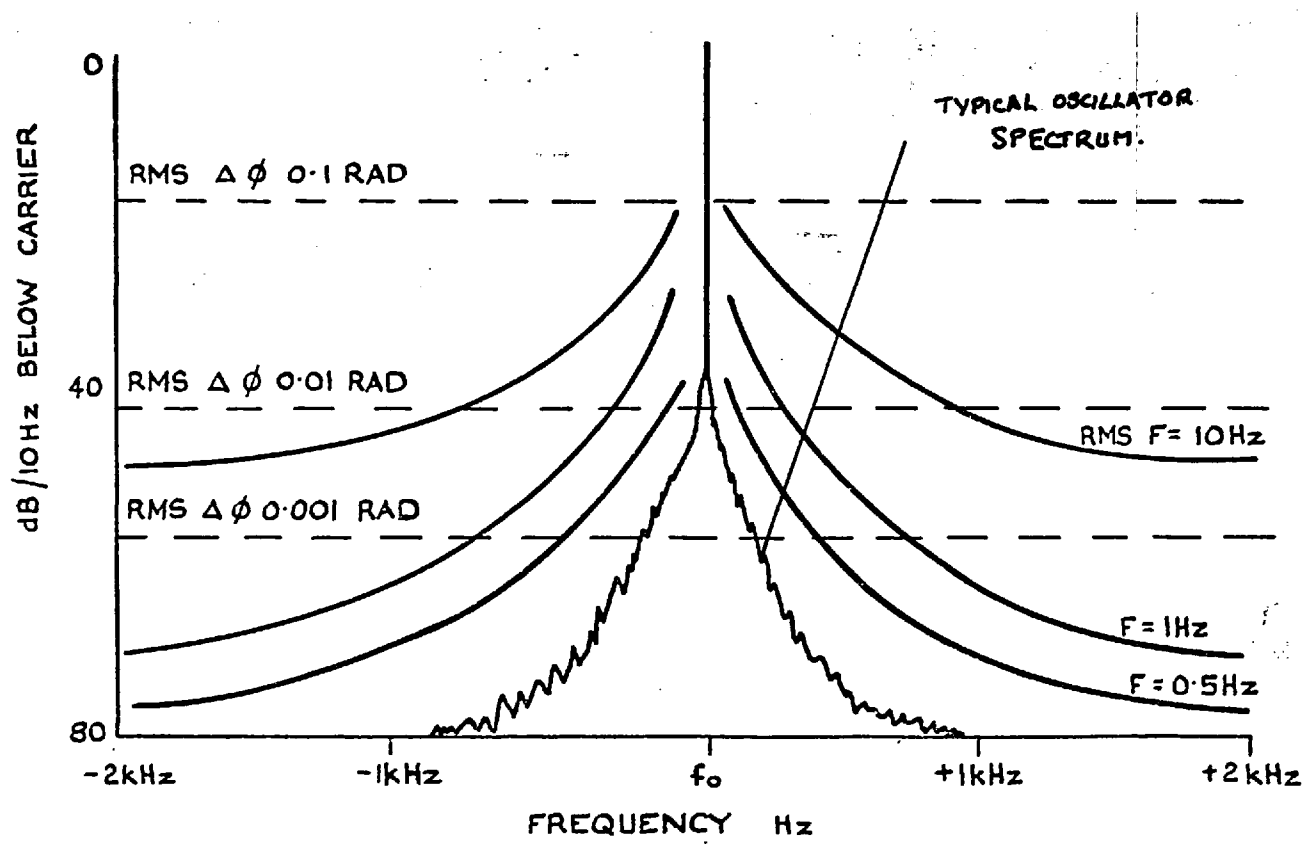


FIG. 2·2 PLOT SHOWING RELATIONSHIP BETWEEN THE DIFFERENT METHODS OF DEFINING FREQUENCY STABILITY.

oscillator is needed. The most common method is to express the spurious output in terms of a frequency modulation. This system equates the noise power in a certain band, b, at a certain frequency separation, f_m, from the carrier with a sinusoidal modulation centred in the bandwidth b and with its deviation proportional to the amplitude of the noise spectrum at f_m. For example the noise at a frequency of 10 kHz from the carrier might be quoted as 1 Hz/kHz. In this case the deviation of the equivalent sinusoid would be 1 Hz at a rate of 10 kHz. The bandwidth of the equivalent noise would be 1 kHz. To specify the total performance the noise power in each band must be separately specified for all frequency separations from the carrier which are important.

The other method of specification which is commonly used is to specify the noise in a certain bandwidth and at a certain frequency separation from the carrier. The noise is usually expressed in decibels relative to the carrier. For example the noise might be 80 dB/kHz below carrier at 10 kHz from the carrier. The two methods of specification are related by:

$$-D \text{ dB} = 20 \log \frac{\Delta f}{2 f_m}$$

where D is the number of dB below carrier

f_m is the deviation frequency

and Δ_f is the deviation

In the above example -80 dB/kHz at 10 kHz separation equates to

$$-80 \text{ dB} = 20 \log \frac{\Delta_f}{2 \times 10^4}$$

$\Delta_f = 2$ Hz ~~kHz~~ (deviation in 1 kHz bandwidth)

This relationship between the two methods of specification and the first method itself are both dependent on the amplitude modulation part of the noise being negligible in comparison to the frequency modulation components. In general this is true.

The relationship between the two methods of specification is more clearly apparent when shown diagrammatically as in Figure 2.2. Which method of specification is used will depend upon the application. Throughout this thesis the dB/Hz below carrier method has been used since this presents the results in a form which is most conveniently related to radar parameters such as clutter cancellation. The methods of specifying frequency stability have been discussed fully by Shields [8] who has compared the methods of specification and the stringency of the stability requirements of the different radar systems discussed in this chapter.

Other papers concerning the stability and performance of different radar systems have been given by Mooney & Ralston [9], Sydnor et al [10], Raven [11], Leeson & Johnson [12] and Bungay & Nesbeda [13].

2.2 Interline Noise

In Chapter 1 interline noise was described as the noise generated between the spectral lines of the spectrum of a pulse train. For most applications the power spectral density of this noise is the important factor influencing the capability of a pulse doppler radar. The power spectral density represents the total noise in a specified band and includes both A.M. and F.M. contributions. In many cases the stability required is specified in r.m.s. frequency deviation which presupposes that the A.M. component of the noise is negligible compared with the F.M.

component. While this is generally true for oscillators it is not necessarily true for the succeeding pulsed amplifiers.

An amplifier cannot produce F.M. noise directly but only phase modulation which can be equated to an equivalent frequency modulation. It is shown in Chapter 3 that most microwave amplifiers will produce phase modulation if their electrode voltages fluctuate. This phase modulation is usually much greater than the amplitude modulation produced by the voltage fluctuations because the amplifiers are run saturated. In general the interline noise produced by electrode voltage fluctuations is considerably greater than the noise produced by the amplification mechanism. However this is not true in the case of Crossed-Field Amplifiers which are less sensitive to voltage variations but produce high levels of self generated noise. The operating mechanism of the most widely used types of high power amplifiers is discussed in Chapter 3 which includes a full discussion of the different sources of interline noise.

Although it is the total noise that determines the performance of a pulse doppler radar a noise measuring system that measured A.M. and P.M. noise contributions separately would have advantages. Some sources of noise can produce more P.M. than A.M. so that a measuring system that differentiated between A.M. and P.M. would help in locating and eliminating unwanted noise components possibly produced by insufficiently stabilised power supplies or by vibration. In addition the noise generated by the source oscillator must be measured since this is likely to be the least stable component.

The techniques used to measure the noise generated by oscillators is quite different from those used for amplifiers. To measure the noise from oscillators a reference signal must be derived from the oscillator itself by using a passive dispersive network, such as a cavity. The

additive noise produced by an amplifier can be measured simply by comparing the input with the output. The Problems become apparent when the very large dynamic range needed is appreciated.

In the next section the methods used to measure oscillator noise are very briefly described and include references to detailed analyses of the circuits involved. The final section discusses various methods of measuring amplifier noise that have been used.

2.3 Oscillator Measurement Techniques

Techniques for the measurement of the noise spectrum and stability of microwave oscillators are now well known and widely applied. In principle the oscillator output is mixed with a sample of a stable reference oscillator at a similar frequency and the resulting low frequency analysed using a spectrum analyser. Provided that the reference oscillator is the quietest of the two the noise measured will be the noise generated by the test oscillator. This is not usually the case with the oscillators designed for use with pulse doppler radar systems and a discriminator must be used instead.

The basic circuit shown in Figure 2.3 compares a sample of the oscillator output which has been passed through a dispersive network with an unmodified sample. The discriminator effectively converts the frequency modulation to amplitude modulation which can be detected and analysed. There are many variants of this basic circuit but one that was developed at the Royal Radar Establishment in 1955 by Drage & Marsh [14] is the most widely used and is shown in Figure 2.4. This circuit uses a cavity as the dispersive element in conjunction with a bridge circuit for accurately matching the cavity to the transmission line. The

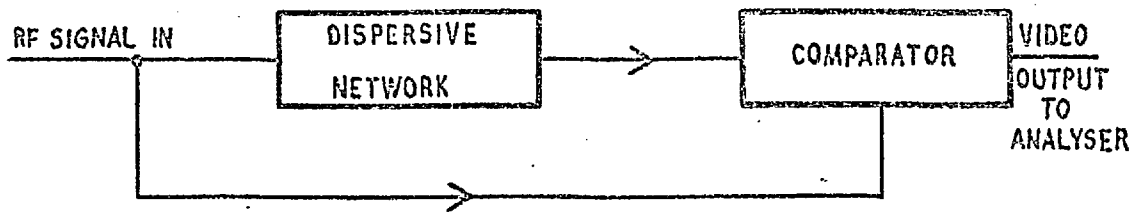


FIG. 2·3

BASIC OSCILLATOR NOISE MEASURING SYSTEM

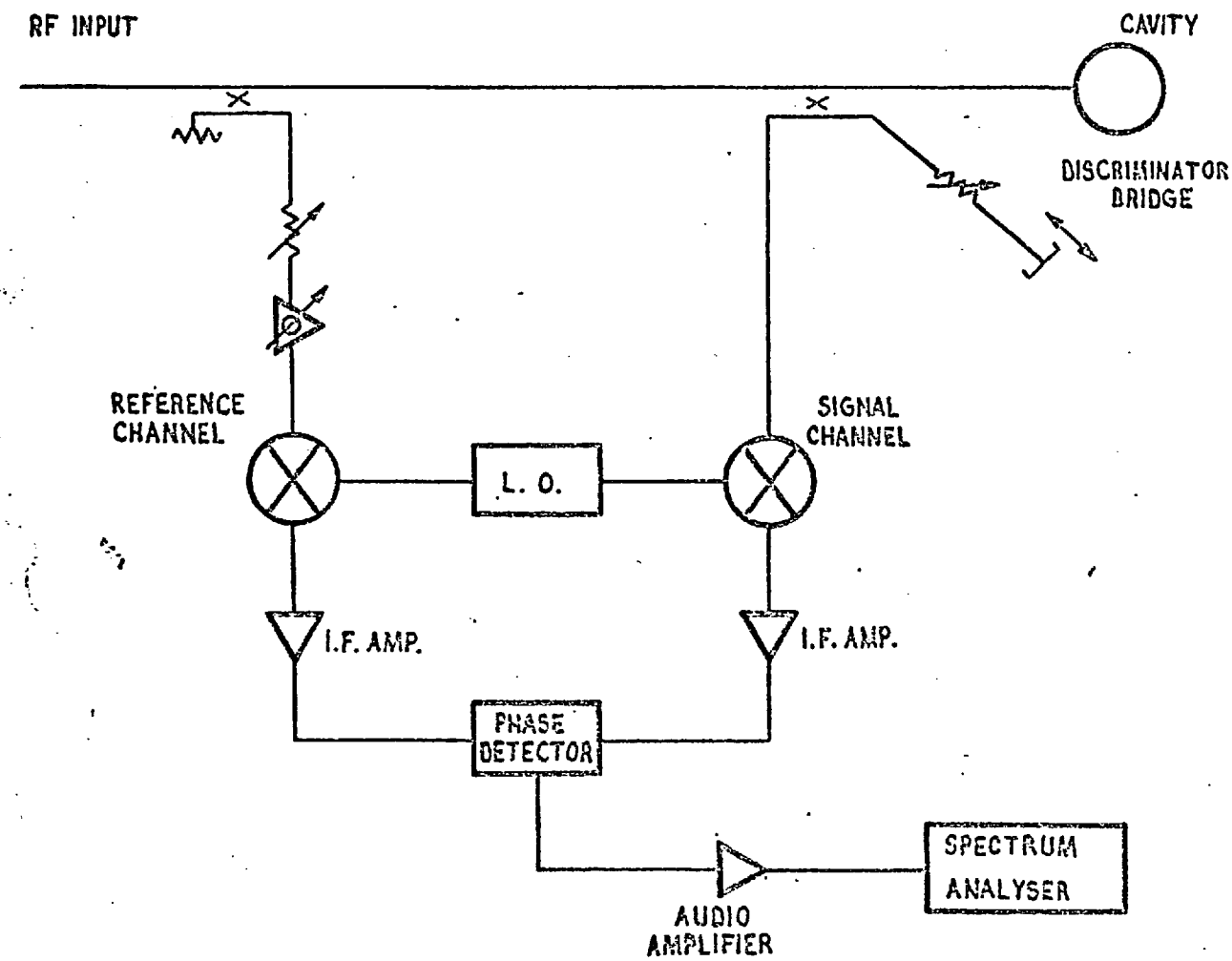


FIG. 2·4

OSCILLATOR NOISE MEASURING SYSTEM

cavity also suppresses the carrier and raises the level of the noise sidebands of the oscillator, increasing the dynamic range and sensitivity of the system by as much as 40 dB.

The RRE discriminator is capable of measuring noise down to 0.001 Hz r.m.s. frequency deviation in a 70 Hz bandwidth. This sensitivity is adequate for most requirements. A full description of this measurement system is not given here since it is already well documented, notably in the manufacturers technical application notes [15] and also by Grauling & Healey [16] and Whitwell & Williams [17]. Improved types of noise measuring system of the same principle have recently been described by Ashley, Searles & Polka [18], Ondria [19] and Blomfield [20].

This type of circuit can be used to measure noise in pulsed signals but the dynamic range and sensitivity is very low because the spectrum of a pulsed signal occupies a much broader band than a CW signal and the cavity can no longer act as an effective discriminator because of its narrow bandwidth. A full analysis of the potential of this system for pulsed signals has been made by Cooper [21] who draws similar conclusions.

2.4 Pulsed Amplifier Measurement Techniques

Until 1960 little interest was taken in the close-to-carrier noise of pulsed high power amplifiers. Up to this time the stability needed by the systems in use had been such that noise introduced by the power amplifiers was insignificant. After 1960 the stability needed increased due to the higher performance and changing needs of civil and military systems. It was then apparent that some means of investigating the close-to-carrier noise of high power amplifiers was required.

An instrument designed to measure the interline noise generated by a pulsed amplifier must be capable of discriminating between individual spectral lines of the sin x/x spectrum and it must measure the noise generated between these lines. The magnitude of this task can be appreciated if the sensitivity and discrimination required are calculated. Most radars operate at P.R.F.s. of between 200 Hz and several kilohertz and this determines the spacing of the spectral lines. In addition a resolution of down to about 10 Hz is necessary if discrete modulation lines due to mains ripple are to be measured. The sensitivity and dynamic range of the instrument are set by the duty ratio of the radar system and by the noise levels to be measured. In Chapter 1 a noise level of 120 dB/Hz below one spectral line was quoted as a typical specification. The measurement system should therefore be able to measure down to 130 dB/Hz. A single spectral line, near the centre of the sin x/x envelope, has an amplitude which is a factor D^2 below the peak power of the pulse, where D is the duty factor. So, for a system with a duty factor of 0.05 a spectral line is 26 dB below the peak power of a single pulse. Since the measuring system must accept the peak power without introducing any distortion or gain compression the dynamic range required is in excess of 156 dB.

The conventional type of microwave panoramic spectrum analyser is not capable of the resolution required, nor would any technique that relied on a free running transfer oscillator to mix the microwave signal to a convenient low frequency for analysis. This is because the transfer oscillator instabilities could not be separated from the noise modulation on the signal to be analysed. These problems were first examined by Koontz [22] in 1962. Koontz used a coherent converter to mix the microwave signal to a low frequency for analysis. In this technique a stable low frequency

signal is upconverted to the microwave frequency, passed through the amplifier and downconverted to the original low frequency using the same local oscillators. Provided that the delay between mixing up and down is small the noise introduced by the transfer oscillators will not decorrelate and will cancel out. The low frequency output signal contains the noise introduced by the amplifier and can be analysed using an audio spectrum analyser. Koontz' system had a dynamic range of 50 dB with respect to a single spectral line and with a measurement bandwidth of 2 Hz. The sensitivity was limited by the spectrum analyser although the basic system should have been capable of far greater sensitivity. No measure of the amplifier noise was achieved but only of the spectrum of some of the spurious modulation introduced by the power supplies and cooling system.

A similar technique was reported by Burnsweig et al [23] at the 1964 IEEE Electron Devices Meeting in Washington. They measured the interline noise of several different types of X Band amplifier and achieved a sensitivity of 75 dB below a single line in a 1 Hz bandwidth. However the characteristics of the analyser filter did not give good resolution of the noise and modulation components. Both this and Koontz' method measured the total noise contribution from the amplifier and did not distinguish between amplitude and phase modulation components.

In 1966 Smith [24] used a modified oscillator measuring system of the sort described in the previous section to measure the noise generated by a pulsed electrostatically focused klystron amplifier. The sensitivity was limited by the response of the discriminator cavity and by the imperfect cancellation of the spectral lines. The reasons for this were discussed in the previous section and analysed by Cooper [21]. The system was able to distinguish between A.M. and P.M. sidebands but as it was not an

additive noise measuring system the noise detected was largely that produced by the source oscillator.

A study of a modified form of oscillator measurement system was performed by the manufacturers [25]. They proposed to fill the gaps between pulses with a clean r.f. signal turning the pulse train into a CW signal which could be analysed using the conventional cavity discriminator system. This cumbersome approach was abandoned in favour of an additive noise measurement system where a sample of the amplifier output is compared with a sample of its input. This basically simple method provides a means of making very wide dynamic range measurements of pulsed tubes. It allows separate measurements to be made of the A.M. and P.M. components of the noise and also suppresses the noise from the preceding stages of the amplifier chain.

This technique was adopted and refined for the work described in this thesis and a detailed description of the operation and development of the method is given in Chapter 5. Since the start of this work other people have reported measurements using similar types of equipment. Sann [26] and Straub [27] have achieved a sensitivity of up to 150 dB/Hz below a spectral line which is approaching the theoretical limit using available components. Sann used the equipment to measure the noise on some medium power klystron amplifiers and found that the noise generated by the tube itself closely approached the noise that could be expected if the tube has a noise figure of 30 dB which is typical for tubes of this type. Better performance than this has been shown by Warren [28] using an X Band travelling wave tube.

Measurements on crossed field amplifiers have been performed by Crowfoot [29], Clark [30] and Hollis et al [31]. Crowfoot and Clarke were evaluating the performance of C Band and X Band Amplitrons (a Raytheon backward wave CFA) and they showed that this type of tube produced noise

typically 75 dB/Hz below one spectral line. Hollis et al were using an L Band forward wave CFA of the same type described in Chapter 3. They found that the noise was about 80 dB/Hz below a spectral line, a similar result to that described later in this thesis.

The increasing interest in this type of measurement indicates the importance now placed on the type of system which demands such high spectral purity.

CHAPTER 3

NOISE MECHANISMS IN TRANSMITTER TUBES AND POWER SUPPLIES

All high power coherent radars use amplifier chains to develop the high energy pulses radiated by the system. In general vacuum tube amplifiers must be used because of the high power levels and the high frequencies used. Before designing a low noise amplifier chain using microwave tubes it is necessary to know something of their operating characteristics and noise mechanisms. This chapter gives a brief description of some of the more common types of microwave tube amplifier. The description of their very complex operating mechanisms is inevitably very much simplified but these types of tube have been fully described in the references quoted.

3.1 The Travelling Wave Tube

The conventional vacuum tube such as the triode is limited by transit time effects at microwave frequencies and only low power tubes have been built for operation at microwave frequencies up to 3 GHz. Another type of electron stream/r.f. interaction must be used - velocity modulation. In this type of interaction the velocity of a beam of

electrons is modulated by the r.f. signal as distinct from the space charge modulation used in the triode and related types of low frequency vacuum tube amplifiers. One class of tubes using velocity modulation is called the travelling wave tube (TWT).

In this type of tube energy is transferred from an electron beam to an r.f. wave carried on a 'slow wave structure' in close proximity to the beam. The slow wave structure has two important functions; i) it must support an r.f. wave with a phase velocity very much below the velocity of light and ii) it must be so arranged that a component of the E field of the r.f. wave is directed along the axis of the electron beam. If the axial component of the E field of the r.f. wave is high in the region of the electron beam interaction between the two will occur providing that the r.f. wave and the electron beam are travelling at approximately the same velocity. If these conditions are satisfied electrons in some parts of the beam see an accelerating potential applied by the r.f. wave and those half a circuit wavelength along the beam from there see a retarding potential. Therefore some electrons will be accelerated and some retarded leading to the formation of bunches in the electron beam and these bunches will travel in near synchronism with the circuit wave. If these bunches are travelling at a slightly faster velocity than the r.f. wave on the circuit then the bunches will move into a region of retarding r.f. field. This field will slow the electron bunch which will lose kinetic energy. Because energy must be conserved the r.f. wave will grow which will increase the retarding r.f. field so slowing the electron bunch still further. In this way the r.f. wave will grow in power exponentially at the expense of the kinetic energy of the electron beam. This growth continues until the velocity of the electron beam falls sufficiently for synchronism to be lost. This explanation is a gross simplification of the interaction mechanism of the

travelling wave tube since the interaction between the electron beam and the r.f. wave on the slow wave circuit is so complex that a full description would be beyond the scope of this thesis. Many books have been written on this topic, notably by Pierce [32] who first described the operating mechanism and more recently by Gittins [33] in a book on high power travelling wave tubes. Gittins describes the interaction mechanism using vector diagrams which enables him to give a very lucid explanation of the process. Gittins' book is strongly recommended to the reader who is not already familiar with travelling wave tubes.

The simplest type of slow wave circuit that satisfies the requirements to provide an E field along the axis of the electron beam and an r.f. wave travelling at a velocity similar to the beam, is a helix. A schematic diagram of a TWT using a helix is shown in Figure 3.1. A high velocity electron beam is formed by an electron gun and injected down the axis of the helix. The beam tends to spread because of the mutual repulsion of the individual electrons and an axial magnetic field is used to constrict the beam. The spent electron beam is collected by a collector. The r.f. signal to be amplified is launched at the gun end of the helix and travels along the helix to the collector end where the amplified signal is extracted.

The propagation characteristics of a helix, or any other form of slow wave structure, can be described by an w-β diagram which is a plot of angular frequency against phase change per unit length. On an w-β diagram the phase velocity at any point is the slope of the line joining that point to the origin since

$$v_p = w/\beta$$

The electron beam can be represented by a line drawn through the origin whose slope is the beam velocity. At those points where this line cuts

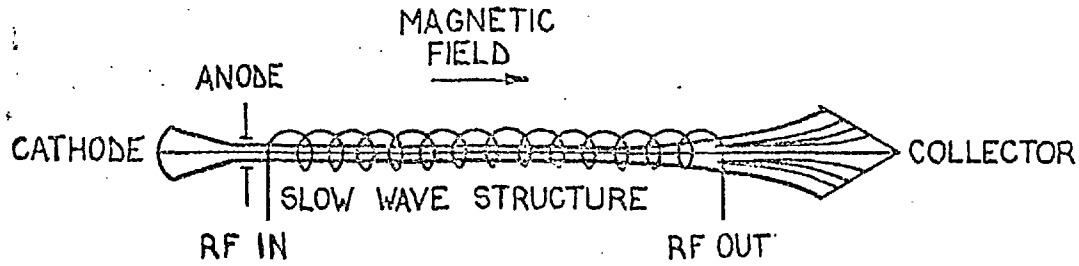


FIG. 3·1 SCHEMATIC DIAGRAM OF HELIX TWT

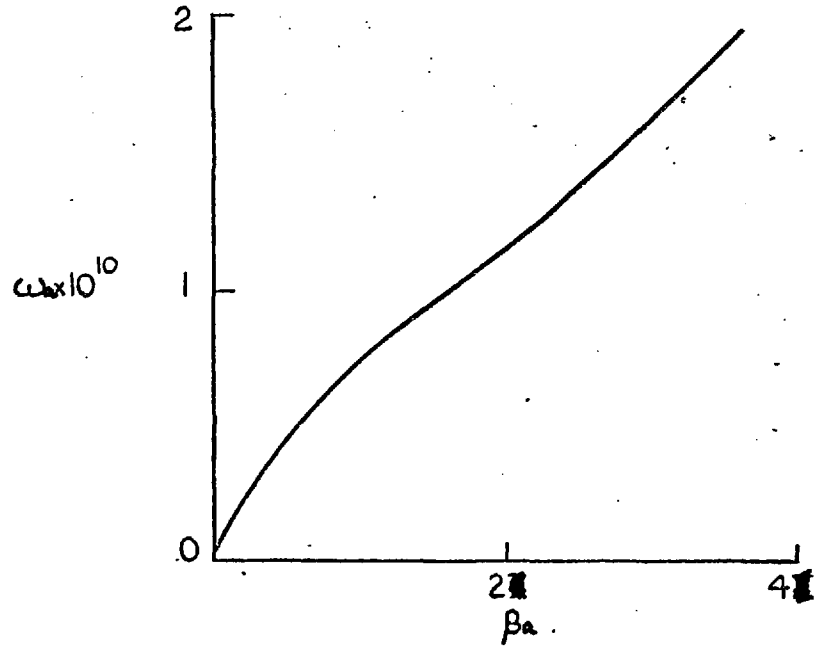


FIG. 3·2 $\omega - \beta$ DIAGRAM FOR A 10^0 HELIX

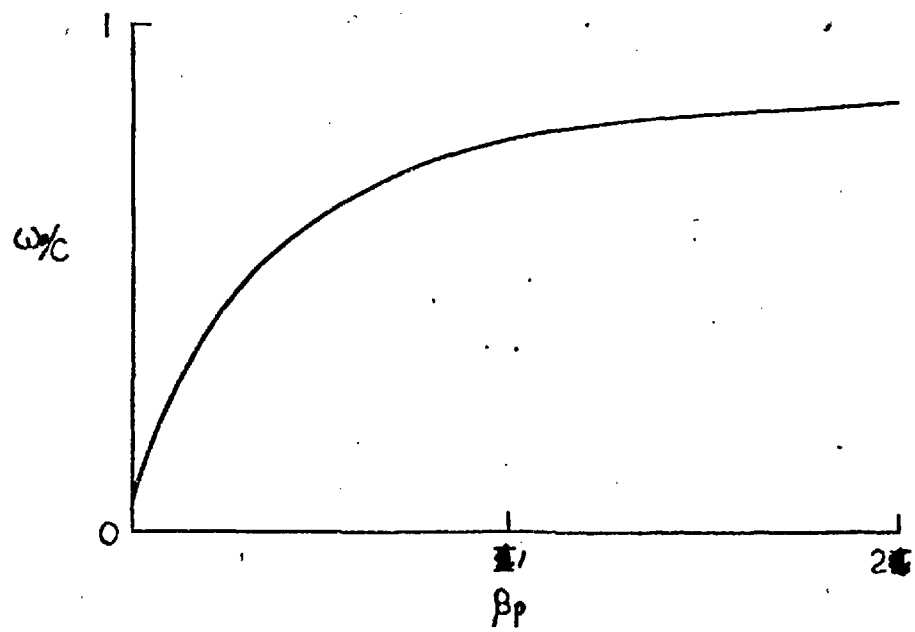


FIG. 3·3 $\omega - \beta$ DIAGRAM FOR A RING & BAR STRUCTURE

the phase-frequency characteristic of the structure the beam and circuit wave have nearly the same velocity and amplification may be possible. An w-β diagram for the helix taken from Gittins book is shown in Figure 3.2. The curve approximates to a straight line through the origin from which it may be inferred that synchronous operation can be obtained over a large bandwidth. This is true in practice and the helix has been used in travelling wave tubes with multi-octave bandwidths. The bandwidth is limited at the high frequency end by falling coupling between the r.f. wave and the beam. This occurs because there are fewer turns of helix per wavelength and a consequent reduction in the component of the E field along the beam which produces the interaction. At the low end of the band there are too few wavelengths along the length of the tube to produce sufficient gain.

The gain of the simple TWT shown in Figure 3.1 is limited by the input and output VSWR between the helix and the external transmission line. A small amount of power reflected from a mismatch at the output transition will travel back along the helix to the input transition where a similar small amount of this reflected power will be reflected back along the tube in the direction of amplification. If the gain of the TWT is too high and the phase of the reflected signal is correct then the TWT will oscillate. This usually occurs for tubes with a gain of 20-25 dB. To overcome this problem an attenuator or sever is used on or in the slow wave circuit. The r.f. drive signal is used to modulate the electron beam and is then attenuated. The modulated electron beam then excites an r.f. wave on the output half of the structure. Using severs [redacted] power TWTs can be made with gains of 50 dB.

The helix is a low power circuit. To generate high power the electron beam voltage must be increased to raise the beam power since both cathode loading and space charge forces limit the beam current. This

produces a faster electron beam and a faster circuit must be produced by increasing the pitch of the helix. Unfortunately this reduces the coupling between the beam and the r.f. wave because there is now a smaller component of the E field along the axis of the beam. The helix is also a fragile circuit and is not capable of withstanding very much electron beam interception.

At moderate power levels of 1-100 kW peak power a modified helix structure called the ring-bar structure is used. This is a robust structure and gives good coupling between the circuit wave and the beam. However it is more dispersive than the helix as the w-β diagram of Figure 3.3 shows. This limits the bandwidth of the ring-bar structure to 20-30%.

For very high power tubes a completely different type of structure is used as described in the next section.

3.2 High Power Travelling Wave Tubes

At power levels ranging from about a hundred kilowatts to several megawatts a very robust structure is required and takes the form of a series of coupled cavities. These can carry a travelling wave of the correct velocity, provide good coupling between the r.f. wave and the beam and withstand high interception currents. The most widely used structure was invented by Chodorow and is called a cloverleaf structure because of its resemblance to the leaf of a four leaf clover. A single cavity is shown in Figure 3.4.

E The noses distort the r.f. magnetic field inside the cavity to provide a strong radial component so that when alternate cavities are rotated through 90° a negative mutual inductance coupling is provided, giving a forward-fundamental passband.

~~next~~. The circuit has a complex w-β diagram as shown in Figure 3.5 and

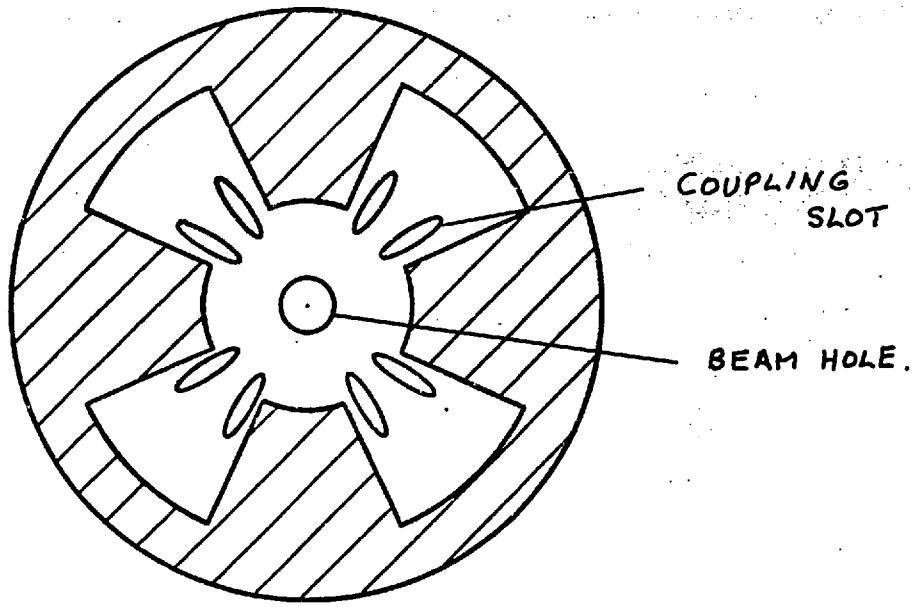


FIG. 3·4 THE "CLOVER LEAF" STRUCTURE

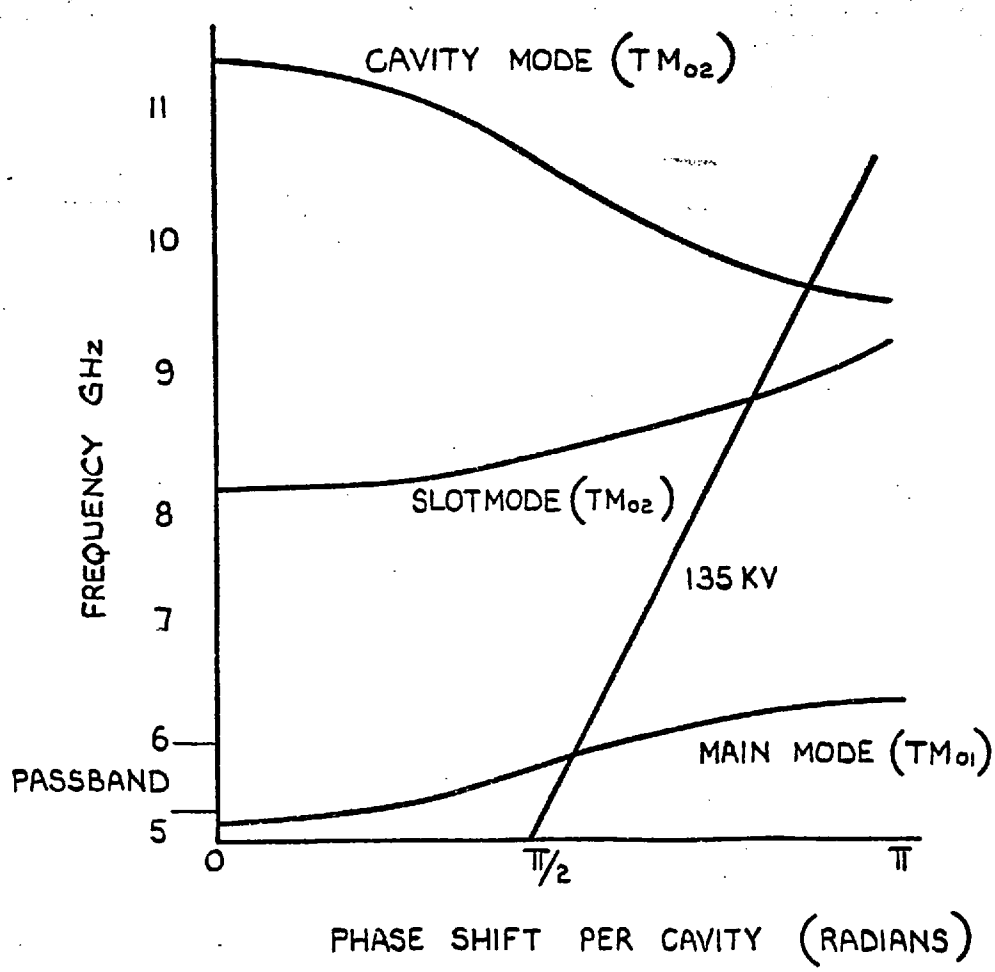


FIG 3·5 ω−β DIAGRAM FOR A TYPICAL CLOVERLEAF TUBE

care has to be taken with the design to suppress competing modes which the circuit is capable of propagating. These are usually eliminated by inserting lossy material in those areas of the cavities in which the field strength of the competing modes is high.

Clover-leaf TWTs have been built with power outputs of several megawatts and bandwidths of 10%. The gain is typically 30 dB and the efficiency 30-40%. These tubes are inevitably fairly large and can require beam voltages well in excess of 100 kV.

The TWT belongs to a class of travelling wave amplifiers known as linear beam tubes because the electron beam follows a straight path, constricted by an axial magnetic field which plays no part in the interaction. Another type of travelling wave amplifier exists, the crossed field amplifier or CFA, in which the accelerating electric field and a magnetic field are arranged orthogonally to each other and to the electron beam.

3.3 The Crossed Field Amplifier

Crossed Field Amplifier or CFA is the generic name for a large family of amplifiers all of which share a similar interaction mechanism. These devices are called CFAs because the electronic interaction occurs in a region of crossed electric and magnetic fields like a magnetron. In other respects the CFA is similar to the TWT since it has a slow wave circuit and a beam forming system which provides a stream of electrons moving in proximity to the r.f. wave on the slow wave structure. However, the energy transferred from the electron beam to the circuit wave is largely potential energy. This feature accounts in part for the much higher conversion efficiencies achieved with CFAs since it is possible

for the electron beam to be collected with low or zero velocity.

The CFA can take many forms but the two most common types are shown diagrammatically in Figure 3.6. They are called the injected beam CFA and the distributed emission CFA. In the injected beam tube a beam of electrons is formed by a crossed field gun and injected into the interaction region formed by a slow wave circuit carrying the r.f. wave and a non-emitting sole electrode. The spent electron beam is collected partly by the circuit and partly by a collector. The electrons injected into the interaction region will move parallel to the circuit at a velocity determined by the sole-circuit voltage and the transverse magnetic field. This velocity is arranged to be in near synchronism with the r.f. wave on the circuit. Bunching of the electron beam occurs in a similar manner to the TWT and energy is passed from the electron beam to the circuit wave. The electrons lose kinetic energy and consequently drift closer to the circuit thereby moving down an electric field giving up potential energy. Some of the electrons will hit the circuit which must be robust enough to dissipate the heat generated. The gain per circuit wavelength is higher than for a TWT and consequently the circuit length required for the same gain is less. However the gain of this type of CFA is limited to 17-20 dB for the same reasons as the unsevered TWT - the mismatch at the input and output transitions to the slow wave structure. The problem is accentuated in the CFA because of the possible generation, at discontinuities in the circuit such as transitions, of fast waves. These are competing modes in the structure which travel at very much higher phase velocities than the natural circuit wave. Fast waves can also propagate unattenuated past severs in the structure negating their value. Although severs have been tried in CFAs they have not yet proved successful, probably because of fast wave feedback.

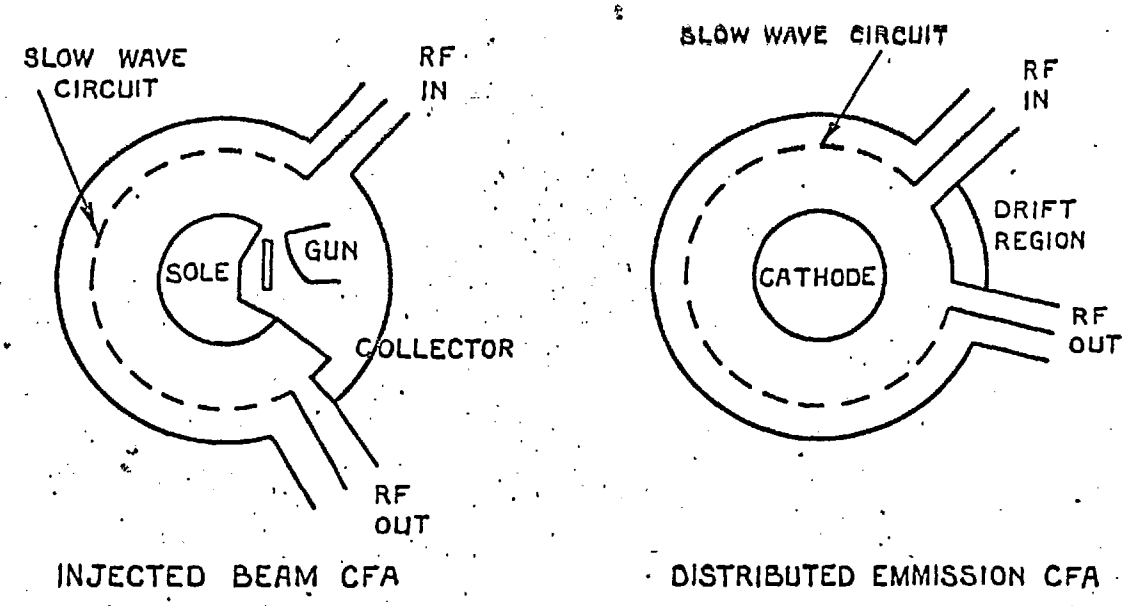


FIG. 3·6

SCHEMATIC OF THE TWO BASIC TYPES OF CFA

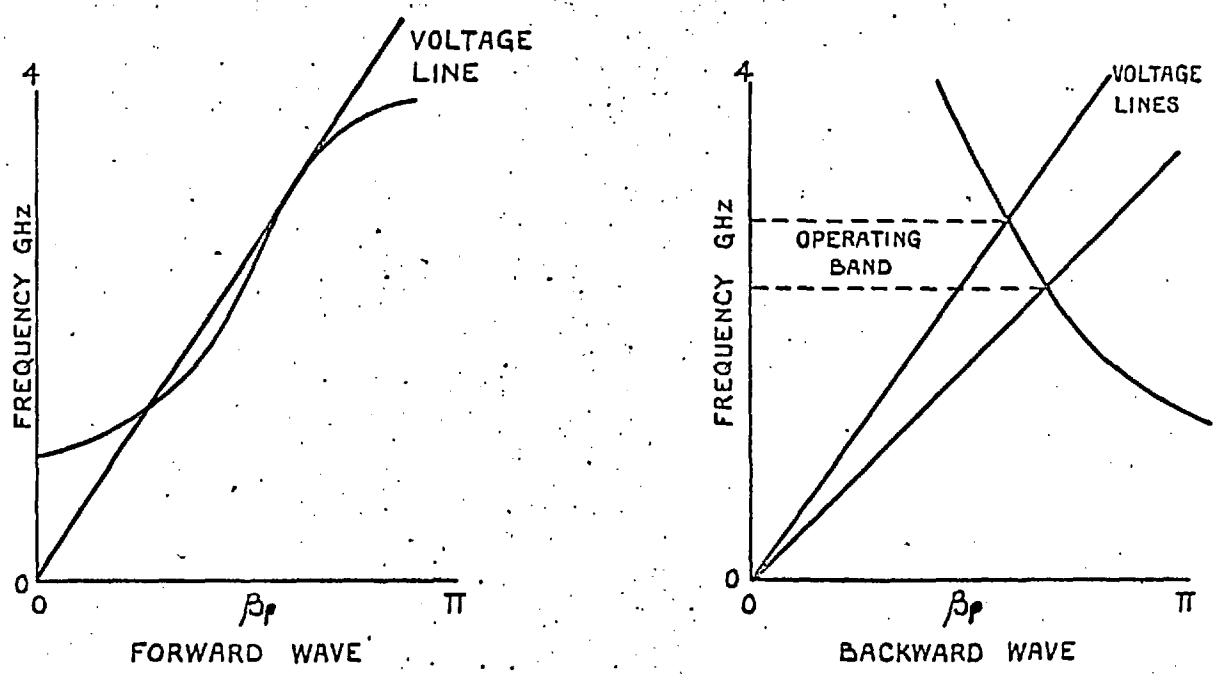


FIG. 3·7

ω-β DIAGRAMS FOR FORWARD & BACKWARD WAVE CFA CIRCUITS

The distributed emission CFA has the same sort of electronic interaction as the injected beam CFA but the beam is formed in a different way. A centrally placed circular cathode emits electrons which rotate around it under the influence of the crossed electric and magnetic fields. A slow wave circuit surrounds the cathode with a gap called the drift space between the input and output transitions. Bunching of the electron cloud occurs and the electrons give up energy to the r.f. wave and are finally collected on the circuit.

The circuit can be arranged to support either a forward wave or a backward wave as shown in the w-β diagrams of Figure 3.7. In the forward wave case bandwidth is achieved at a fixed voltage while in a backward wave tube some voltage tuning is required. (In a real backward wave CFA the operating impedance of the tube changes with frequency. This change in impedance is readily accommodated using a line-type modulator discussed later in this chapter.) In forward wave CFAs the electron beam and circuit wave move in the same direction and in backward wave CFAs they move in opposite directions.

The electron beam in these tubes is re-entrant since it circulates round the structure via the drift space, the length of which greatly affects the operation of the tube. If it is short then the electron beam is still heavily bunched when it re-enters the interaction region and produces strong electronic feedback. This feature can be used to get very high efficiency at the expense of stable gain. Efficiencies of 80% have been observed but at gains of only 8-10 dB. The noise generated by such tubes is also high.

If the drift space is long then space charge forces de-bunch the electron beam and eliminates this source of electronic feedback. Most distributed emission CFAs made now have long drift spaces. The efficiency is reduced to about 50% but stable gains of up to 17 dB have been

demonstrated. Such tubes also produce less noise and are less prone to burst into oscillation.

CFAs in general are characterised by quite high levels of noise output compared to TWTs. Figure 3.8 shows a comparison of the broad-band spectrum of an L Band forward wave CFA with an L Band TWT. The differences in noise are quite striking. The spectra are typical of a good CFA and a good TWT.

3.3.1 Cold cathode CFAs

The electrons in all CFAs tend to move in cycloidal paths and many are returned to the cathode of distributed emission CFAs. These electrons can generate secondary electrons and supplement the thermionic emission. The effect can also be used in some tubes to provide heaterless operation. The cathode is made of a material such as beryllium oxide or platinum with a high secondary emission coefficient. Stray electrons and ions are always present in the tube vacuum and these bombard the cathode under the influence of the combined d.c. and r.f. fields. Secondary electrons are produced some of which in turn bombard the cathode and full conduction builds up in about 10 ns.

At high power levels platinum can be used despite its relatively low secondary emission coefficient of 2. For lower powers a higher coefficient is required and a material such as beryllium oxide with a coefficient of 4 must be used. Such a cathode would be made of beryllium with a thin oxide layer allowed to form on the outside. Unfortunately in the severe environment inside a CFA the oxide layer tends to get stripped off by bombarding ions and electrons, exposing the bare beryllium which has a lower secondary emission coefficient. Tube performance then degrades.

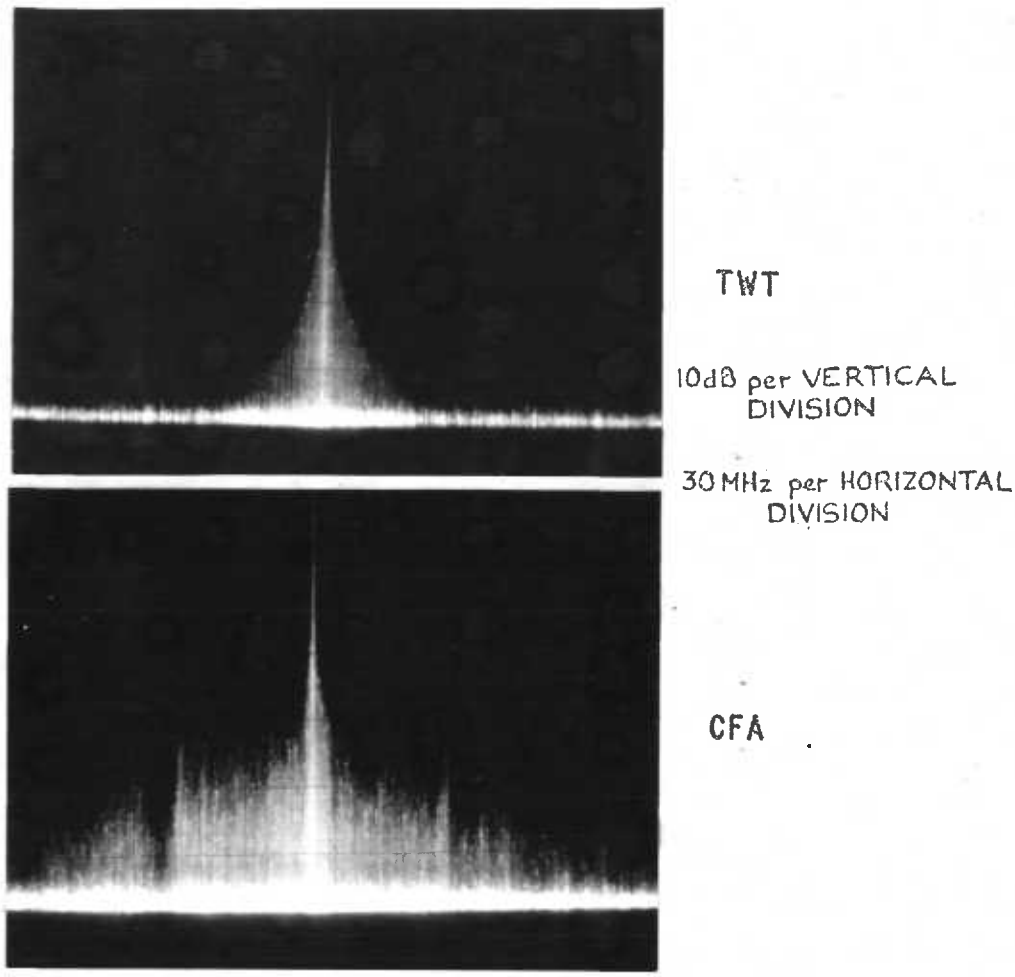


FIG. 3·8

COMPARISON OF TWT & CFA BROADBAND NOISE

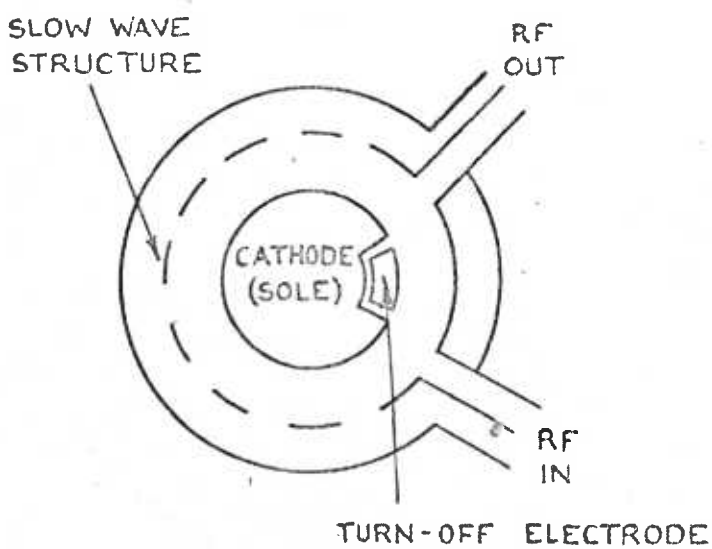


FIG. 3·9

COLD CATHODE, RF SWITCHED CFA

To prevent this a small amount of oxygen can be released inside the tube to combine with the beryllium and renew the oxide coating. The oxygen is usually absorbed into a wire element within the tube and is released in a controlled manner by heating the wire with a small electric current. In general platinum cathodes are preferred for cold cathode operation since they do not suffer from poisoning or oxide layer depletion.

Using cold cathode operation, conduction cannot start unless both the HT voltage and the r.f. drive are present. This gives the possibility of d.c. operation of the tube if some means of gathering up the circulating electron cloud at the end of each pulse is used. A diagram of such a tube is shown schematically in Figure 3.9. When r.f. drive is applied to the tube conduction and amplification begins. At the end of the r.f. drive pulse that portion of the cathode opposite the drift space and called the turn-off electrode is pulsed positively with respect to the cathode and collects the electrons as they pass. Beam shut-off is usually achieved within 100 ns. This type of operation can simplify the power supplies for the transmitter since instead of a high voltage pulse modulator only a d.c. power supply and a low power modulator are needed. This technique is especially useful if it is desired to transmit complex pulse trains where a conventional pulsing circuit becomes very complicated.

This description of the operation of some of the different types of CFA is again brief but a very comprehensive book on crossed field devices has been written by Okress [34].

3.4 Noise in Transmitter Tubes

An ideal pulsed microwave amplifier will produce a frequency spectrum made up of a theoretically infinite number of discrete spectral

lines. A standard fourier analysis of a pulse train shows that these lines have an envelope which is a $|\sin x/x|$ function with lines spaced apart by an amount equal to the pulse repetition frequency. A spectrum of this type is shown in Figure 3.10a. No real pulse train can have pulses with zero rise and fall time and since these parts of the pulse contribute the higher order spectral lines no real spectrum is infinite.

All amplifiers produce noise which degrades this perfect spectrum. The first type of noise is called extra-spectral noise and is the noise generated by the amplifier outside the band of frequencies occupied by the sin x/x spectrum of the pulse train. This is illustrated in Figure 3.10b. TWTs typically produce extra-spectral noise levels of better than 80 dB/MHz below the transmitted power. However coupled cavity TWTs can oscillate on the rise and fall of the voltage pulse as the voltage sweeps through a value which excites an unwanted mode on the circuit. The peak power level of the oscillation can approach the peak power output of the tube although the mean power level is small in most cases since the oscillation only lasts for 50-100 ns. The frequency of the oscillation is always outside the operating band of the radar and is rarely troublesome to the radar itself although it can interfere with other systems operating on neighbouring frequency bands. A broad-band spectrum of a TWT is shown in Figure 3.11a. The effect of oscillations on the rise and fall of the voltage pulse can be clearly seen.

The CFA produces very much higher levels of extra spectral noise and spurious oscillations. The broad-band spectrum of a 'quiet' CFA is shown in Figure 3.11b. The general background noise is about 50-55 dB/MHz below the transmitted power and in this spectrum there is no sign of spurious oscillations, although slight misadjustment of the operating conditions can produce these.

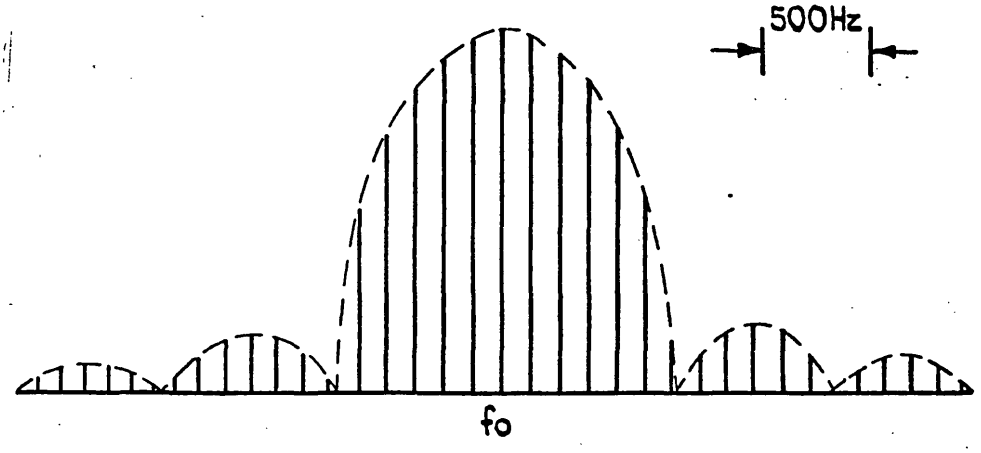


FIG. 3·10 a

SIN x/x SPECTRUM OF A PULSED SIGNAL

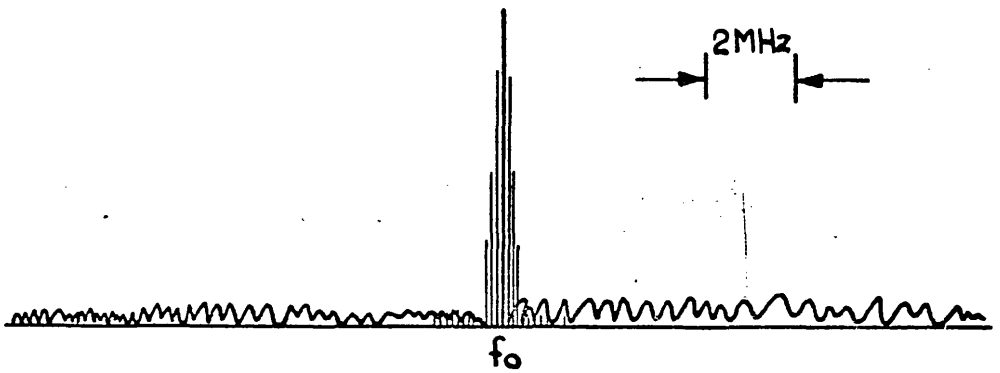


FIG. 3·10 b

EXTRA–SPECTRAL NOISE ADDED

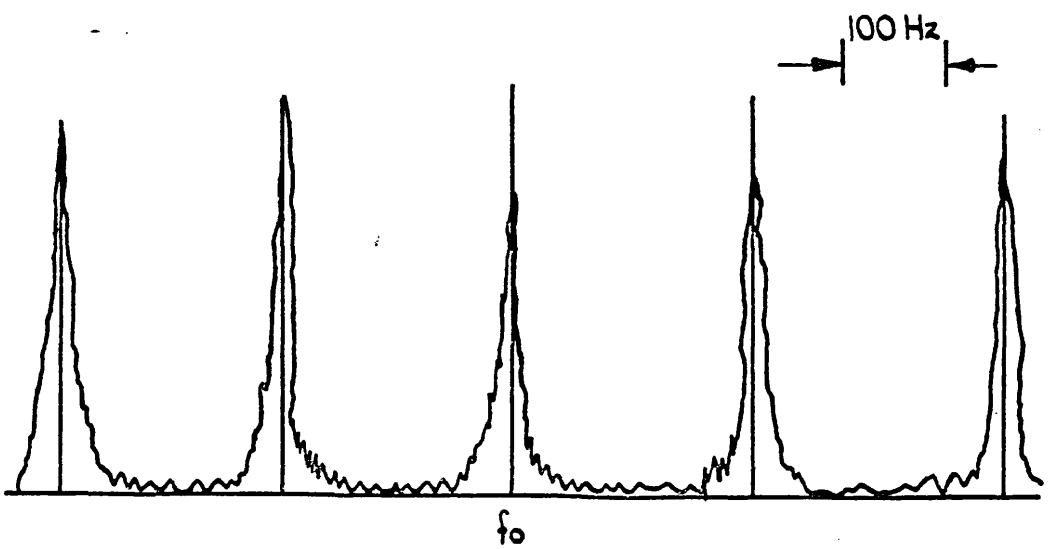


FIG. 3·10 c

INTER–LINE NOISE ADDED

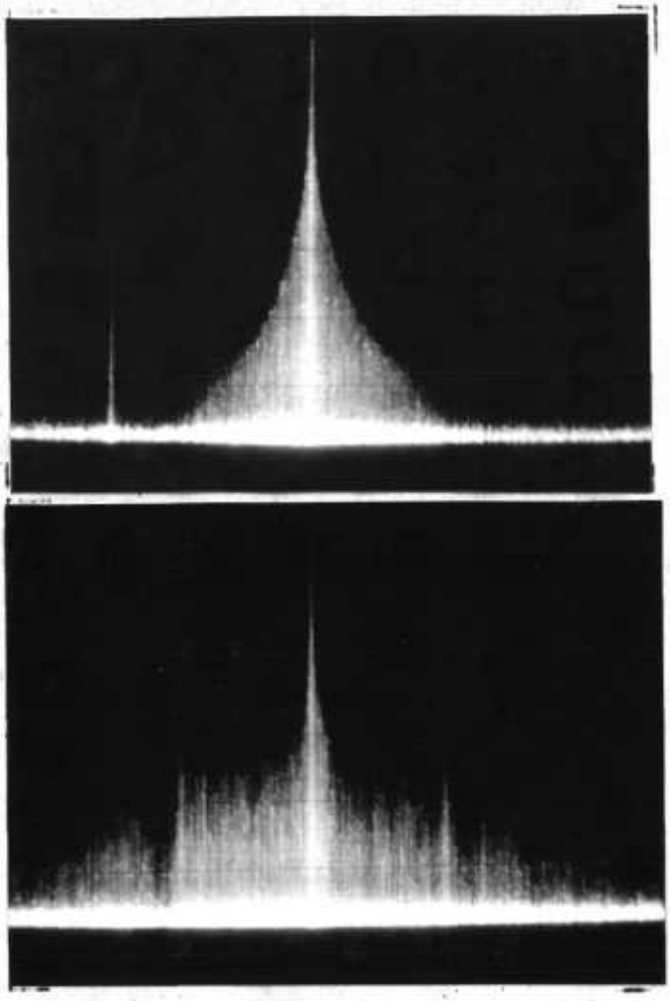


FIG. 3·11
a) SPECTRUMS OF ATWT & ACFA

b)

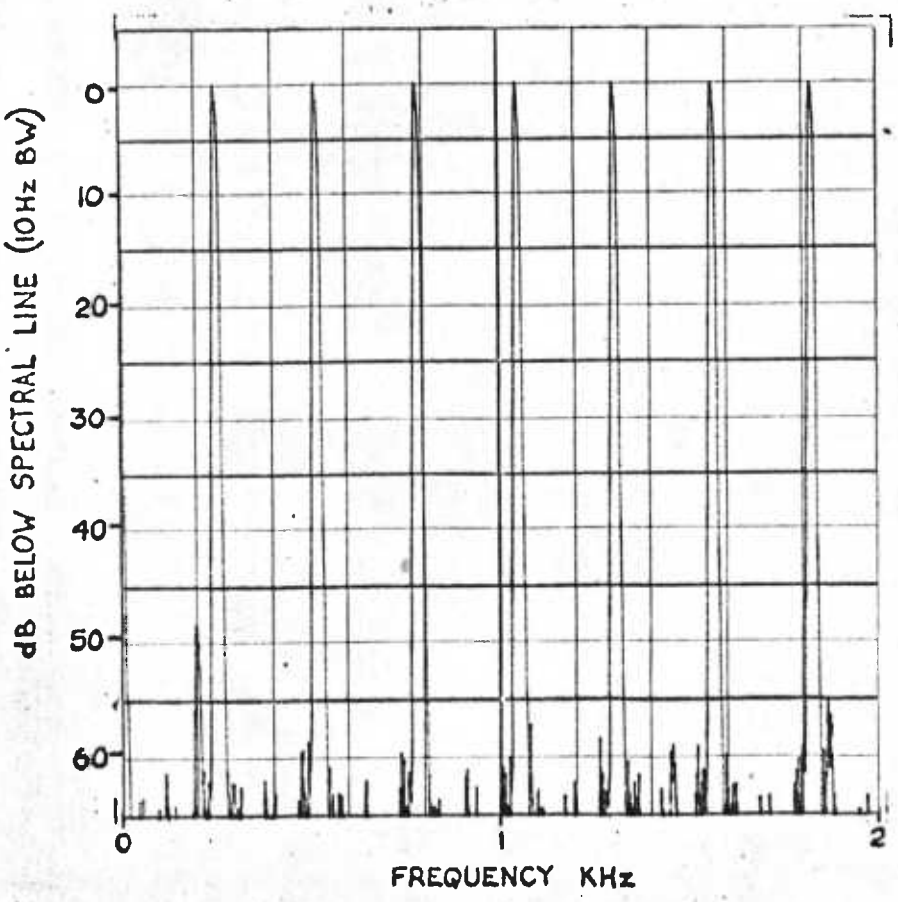


FIG. 3·12
INTERLINE NOISE GENERATED BY A SMALL TWT

The second important type of noise is Intra-spectral or interline noise. This is noise generated between the lines of the sin x/x spectrum of the pulse train and is illustrated in Figure 3.10c, and an interline noise spectrum of a small TWT is shown in Figure 3.12. As has been shown in Chapters 1 and 2 interline noise degrades the performance of radars which use doppler signal processing. The causes and effects of interline noise are discussed fully in the next section.

The last type of noise generated by pulsed amplifiers is called interpulse noise and is generated between pulses when the amplifier is quiescent. It only occurs in d.c. operated tubes such as grid pulsed TWTs and cold cathode r.f. switched CFAs. The noise is produced by leakage currents flowing between the electrodes within the tube. If the tube is properly designed the noise produced is less than thermionic noise (< 110 dBm/MHz). In these circumstances this type of noise would not degrade the output spectrum of the tube. If this type of noise was significant it would have the effect of raising the general noise level of the output spectrum. A worse effect would be the degradation of the receiver noise figure of the radar set in which the amplifier was operating. During the interpulse period the receiver is turned on and noise generated by the amplifier would leak into the receiver via the duplexer and degrade the receiver noise figure and the sensitivity of the radar.

3.4.1 Sources of Interline Noise

Interline noise in a radar system is produced by a number of different sources amongst which are the power amplifier and its power supplies. These sources are made up of the following:

a. Noise and instability of the r.f. source oscillator in the system.

b. Time jitter of the r.f. pulse applied to the power amplifier, produced by instabilities in the timing and prf generating circuitry.

c. Random phase modulation produced by vibration of the waveguide components in the system.

d. Noise and ripple on the power supplies to the power amplifier.

e. The inherent noise generated by the power amplifier itself.

In general most of the interline noise in a system is introduced by the r.f. source oscillator. The next major contributors are the power amplifiers and their associated power supplies.

a. Noise introduced by the source oscillator

There are two types of oscillator which can be used in systems requiring low interline noise - the multiplier and the cavity controlled r.f. oscillator.

A multiplier consists of a crystal controlled master oscillator running at a frequency of 10-100 MHz which is multiplied to the required microwave frequency by either a varactor or step recovery diode multiplier. Both types of multiplier rely upon the very non-linear characteristics of the diodes to produce many harmonics of the fundamental crystal frequency. The required harmonic is filtered out to produce the microwave signal. Varacter diodes are less efficient at producing harmonics than step recovery diodes and several multiplier stages are needed with intermediate

amplifiers to achieve the required microwave frequency. The efficiency of the varacter multiplier is about $1/n^2$ where n is the multiplication ratio. The step recovery diode is a very much more efficient harmonic generator and only one multiplier stage is normally required. The multiplication efficiency can be as high as 30% if complex harmonic filtering is used.

The noise produced by a multiplier depends upon the stability of the master crystal oscillator and the multiplication ratio. The noise produced by the oscillator is enhanced by 6 dB per octave of multiplication. This is simply demonstrated as follows:

The ratio of noise sidebands to the carrier is expressed in the form:-

$$\left(\frac{V_{sb}}{V_c}\right)_{dB} = 20 \log \frac{\Delta f}{2fm}$$

Multiplication of the carrier frequency by a factor n has the effect of multiplying the frequency deviation by n. This raises the deviation by a factor n at the higher frequency and increases the sideband accordingly:-

$$\left(\frac{V_{sb}}{V_c}\right)_{dB} = 20 \log \frac{n\Delta f}{fm}$$

$$= 20 \log \frac{\Delta f}{fm} + 20 \log n$$

If n = 2 for a doubler then the sideband amplitude increases by 6 dB. To minimise this effect the master oscillator is made as quiet as possible and operated at the highest frequency which is practical to minimise the multiplication ratio needed. At low microwave frequencies (1-4 GHz) multiplier sources produce noise levels of 100 dB/Hz below the carrier

measured at 1 kHz from the carrier frequency. At higher microwave frequencies the noise produced increases at the rate of 6 dB per octave of multiplication. The crystal controlled multiplier also has good long term frequency stability, especially if the crystal oscillator is termperature controlled.

Low noise microwave oscillators can either use klystrons, transistors or bulk effect devices. At the lower microwave frequencies transistors predominate while at higher frequencies bulk effect devices or klystrons are used. The noise performance of all these devices is largely determined by the resonator cavity used to complete the oscillator. Bulk effect devices are particularly noisy and oscillators using these devices rely heavily upon the resonator cavity to obtain satisfactory noise performance.

Typically, the noise from a good microwave oscillator is about 80 dB/Hz below the carrier measured at 1 kHz from the carrier frequency. Noise as low as 90 dB/Hz has been measured in some cases.

At the lower end of the microwave frequency band the crystal controlled multiplier has the best noise performance and is used widely in radar systems. At higher frequencies the noise performance degrades below that of microwave oscillators due to the effects of the higher multiplication ratio. Generally in radar systems operating at high microwave frequencies microwave oscillators are used although these are frequently phase locked to a multiplied source with a very narrow band phase locked loop. This has the advantage that the microwave oscillator gains the long term stability derived from the low frequency crystal controlled oscillator whilst retaining its own superior noise performance. Another way in which microwave oscillators can be made with an improved noise performance is to operate them with a very high Q resonator. Blomfield [35] has constructed an L Band oscillator using a superconducting

lead plated cavity cooled to 4 ^{o}K. The cavity Q was measured as 10^{6} which is similar to that for a low frequency quartz crystal. The measured noise was 110-120 dB/Hz below carrier at 1 kHz from the carrier. The noise performance at frequencies very close to the carrier was also very good. This technique could well find application in systems provided the complexity of the cryogenic equipment could be accepted.

b. Time Jitter

Timing jitter can be a major contributor to the interline noise produced by a transmitter. Jitter is an imperfection of the modulation system of the transmitter where the edges of the pulses are displaced from their correct position with respect to one another in a periodic or random fashion.

Jitter can be caused in a number of ways. Radar systems which require accurate timing signals normally have a master crystal controlled oscillator from which all the timing and r.f. signals are derived either by multiplication or division. Jitter in the division circuitry is caused by random or periodic (eg power supply ripple) noise which introduces a certain timing error in the operation of the flip-flops used in such circuits. The effect is minimised by using clocked flip-flops where the actual timing of the switching of the flip-flop is controlled directly by the master oscillator. In this way the uncertainties in timing introduced by the divider are reduced to those introduced by only one element of the divider.

The second way in which jitter can be introduced on to the transmitted pulse train is by the modulator which pulses the transmitter amplifier. The pulse modulator can take one of four basic forms.

The most commonly used system is called the line type modulator where a delay line is discharged through the tube via a pulse transformer. The delay line is usually formed of an array of discrete inductors and capacitors and it is discharged through the tube by a thyratron or thyristor switch. The length of the pulse is very accurately determined by the line and is not likely to vary and produce jitter. The start of the pulse is determined by the firing of the switch and this is likely to introduce jitter. The thyratron switch is more likely to introduce jitter than the thyristor switch since it relies upon a gas discharge. This type of modulator will therefore introduce jitter in the pulse timing but not in pulse length.

A similar type of modulator is termed the 'hard tube modulator' where a vacuum tube is used to pulse the power amplifier. In this system the energy for the pulse is derived from a storage capacitor charged by a d.c. power supply. The timing and duration of the pulse are determined entirely by the vacuum tube so there is likely to be jitter in both pulse length and pulse timing. However the jitter produced by a vacuum tube is likely to be small.

The third method of modulating the tube is only applicable to low and medium power TWTs where it is practical to incorporate a control grid into the gun of the tube. The tube is supplied from a d.c. power supply with a suitable reservoir capacitor to supply the pulse current. The tube can then be switched on and off by means of a relatively low powered pulse applied to its grid. Like the hard tube modulator jitter in both pulse timing and pulse length is possible but again this is likely to be small for similar reasons.

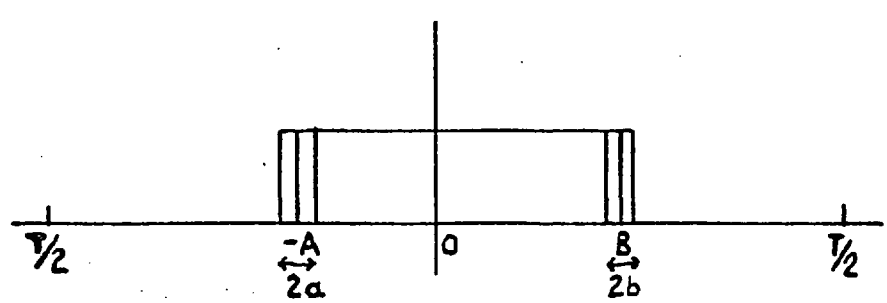
The last modulation method is only applicable to r.f. switched cold cathode CFAs the operation of which was described in Section 3.3. These run with a d.c. power supply and the tube is turned on by the effects of

the r.f. drive pulse. Beam shut-off is accomplished by pulsing part of the cathode positive to collect the rotating electron cloud. The start up jitter of these devices has been assessed by the manufacturers who state that this is less than 3 ns. There is also likely to be jitter of the trailing edge of the pulse introduced by jitter in the shut-off pulse modulator.

The r.f. switched CFA is then likely to introduce jitter into the front and back edge of the pulse. This is a complex interaction of both pulse timing jitter and pulse length jitter.

In this brief review of the various modulation systems that can be used to pulse power amplifiers, two types of jitter have been shown to occur to various extents. These are jitter in the pulse timing and jitter in the pulse length. In order to assess the contribution of jitter to the interline noise level of a pulse amplifier chain it is necessary to analyse the form and magnitude of the spectral contributions of these two types of jitter. This analysis is included in Appendix 1.

The analysis is generalised to include independent jitter on the leading and trailing edges of the pulses. For ease of analysis periodic jitter is considered and it is demonstrated that this is in fact the worst case condition from the point of radar performance. From this general analysis the effects of the ~~type~~ types of jitter of most concern can be derived.

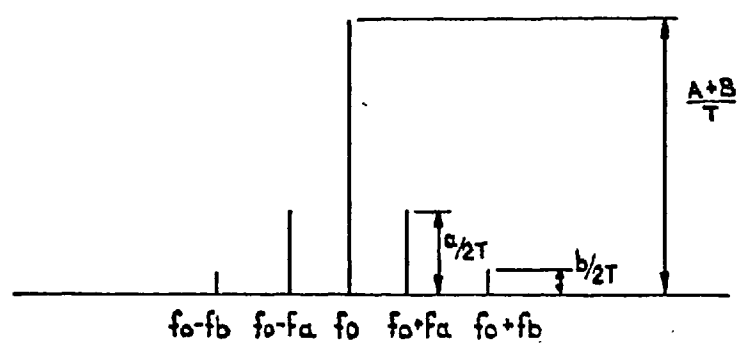


The above diagram represents one pulse, length A+B, of a pulse train with an interpulse period T. Periodic jitter, amplitude a and b is assumed to be present on the leading and trailing edges of the pulse respectively, of frequencies ω_a & ω_b.

The amplitude of the central spectral line of the pulse spectrum is given in Appendix 1 as:-

$$C_o = \frac{A+B}{T} + \frac{a}{2T}\left[e^{jw_at} + e^{-jw_at}\right] + \frac{b}{2T}\left[e^{jw_bt} + e^{-jw_bt}\right]$$

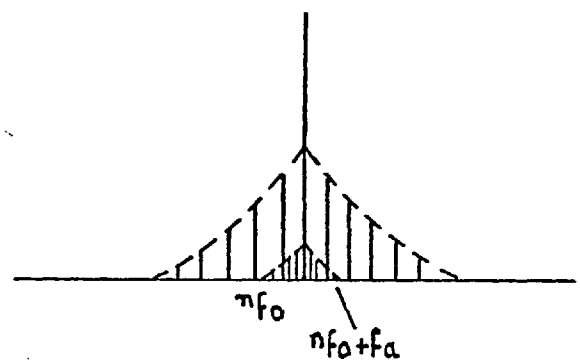
This equation represents 5 spectral lines. The first term (A+B)/T represents the amplitude of the fundamental line of the pulse spectrum and is unchanged by the jitter on the pulse. The other 4 terms represent 2 pairs of modulation lines spaced about the fundamental line, provided that the jitter amplitudes are small. The resulting spectrum would have the appearance shown in the diagram below.



The amplitude of the other spectral lines are represented by:-

$$C_n = \frac{1}{2\pi nj}\left[e^{jnwA}\sum_{m=-\infty}^{\infty} J_m(nwa)e^{jm(w_at+\pi/2)} - e^{-jnwB}\sum_{l=-\infty}^{\infty} J_l(nwb)e^{jl(w_bt-\pi/2)}\right]$$

Both of these terms represent an infinite series of lines spaced at their respective jitter frequencies with amplitude terms controlled by the Bessel functions. It is shown in the appendix that for a real situation where the jitter amplitude is small that the terms rapidly diminish as m or l increases. The n^{th} spectral line would then take the form shown in the diagram below:-



The combined effects of leading and trailing edge jitter may be used to examine the effects of pulse position and pulse length jitter.

For pulse position jitter it is shown in Appendix I that there are no lines modulating the fundamental although there are lines about all the other harmonics of the PRF. This is a very interesting result since in a pulse doppler radar the clutter filter pass bands are situated on either side of the fundamental PRF line. Their pass bands extend to half way between the fundamental and first PRF line. Consequently modulation on the fundamental line is of greater importance than modulation on other PRF lines. Because pulse position jitter does not introduce lines about the fundamental this type of jitter is of less importance to the system.

Pulse length jitter will take a similar form to that caused by leading and trailing edge jitter and will produce lines about the fundamental.

It is now convenient to insert some values into these equations to determine what amplitudes of jitter can be tolerated by a system.

Suppose that the pulse length A+B = 5 μs, the PRF = 10 kHz, and that the required interline noise level is 100 dB below the fundamental.

For pulse length jitter the amplitude of the largest modulation line about the fundamental is given by:

$$\frac{a}{2T}$$

where a is the time jitter.

The amplitude of the fundamental line is:

$$\frac{A+B}{T} = \frac{5 \times 10^{-6}}{10^{-4}} = 5 \times 10^{-2}$$

Now the ratio of the modulation line to the fundamental must be 10^5 to achieve a 100 dB interline noise level. So:-

$$\frac{a/2 \times 10^{-4}}{5 \times 10^{-2}} = 10^{-5}$$

$$\text{giving } a = 10^{-10} \text{ seconds}$$

So to achieve the required level of interline noise of 100 dB the pulse length jitter should not be more than 100 ps. This is a very stringent requirement and very careful design of the transmitter modulator is needed to achieve such low levels of jitter.

The analysis given in Appendix 1 also includes the effects of multiple frequency jitter and random jitter but it is shown qualitatively that these would not produce worse effects than periodic jitter.

c. Phase Modulation due to vibration of Waveguide components

Vibration of the waveguide run may give rise to phase modulation of the microwave signal. There are many different ways in which a length of waveguide can be vibrated and certain assumptions and simplifications must be made. Firstly there are two dimensions that can influence the propagating characteristics of a length of waveguide. These are its broad wall dimension which determines the guide wavelength, its length, which determines the phase shift between its ends. Any vibration which changes either of these dimensions will produce modulation on the signal carried by the waveguide.

Both modes of vibration have been analysed in Appendix 2. The vibration levels have been calculated that will produce interline noise of 100 dB below the fundamental line of the pulse spectrum. Vibration of the broad wall dimension of L Band waveguide WG6 must not exceed 0.18 μm, and vibration in length of the waveguide must not exceed 4.4 mm per metre length. Although vibration of the broad-wall of the waveguide must be so small this mode of vibration is unlikely to be severe because of the stiffness of the waveguide in this dimension. Vibration in length due to flexing is a much more likely mode and fortunately the modulation produced is very low for quite high levels of vibration.

d. Noise produced by instabilities in the power supplies to the power amplifiers

Both the travelling wave tube and the crossed field amplifier are sensitive to changes in their supply voltages. Each type of tube will require several supplies to different electrodes (eg main HT voltage,

heater supplies - grid bias etc) and variation in each of these supplies will modulate the r.f. signal to a greater or lesser extent. In general the TWT is very much more susceptible to power supply instabilities than the CFA. The beam voltage which controls the velocity of the electron stream has the greatest effect on the r.f. signal since any variation in beam voltage produces a corresponding variation in the beam velocity which alters the phase shift through the tube.

If ϕ_o is the total phase shift through the tube then

$$\phi_o = \frac{wd}{v_B}$$

where d is the length of the tube

w is the angular frequency

and v_B is the beam velocity.

If V_o is the accelerating voltage

then $e V_o = 1/2\ m v_B^2$

so $v_B = \sqrt{\frac{2e}{m} V_o}$

and $\phi_o = \frac{wd}{\sqrt{2\ e/m}} \quad \frac{1}{\sqrt{V_o}}$

$$\frac{\Delta\phi_o}{\Delta V_o} = -1/2 \frac{wd}{\sqrt{2\ e/m}} \quad \frac{1}{V_o^{3/2}}$$

$$= -1/2 \frac{wd}{\sqrt{2\ e/m}} \quad \frac{1}{V_o\sqrt{V_o}}$$

$$= -\frac{\phi_o}{2} \quad \frac{1}{V_o}$$

so $\frac{\Delta\phi_o}{\phi_o} = -\frac{1}{2} \frac{\Delta V_o}{V_o}$

This equation applies to TWTs and gives results which agree quite well with measurements on real tubes. Consider a high gain TWT with a total phase length, ϕ_o, of 50 wavelengths and operating at a beam voltage of 40 kV.

$$\phi_o = 50 \times 360 \text{ degrees}$$

$$\frac{\Delta V_o}{V_o} = 0.01 \text{ for a 1\% change in beam voltage}$$

$$\therefore \quad \Delta\phi_o = -\frac{50 \times 360}{2} \times 0.01$$

$$= 90 \text{ degrees per 1\% change in } V_o$$

The sensitivity to beam voltage quoted by the manufacturers of such a TWT is 120 degrees per 1% change in V_o - quite good agreement.

A similar expression can be derived for CFAs.

$$\text{Again } \phi_o = \frac{wd}{v_B}$$

$$\text{but } v_B = \frac{V_o}{rB}$$

where r is the line-cathode spacing

and B is the transverse magnetic field

$$\text{and } \phi_o = \frac{wdrB}{V_o}$$

$$\frac{\Delta\phi_o}{\Delta V_o} = -\frac{wdrB}{V_o^2}$$

$$= -\frac{\phi o}{V_o}$$

$$\text{so } \frac{\Delta\phi_o}{\phi_o} = -\frac{\Delta V_o}{V_o}$$

A CFA with a similar power output to the TWT previously discussed might have a phase length, ϕ_o, of 10 wavelengths so

$$\phi_o = 10 \times 360 \text{ degrees}$$

$$\frac{\Delta V_o}{V_o} = 0.01 \text{ for 1\% change in } V_o$$

$$\therefore \Delta\phi_o = -10 \times 360 \times 0.01$$

$$= 36 \text{ degrees per 1\% change in } V_o.$$

In practice however such a CFA would only produce a phase shift of about 5 degrees per 1% change in beam voltage. This difference is due to the very complex nature of the crossed-field interaction which introduces what can be described as "phase-locking" which improves the phase stability.

The beam voltage is generally the only supply to a CFA apart from the heater which has little effect on the phase characteristics. The TWT needs several other supplies if it is grid modulated. The heater can also influence the phase characteristics but only to a limited extent. Because the control grid of a grid pulse TWT is close to the cathode and in a region where the electron beam is still accelerating the grid voltage can have a substantial influence over the final beam velocity and hence the phase characteristics. A typical value of phase change with grid voltage would be 5^o/volt, which represents about 2^o per 1% change in grid voltage. The grid voltage is normally about 250 V with respect to the cathode. This figure is less than the corresponding sensitivity to changes in beam voltage but is sufficiently high to require careful stabilisation of the voltage on the grid.

Again it is of interest to determine the stability required of the power supplies for a low interline noise level. The characteristics of phase modulation of a pulsed microwave signal have been calculated ~~in Appendix 7 where it is~~ * it can be shown that for a system requiring an interline noise level of -100 dB the maximum single frequency phase ripple that could be tolerated is 0.01 degrees peak to peak. For a TWT the sensitivity to beam voltage variation is approximately 100^{o} per 1% change in beam voltage. To stabilise the phase ripple to 0.01^{o} requires a stability of one part in 10^{6} in beam voltage or 40 mV in 40 kV for a typical TWT. The CFA, however, because of its superior phase characteristics will only require a voltage stabilised to one part in 10^{4} or one volt in 10 kV, a much easier task.

The effects of electrode voltage changes on the amplitude of the signal produced by either a TWT or a CFA will be less than the phase modulation. This is because both types of amplifier are run saturated and little variation in amplitude can occur. The amplitude modulation that occurs is generally about an order lower than the phase modulation produced.

e. Noise generated by the power amplifier

A great deal of work has been done to investigate and improve on the noise performance of low power receiver TWTs but no work has been done on high power tubes. Apart from broad-band noise which is easily measured using conventional techniques no measurement of the close to carrier noise of TWTs or CFAs has been made using equipment sensitive enough to detect the noise generated by the tubes themselves. The measurements described in Chapter 6 show that the noise from TWTs is lower than

120-130 dB/Hz below one spectral line and this is unlikely to cause any degradation in system performance. CFAs however produce very much more noise and would not be acceptable for some systems.

The theoretical aspects of noise generation in both TWTs and CFAs is very complex and will not be dealt with in any greater detail in this work which is mainly concerned with the measurement of the noise generated.

CHAPTER 4

THE EXPERIMENTAL TRANSMITTER

The two-stage transmitter on which the measurements which are described in Chapter 6 were performed was built as part of an experimental pulse doppler radar. The advantage of this type of radar is its excellent performance in a dense clutter environment as described in Chapter 1. The penalties paid for this advantage are the complexity of the receiver, the stability required from the transmitter system and problems associated with the computer programming. The experimental radar was built in order to evaluate the performance of a pulse doppler radar and to investigate the extent to which these penalties are serious.

4.1 The Experimental Radar

The radar was required to detect airborne targets of down to 4 m^2 echoing area at ranges out to 150 km and moving at speeds up to Mach 3. The angular accuracy of the radar had to be better than 0.5° which limits the aerial beamwidth to 2°. The clutter peaks expected were likely to be 90 dB above the receiver noise level and ideally the clutter cancellation of the radar should have approached this value. Since this was thought impractical at the time a figure of 70 dB was chosen.

Because of physical limitations to the size of the aerial the lowest radar band that could be used, whilst retaining the angular resolution, was L band (approximately 1200-1400 MHz). At higher frequencies the aerial would be smaller and easier to install. The measurement of a target velocity was chosen to be unambiguous which means that the P.R.F. and therefore the spacing between the spectral lines of the radiated sin x/x spectrum must be greater than the maximum doppler-shifted target return expected. For a target moving at 900 m/s (Mach 3) the doppler shift at 1200 MHz given by $f_D = \frac{2\ Vr}{\lambda}$ is 7200 Hz. At higher radar frequencies the doppler shift increases. Since the P.R.F. of the radar determines the maximum unambiguous range it is desirable to keep it as low as possible (ideally below 900 Hz for 150 km range). It is obvious that because of the aerial size limitation some compromise must be made between velocity and range ambiguities and the frequency of transmission. For this experimental radar the frequency chosen was the lowest possible, 1200 MHz, and the measurement of velocity was made to be unambiguous. This results in a P.R.F. of 8600 Hz, giving an unambiguous range of 17.4 km with 8 range ambiguities out to the 150 km range desired. These ambiguities would be resolved by changing the P.R.F. by up to 10% during the time the aerial beam was moving past the target.

The mean power of the radar was determined by the target echoing area and the maximum range and is approximately 2-3 kW. The pulse length determines the resolution in range and also the number of range gates and receiver channels as described in Chapter 1. For this radar a pulse length of 5 μs was chosen resulting in 27 range channels. The combination of pulse length, P.R.F. and mean power determined the peak power of approximately 100 kW. These parameters were also influenced by the choice of microwave power amplifiers available 'off-the-shelf'.

TABLE 4.1

MAIN PARAMETERS OF EXPERIMENTAL RADAR

Frequency	-	L-band.
Peak Power	-	5 kW or 100 kW.
Pulse length	-	5 μs
Duty cycle	-	Up to 5% at 5 kW.
		Up to 3% at 100 kW.
P.R.F.	-	8.6 kHz ± 10% at 5 kW.
		4.3 kHz ± 10% at 100 kW.
Aerial Beamwidth	-	4° or 2°.
Aerial gain	-	32 dB.
Aerial rotation rate	-	30 r.p.m.
Receiver noise figure	-	10 dB.
Receiver	-	Range gated with 27 range bins.
Data Handling	-	Elliott 920C computer, 16 K Store.
Display	-	Synthetic TV type display updated and refreshed by the 920C.

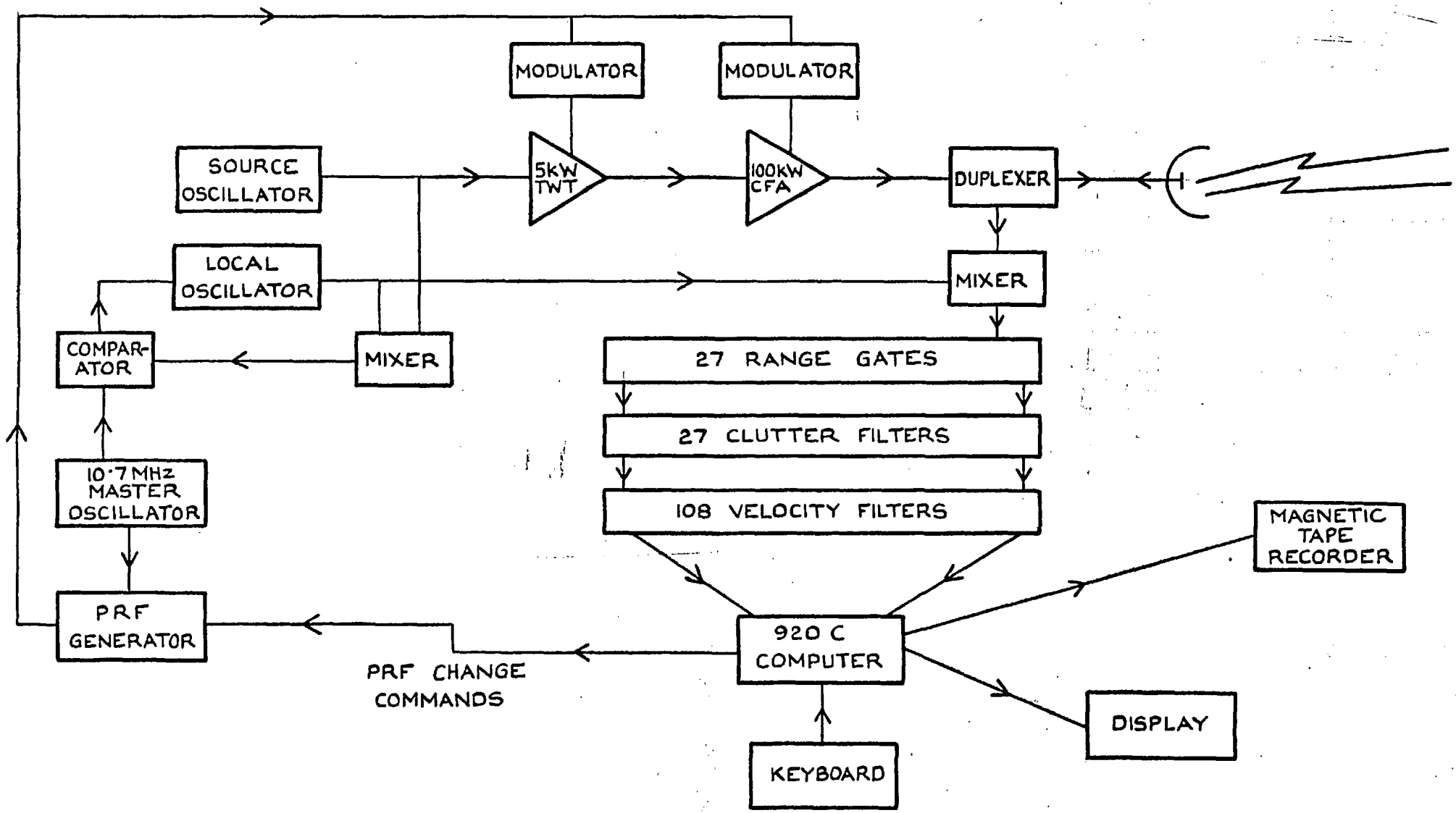


FIG. 4·1 BLOCK DIAGRAM OF THE EXPERIMENTAL RADAR

The main parameters of the radar are summarised in Table 4.1 and Figure 4.1 shows a block diagram of the complete radar. The radar can be broken down into a number of sub-systems as follows:-

(a) The frequency generation equipment;

(b) The transmitter, duplexer and aerial combination;

(c) The receiver;

(d) The timing circuits;

(e) The data handling and control computer.

Each of these sub-systems is briefly described except for the transmitter which is described in detail since all the work described later in this thesis was done using this transmitter.

(a) The Frequency Generation Equipment

The radiated signal is generated by a free running L-band oscillator producing about 200 mW which is sufficient to drive the first stage amplifier of the transmitter. The local oscillator is derived from this signal by phase locking a similar oscillator displaced upwards in frequency by 10.7 MHz using a crystal controlled oscillator to produce the 10.7 MHz signal. The microwave oscillators were specially selected for their good noise performance of 90 dB/Hz below the carrier at 3 kHz from the carrier frequency. The free running oscillator has now been replaced by a multiplier using a crystal controlled oscillator as its source. This improved the noise level by 15 dB.

(b) The Transmitter, Duplexer and Aerial

The transmitter consists of a two-stage coherent amplifier. The first stage is a travelling-wave tube with 47 dB gain producing 5 kW peak power output. The second stage is a crossed-field amplifier with 13 dB gain and an output power of 100 kW peak. Both amplifiers need very stable power supplies in order to achieve the low interline noise levels required. These tubes and their power supplies are described fully in the following sections.

The duplexer used is a balanced, twin TR cell duplexer designed to have a short recovery time following the transmitter pulse. A pin diode attenuator is used to further attenuate any leakage through the duplexer that might damage the front end of the receiver.

Two aerials have been used with the radar. The first was a simple parabolic dish with a coaxial probe feed giving a pencil beam with a beamwidth of 4°. This aerial was limited to operation at a peak power level of 5 kW. The second aerial was designed for operation at 100 kW and consisted of an end-fed array. This gave a fan beam with 20° beamwidth in elevation and a 2° beamwidth in azimuth.

(c) The Receiver

The front end of the receiver is a mixer translating the received signal to the first i.f. frequency of 10.7 MHz. After amplification the i.f. signal is mixed down to 1.6 MHz. At this point the signal is passed into 27 separate identical receiver channels via 27 range gates. Range gating is required to retain the range information which is destroyed by the narrow band clutter filters. The clutter filters are tailored to fit

between two spectral lines of the transmitted pulse spectrum and pass only one spectral line of any doppler shifted target echo. The range of the target is determined by the pulse timing which is destroyed by the clutter filter since the single spectral line accepted approximates to c.w.

The range gates open and close sequentially after the transmitted pulse and effectively pass only those target echoes from a particular range into any one receiver channel. All signals in any one receiver channel therefore come from targets at the same range or from one of the outer range ambiguities. Clutter filters follow the range gates and any clutter echoes are rejected. Target echoes are shifted in frequency due to the target's motion relative to the radar and are passed through the filter.

Following the clutter filters the signals in each channel are again mixed to a lower frequency, in this case 10 kHz, where further filtering is done by a bank of 4 narrow band velocity filters. These give a crude measurement of target radial velocity. Each of the 108 outputs of the receiver bank is passed through a threshold detector and coded for transmission via an interface to the data handling equipment.

Although the receiver is complicated many of the circuits are duplicated which helps to reduce the cost. Problems do arise however in attempting to match the gains of the channels which must be identical to one another. In this experimental system the channels were individually matched and rechecked periodically. In a developed system automatic gain control would have to be used.

(d) The Timing Circuits

All the timing pulses throughout the system are derived from a master crystal-controlled oscillator. This is counted down using clocked J-K flip flops to derive the trigger pulses. To minimise the jitter between pulses the number of gates following a clocked counter was reduced to one.

(e) The Data Handling and Control Computer

Information from the 108 receiver outputs, the aerial bearing encoders and the P.R.F. generator is passed to an on-line Elliot 920C computer via an interface unit. When a target is detected in any of the receiver channels all the information on the target such as apparent range, bearing and velocity is passed to the computer and the 'housekeeping' program is interrupted. The computer will immediately process the data and if necessary order a P.R.F. change to measure the true range of this target. The entire operation is completed during the time the aerial beam is scanning through the target (approximately 22 ms for a 4° beamwidth and a rotation rate of 30 r.p.m.). Between target detections the computer provides information to a synthetic display which includes an alpha-numeric tote for displaying target information at the control of a rolling ball marker and a keyboard. The keyboard can also be used to change the mode of operation of the radar, depending upon the type of program used.

Some photographs of the radar are included to indicate the general scale of the hardware involved. The transmitter and receiver are housed in two separate screened, air-conditioned cabins which are linked together by a removable lobby. To move the radar to a new site the lobby is removed





FIG. 4·2

GENERAL VIEW OF THE RADAR SET & OF THE TRANSMITTER CABIN

and each cabin can then be transported on a low-loading truck. A third, smaller, cabin houses a motor generator providing a 400 Hz 3-phase supply for the transmitter and a recirculating, purified water cooling system for the transmitter tubes. The aerial system is demountable and only requires a prepared reinforced concrete raft for installation on a new site.

4.2 The Power Amplifiers

The stability requirements imposed on the transmitter by the clutter suppression needed determines the tube types that can be used. Experience with c.w. doppler radars has shown that linear beam tubes are more likely to give adequate noise performance. Crossed-field amplifiers have always been regarded as inherently noisy devices but little was known about their noise performance close to the carrier frequency. When this radar was first envisaged the choice of tube lay between a TWT/CFA combination or a single klystron amplifier. Doubts existed about the CFA noise performance. However, the klystron is not capable of operating over the bandwidth required for certain experiments and so it was decided to use the TWT/CFA combination. It would be possible to do many of the experiments using the TWT alone if the CFA proved too noisy. It would also be possible to evaluate the CFA which was of a new type, untried in the UK.

(a) The 5 kW Travelling-Wave Tube

This tube is a VA 133G manufactured by Varian-Associates. It is a grid-pulsed, periodic-permanent-magnet focused, TWT. It has a saturated gain of 47 dB and a peak power output of 5 kW at a maximum duty ratio of 6%. The slow wave structure is a helix-derived circuit with an operating band-

width of 1250-1350 MHz. The tube operates from a 10 kV d.c. power supply and is switched with only a few hundred volts applied to the grid. The efficiency is only about 20% and the tube requires water cooling. A data sheet is included in Appendix 3.

(b) The Crossed-Field Amplifier

This is a Raytheon tube, type QKS 1319, capable of generating 100 kW peak power at a duty ratio of 3% over the frequency band of 1250-1350 MHz. The tube is a forward wave, re-entrant beam device. The cathode is made of beryllium with a surface layer of beryllium oxide which has a high secondary emission coefficient of 4. The tube is operated with the cathode cold and the h.t. voltage of 10 kV applied continuously. When the r.f. drive is applied it ionises the residual gas particles. These ions move in cycloidal paths under the influence of the crossed electric and magnetic fields and bombard the cathode producing many secondary electrons. These in turn bombard the cathode and full conduction builds up within a few nanoseconds. Interaction then occurs between the orbiting electron cloud and the r.f. wave on the slow wave structure. At the end of the r.f. drive pulse a section of the cathode, opposite the drift space, is pulsed to a positive potential of 9 kV with respect to the cathode and this gathers up the electron cloud. The tube is then quiescent until the next r.f. drive pulse. A fuller description and a schematic diagram of the tube was given in Chapter 3.

The tube only requires a simple low power modulator to provide the turn-off pulse and a 10 kV d.c. power supply and energy storage capacitor. This simplicity combined with a conversion efficiency of 50% and the small size of the tube enables a very compact transmitter to be made. A data sheet on the CFA is included in Appendix 3.

4.3 Power Supply Stability Requirements

(a) The Travelling-Wave Tube

Linear beam devices, because of their long electrical length, have phase characteristics which are sensitive to beam voltage. Typically the VA 133G exhibits 0.3 degrees phase shift per volt change in beam voltage. This sensitivity imposes a very stringent stability specification on the tube power supplies. In order to achieve the sub-clutter visibility required, the phase ripple from pulse to pulse must be less than 0.01 degrees which represents a beam voltage ripple of less than 50 mV in 10 kV - a stability of 5 parts in 10^6. This is extremely difficult to achieve and requires elaborate stabilising and filtering circuits. The other tube supplies for the grid bias and heater must also be stabilised.

(b) The Crossed-Field Amplifier

In general CFAs are not as phase sensitive to beam voltage as t.w.ts. This is partly due to their short electrical length and partly due to their mode of operation. A typical sensitivity for the QKS 1319 is 0.01 degrees phase shift per volt change in beam voltage; over an order of magnitude better than linear beam devices. In order to meet the phase ripple specification the power supply stability need only be 1 part in 10^4, which is relatively easy to achieve. However, it was likely that the CFA would generate excessive noise although cold cathode devices were thought to be much quieter than other CFAs.

4.4 The Design of the 5 kW Transmitter

A simplified circuit diagram of the 5 kW transmitter is shown in Figure 4.3. The 10 kV d.c. beam supply is stabilised by a conventional hard tube series stabiliser. The error signal for the stabiliser is generated by a differential amplifier which compares the output from a resistor divider across the 10 kV line with a reference voltage derived from a temperature-compensated chain of zener diodes. This error signal is then amplified and used to drive the series stabiliser tube. The stabiliser had to be capable of operating with a pulsed load and maintain good stability from pulse to pulse whilst relying on an energy storage capacitor to supply the pulse current. Care had to be taken with the design of the stabiliser to prevent 'lock-up'. If the damping of the response is less than critical the output voltage will overshoot its set value and the excess charge in the capacitor can only leak away through the resistive divider. This means that the output will not stabilise to the correct voltage before the next pulse. This problem was met and overcome by correctly compensating the response of the amplifier. The final stability of the power supply was better than 5 parts in 10^5 and although worse than that desired it was not the limiting factor on radar performance.

The TWT is grid pulsed and the d.c. supplies for the hold-off bias and pulsing circuits must also be stabilised. The grid bias voltage of -150 V with respect to the cathode is supplied from a commercial power supply which is floated up on the -10 kV h.t. supply. The power supply is fed via a 1:1 isolating transformer. A similar principle is used to generate the d.c. heater current for the TWT. To turn the TWT on, a 300 V pulse is applied to the grid to overcome the bias and raise the grid to +150 V with respect to the cathode. This pulse is generated by a

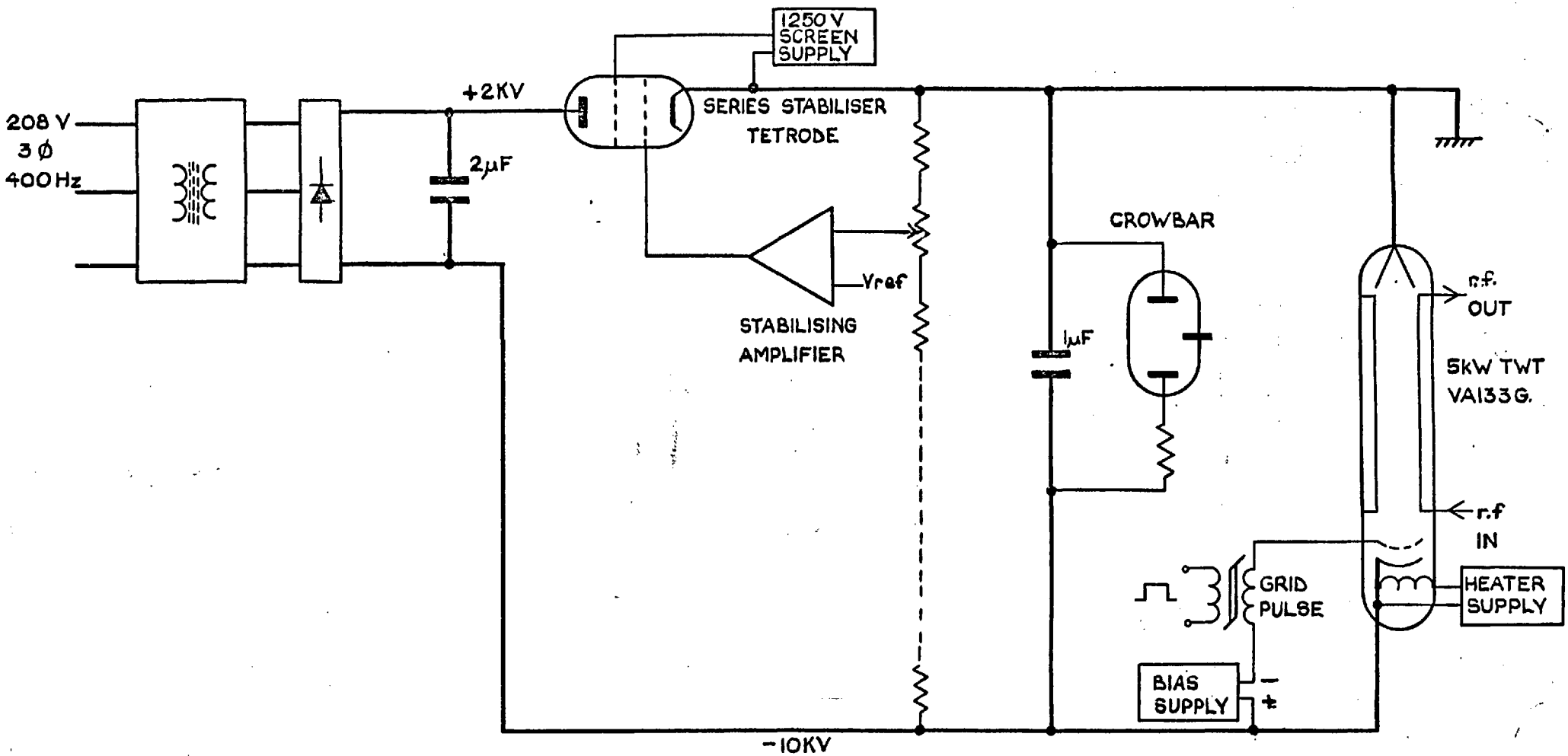


FIG. 4·3
SIMPLIFIED CIRCUIT DIAGRAM OF 5kW TRANSMITTER

transistor switch and fed to the grid via a pulse transformer. The transformer steps up the voltage pulse to the required value and provides the necessary 10 kV isolation between the grid circuitry and the pulse generator which is at ground potential. The effects of amplitude variation and droop on the grid pulse are eliminated using the simple clipping circuit shown on the diagram. This derives its reference voltage from the stable 10 kV supply. The rise and fall time of the grid pulse is not critical since the r.f. drive is gated by a PIN diode switch and 'nested' within the current pulse. However, it is preferable to keep the grid pulse rise time to less than 0.25 μs to improve the efficiency of the system.

4.5 The Design of the 100 kW Transmitter

A simplified circuit of the power supplies for the CFA is shown in Figure 4.4. The 10 kV d.c. supply in this case is generated by an entirely novel method. One of the most difficult problems in designing a stable high voltage power supply of moderate proportions is minimising the size of the step-up transformer. Another problem is stabilising the h.t. voltage, which usually entails using high power hard tubes with their associated bias and heater supplies. Both problems are overcome by utilising the approach used in this transmitter. The 3-phase a.c. mains is rectified directly without a bulky isolating transformer and the raw d.c. is smoothed and stabilised using a water cooled, high current transistor stabiliser. This stable d.c. at about 200 V is then chopped by 8 parallel thyristor inverters running at a chopping frequency of approximately 10 kHz and locked to a multiple of the P.R.F. of the radar system. The chopped waveform is transformed to 1.25 kV and rectified in each of the 8 inverters. The outputs of all the inverters are connected in series and fed to the energy storage capacitor and the CFA. Because the transformation is done at a frequency

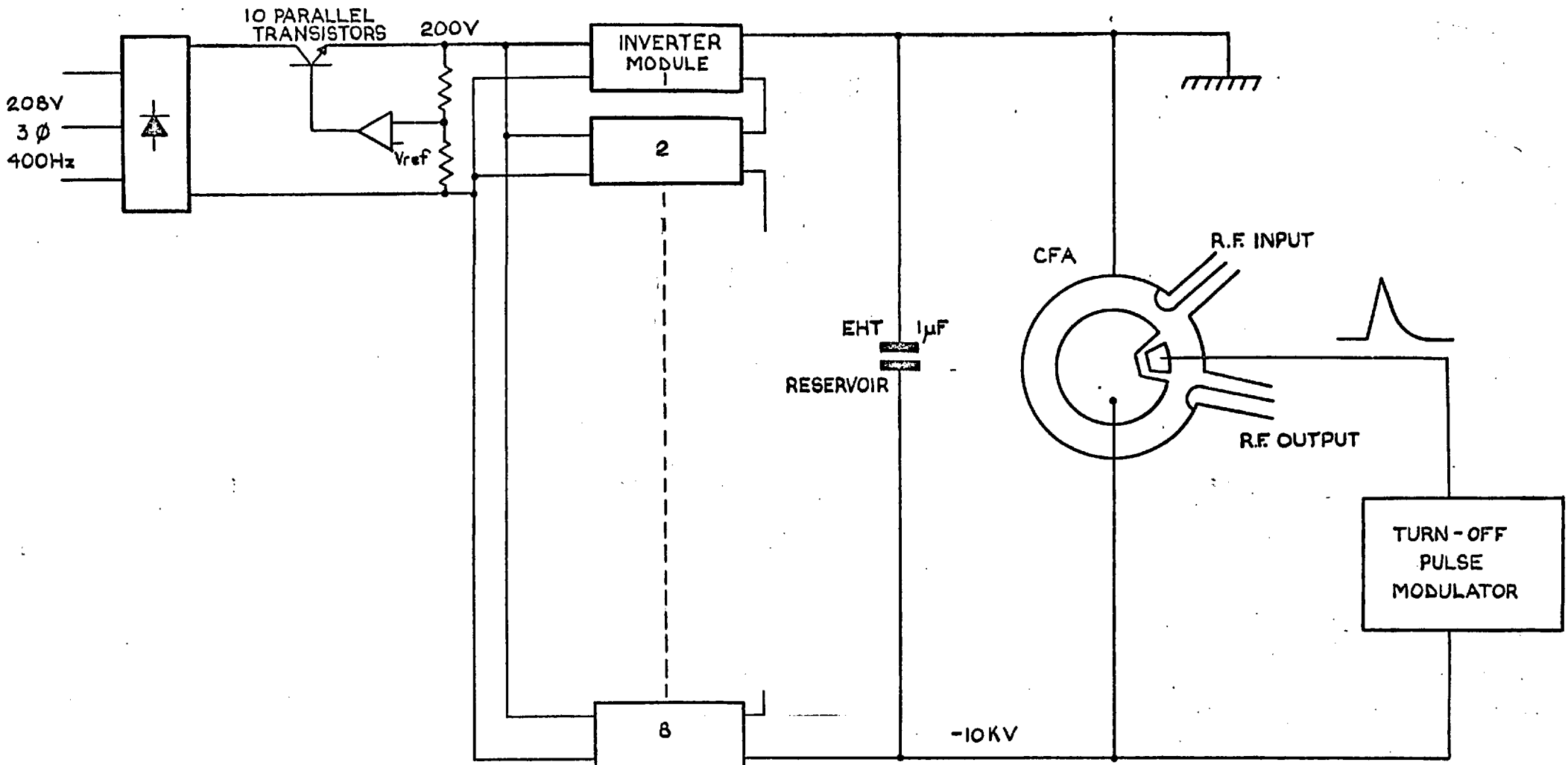


FIG. 4·4
SIMPLIFIED CIRCUIT DIAGRAM OF 100kW TRANSMITTER

of 10 kHz the transformers are very compact and the bulk of the complete power pack is reduced. The second advantage is that the stabilisation is done at low voltage and high current where transistors can readily be used. The inversion process will not produce noise between the spectral lines since the inversion frequency is locked to a multiple of the P.R.F. and any modulation line produced will coincide with a P.R.F. line.

The success of this type of circuit depends upon the availability of fast thyristor switches. At the time when this transmitter was designed only relatively low power thyristors existed (Mullard type BTX 64-600R) and it was necessary to use a number of parallel inverters to handle the power required. The state-of-the-art in thyristor design has now advanced to the extent that inverters of up to 50 kW power output and chopping at frequencies as high as 50 kHz are being designed.

The inverter power supply described here is capable of delivering up to 8 kW of mean power with a stability of 1 part in 10^4 over the doppler frequency band of interest (400 Hz-10 kHz).

The second major component of the transmitter is the modulator for supplying the beam quenching pulse to the turn-off electrode of the CFA. This pulse must have an amplitude of 8-10 kV and work into a load of 400 Ω in parallel with the electrode to ensure that the pulse is not loaded down by the tube impedance which is somewhat more than 400 Ω. To ensure a clean cut-off the rise-time of the pulse must be less than 100 ns. Turn-off is usually accomplished with 150 ns and the pulse width is designed to be 300 ns to allow some margin for error in setting up the exact position of the pulse with respect to the r.f. drive pulse.

A simplified circuit of the turn-off modulator used in the 100 kW transmitter is shown in Figure 4.5. This is a modified form of a standard

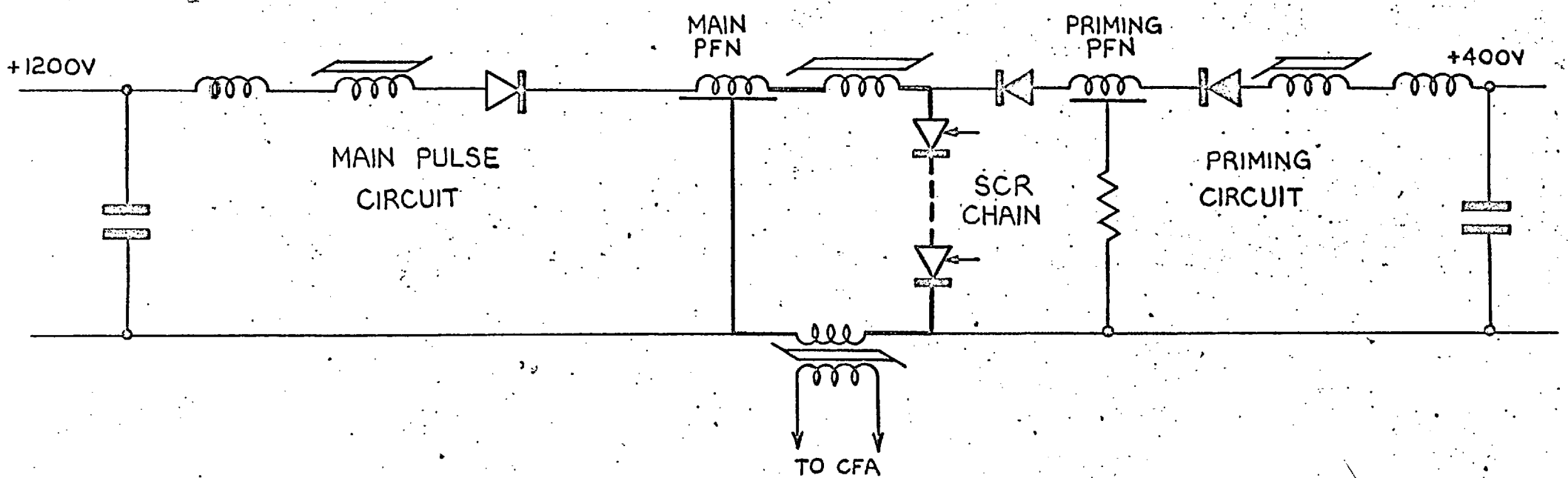


FIG 4·5
SIMPLIFIED CIRCUIT OF THE CFA TURN OFF MODULATOR

line type modulator widely used in radar transmitters. The most significant difference is the use of a stack of thyristors as the switching element in place of the conventional hydrogen thyratron. The thyristor can switch on with very much less jitter than a thyratron which is one of the reasons it was chosen since in this application jitter of the back edge of the r.f. pulse could cause very high levels of interline noise. The thyristor is also small and does not require any heater, reservoir or bias supplies. The very fast rise-time of 100 ns places a di/dt rating of 1600 A/μs on the thyristors and since they will not normally turn-on at this rate a special circuit technique known as 'priming' has to be used to overcome the problem. To prime a thyristor it is initially switched on and passes a low current pulse which conductivity modulates the device and increases the area in conduction so lessening the local loss when the main current pulse is passed. The main current pulse must be delayed during priming and this is done using a saturable reactor. The iron core of the saturable reactor has a square BH loop and will saturate very sharply. The impedance changes from a very high to a very low value in a few nanoseconds. Figure 4.5 shows a simplified circuit of the turn-off modulator and shows the priming arrangements. When the thyristors are switched on the main pulse forming network tends to discharge through the thyristors, saturable reactor and load. However, the saturable reactor presents a high impedance until it saturates and will only pass a small current, its magnetising current. The reactor is arranged to saturate after about 1 μs and the main pulse forming network will then discharge through the load. During this delay time the priming pulse forming network will discharge through the stack of thyristors and open up the conducting area within the devices. The priming current is about 20 A. This system is very effective and rise-times of 100 ns are readily achieved, limited only by the inductance of the circuitry which is primarily that of the saturated saturable reactor. The quality and 'squareness' of the BH

loop of the core material for the saturable reactor are important factors in obtaining optimum performance.

Typical waveforms showing the r.f. drive pulse, CFA current pulse and the action of the turn-off pulse are shown in Figure 4.6.

Great care has to be taken to protect the power tube since it costs more than £10,000 and delivery is in excess of 9 months. The power supplies and cooling supplies are fully interlocked and the h.t. voltage is removed from the tube should any of them fail. In addition the tube must be protected from its own malfunctions such as arcs and failure to turn-off after a current pulse. If the tube arcs internally all the energy in the pulse reservoir capacitor will be dumped in the tube which could cause considerable damage by spluttering copper from the slow wave structure onto the cathode or ceramic insulator. To protect the tube a 20 Ω resistor is placed in series with the tube to limit the arc current and a sensing circuit triggers a triggerable spark gap which crowbars the capacitor within 5 μs of the tube arc. If the tube should fail to turn-off after a current pulse, either through failure of the turn-off pulse modulator or misposition of the turn-off pulse, then the tube will continue to conduct and overheat. Again this condition is sensed by a monitoring circuit which also triggers the spark gap and crowbars the capacitor.

The interlock and control system is fairly complex and forms a significant fraction of the transmitter.

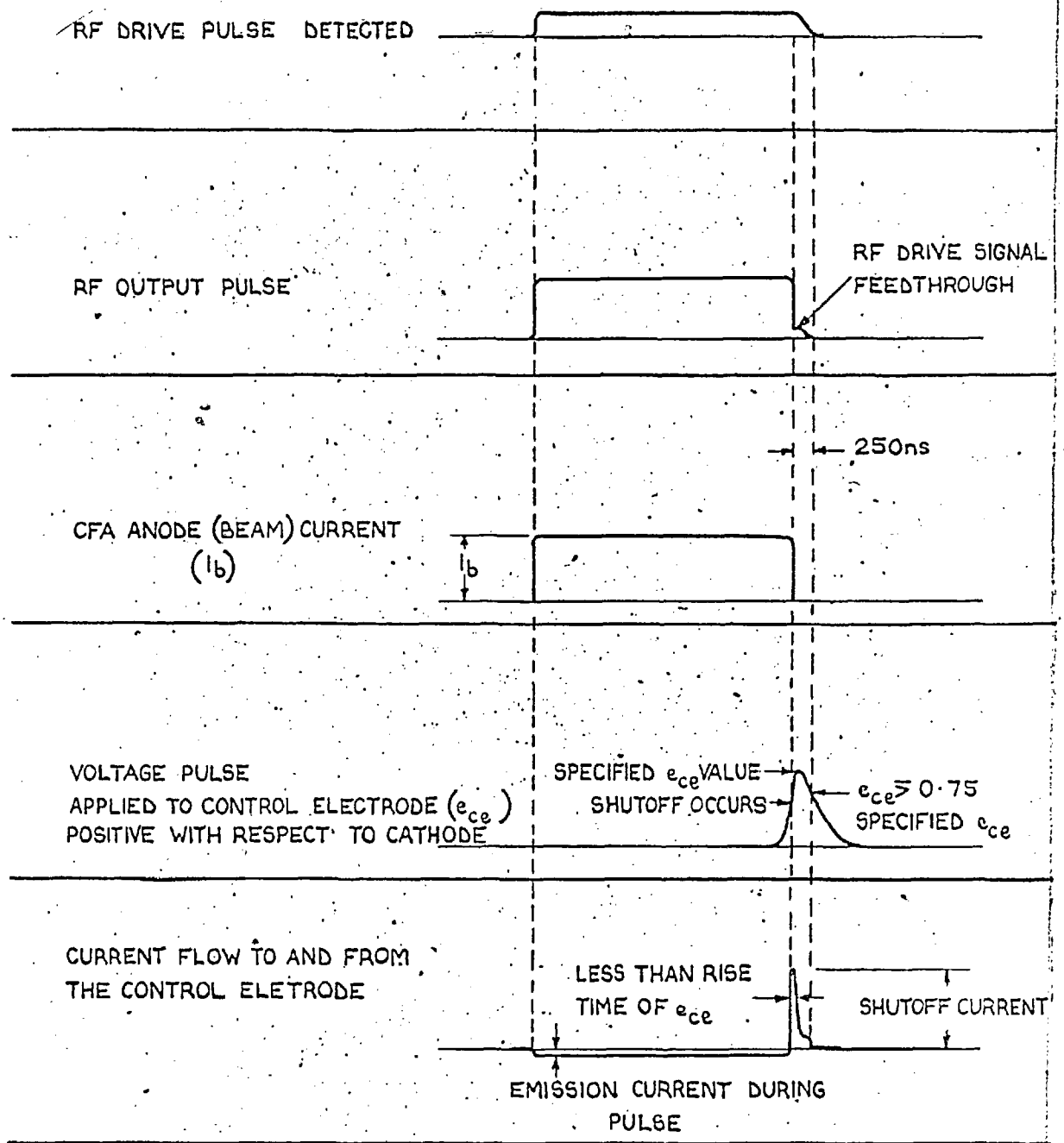


FIG. 4·6
TYPICAL WAVEFORMS DEMONSTRATING THE ACTION
OF THE TURN-OFF PULSE

CHAPTER 5

THE NOISE MEASURING SYSTEM

The pulse doppler radar described in the previous chapter was designed to detect moving targets approaching with radial velocities in the range 100-2000 knots and to attenuate clutter echoes by 70-80 dB. At the frequency of 1300 MHz forced upon the radar by the combination of aerial size and range ambiguities the doppler shift for these targets will lie in the range of 400 Hz to 8 kHz from the transmitted frequency. The P.R.F. of 8.4 kHz was chosen to make the measurement of velocity unambiguous. Only a coarse measurement of target velocity was attempted using filters with a bandwidth of 1 kHz. These factors all combine to define the permitted levels of interline noise produced by the transmitter.

The clutter attenuation of 80 dB and the final detection bandwidth of 1 kHz set by the velocity filters required a maximum level of interline noise of 80 dB/kHz relative to the central P.R.F. line of the pulse spectrum. This is equivalent to 110 dB/Hz assuming the noise to be evenly distributed over the 1 kHz band. If the interline noise transmitted exceeds this level then the noise will modulate high clutter echoes and be detected as targets after passing through the velocity filters.

In the radar system the clutter filters are designed to reject the fundamental P.R.F. line and also any residual noise and modulation out to 400 Hz from that line (equivalent to a 100 knot target). This 400 Hz

guard band eliminates any doppler components on the clutter caused by moving trees, clouds, traffic and motion of the radar platform (in the case of a shipborne radar). The upper cut-off frequency of the clutter filter is determined by the fastest target to be detected, in this case 2000 knots which is equivalent to about 8 kHz. In consequence the interline noise generated must be below the level defined over the band 400 Hz to 8 kHz from the fundamental P.R.F. line. Ideally to ensure that clutter peaks at 80 dB above receiver noise cannot break through, the interline noise should be 120 dB/Hz.

Not all the noise between the lines will be pure noise, much of it being in the form of discrete lines caused by incompletely suppressed ripple on the power supplies to the power amplifier. The permitted level for these lines is nominally 80 dB below a spectral line irrespective of measurement bandwidth since these are at a single frequency. However this level of 80 dB will depend upon the number of such lines in any velocity filter band. A number of lines will add vectorially and, depending upon their phase, may exceed the total 80 dB limit. This effect can be observed by monitoring the radar performance and comparing it with the known noise level determined by a separate measurement of the interline noise. A means of measuring the interline noise is obviously useful as a check on what the radar performance ought to be and for tracking down the causes of interline noise should it prove to be excessive.

At the time this radar was designed little work had been done on measuring interline noise levels as low as 110 dB/Hz. The method used by Koontz [22] and Burmweig et al [23], described in Chapter 2, measured the additional noise introduced by the transmitter amplifier but they only achieved a sensitivity of 75 dB/Hz. Additionally both systems used rather complex up and down converters to transfer the microwave signal to a low

enough frequency for analysis. In many radars these up and down converters are an integral part of the radar but they are not always suitable for noise measurement purposes. The sensitivity of Koontz' system was limited by the spectrum analyser he used and no indication of the fundamental limits of his system were quoted in his paper.

The noise measuring system developed for this radar measures the additional noise generated by the transmitter amplifiers down to a level of 120 dB/Hz. Its principle of operation is basically similar to that used by Koontz since it compares samples of the input and output of the transmitter. In addition it is capable of discriminating between the A.M. and P.M. component of the noise. This system is described in the next section. The system has been further refined enabling measurements down to 150 dB/Hz to be made although this involves selectively cancelling the P.R.F. lines by 20-30 dB using a feed forward system. This involves careful matching of components and is not as easy as using the basic system. This refinement is also described later in this chapter.

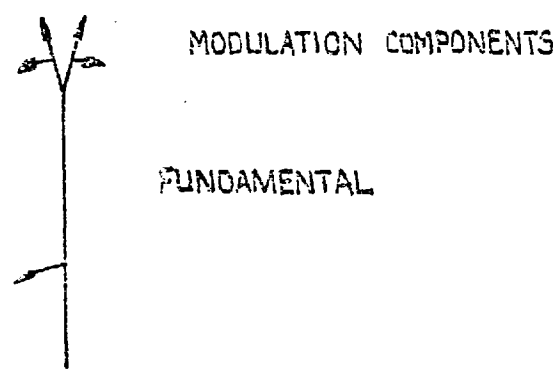
5.1 Additive Noise Measurement System

The noise measuring system described is only capable of measuring the interline noise generated by an amplifier, although this amplifier can be either a single stage of a chain of amplifiers or the complete chain. The system is basically very simple and could be applied to devices operating in any frequency band providing that suitable components such as mixers, couplers, phase shifters etc, existed or could be made.

The technique used is to sample both the input and the output of the amplifier and compare these samples in a phase sensitive detector. The video output of the phase sensitive detector (PSD) is amplified and analysed

using an audio frequency spectrum analyser with a high dynamic range and good resolution. A block diagram of the basic system is shown in Figure 5.1. Small samples are taken from the input and output waveguides by microwave couplers and fed to the two input arms of the PSD via a variable attenuator in the output arm and a variable phase shifter in the reference arm. The way in which the PSD operates allows for separate measurement of the A.M. or P.M. components of the noise depending upon the phase relationship of the reference and output signals. For the PSD to operate in this way the reference signal must be at least an order of magnitude greater than the output signal. The mode of operation is most easily understood if vectors are used to represent the various signals and modulation.

Amplitude modulation can be represented by two vectors rotating in opposite directions on top of the vector representing the fundamental signal:-



As the modulation vectors rotate the resultant of these and the fundamental will vary in amplitude but not in phase. Phase modulation is similar but the modulation vectors are displaced 90° in phase compared to the fundamental.

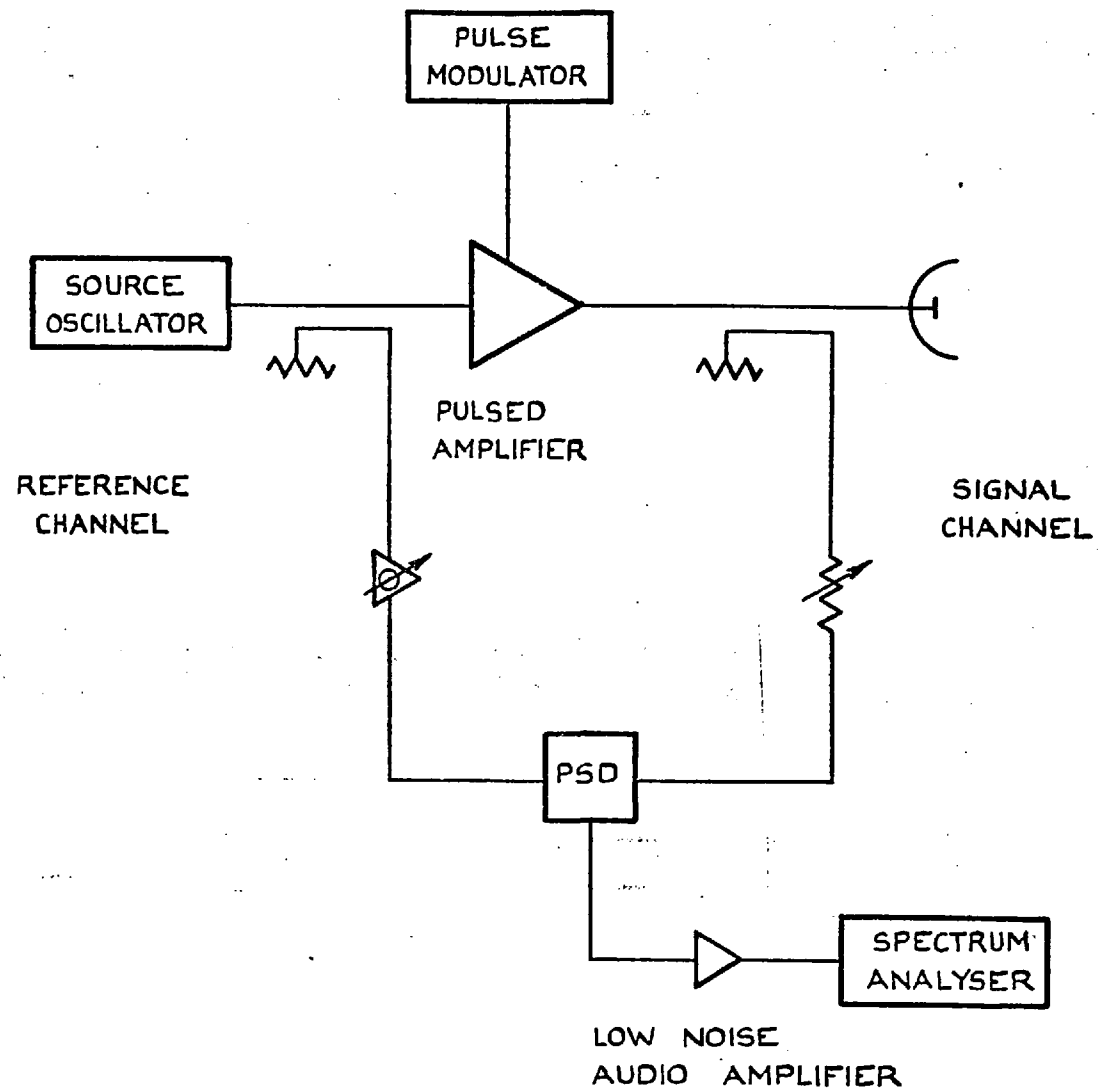
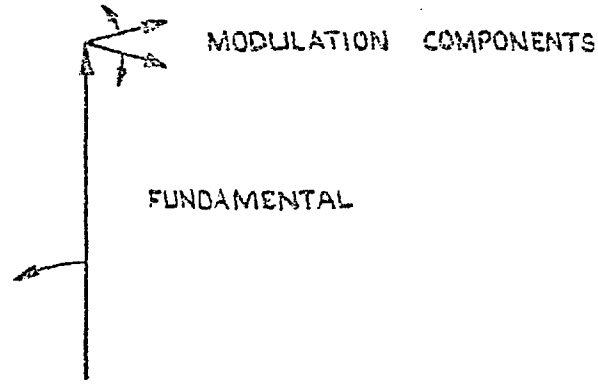


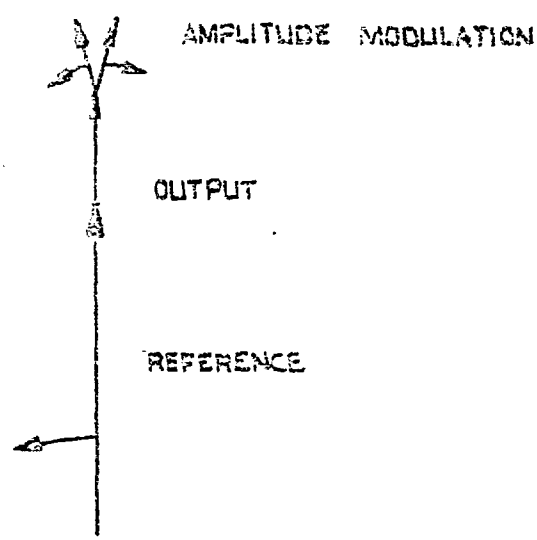
FIG. 5·1

THE BASIC NOISE MEASUREMENT SYSTEM

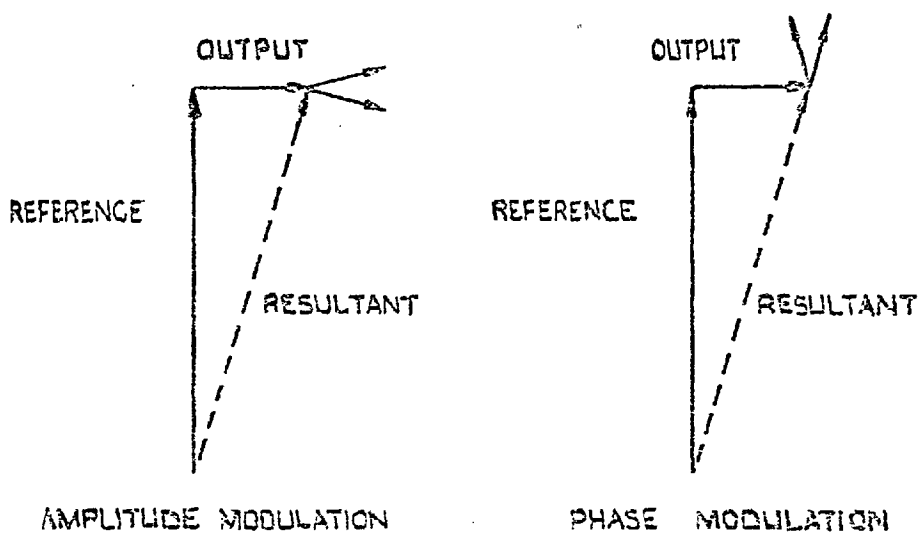


As the modulation vectors rotate the resultant of these and the fundamental swings about the mean position in phase but there is no change in amplitude.

The output of the PSD is simply the detected envelope of the combined reference and output signals and will reproduce either the A.M. or P.M. components of the noise on the output signal depending upon the phase relationship of the two inputs. Firstly consider the two inputs to be in phase with each other and with the reference signal ten times larger than the output signal:-



The amplitude modulation will be detected by the PSD and will appear on the output. The reference and output signals will appear on the output as a d.c. level (assuming in the first instance that the input signals are c.w.). Any phase modulation on the output signal will not be detected since the PSD will only respond to amplitude fluctuations. If the phase relationship between the reference and output signals is altered to be in quadrature then the result is completely different:-



AMPLITUDE MODULATION PHASE MODULATION

In this case the amplitude modulation is effectively converted to phase modulation and is not detected by the PSD. However phase modulation is converted to amplitude modulation as shown above and will be detected. In this way by simply changing the relative phase between the reference and output signals by 90° the A.M. and P.M. components of the noise can be measured separately. This action of the PSD is also demonstrated mathematically in Appendix 4.

In practice the reference signal may be either c.w. or pulsed and the output signal will always be pulsed. This does not change the operation of the circuit since the pulsed output signal can be considered as amplitude modulated c.w. In this case when the reference and output signals are in phase then the output from the PSD will be a pulse, modulated with the A.M. components of the noise introduced by the power amplifier. If the reference and output signals are in quadrature then amplitude modulation is suppressed and the output will no longer be a modulated pulse but a pulsed sample of the P.M. component of the noise introduced by the amplifier. In terms of the spectrum, in the A.M. case the usual sin x/x pulse spectrum will appear with A.M. components of noise modulating each P.R.F. line. Only half of the true sin x/x spectrum will be seen since it will be folded over at zero frequency by the detection process. The power spectral density measured will in fact be twice the true value because of this folding and the central P.R.F. line will appear at zero frequency.

When P.M. is being measured, the P.R.F. lines will be suppressed since these are amplitude modulation components. The phase modulation on the pulsed signal will now appear as a periodic spectrum with phase modulation components appearing on either side of the cancelled P.R.F. lines of the sin x/x spectrum. This effect is shown in Figure 5.2 which shows what typical amplitude and phase modulation spectrums would look like. The cancellation of A.M. or P.M. components of noise is never complete but in practice 40-50 dB cancellation can be achieved. Appendix 4 shows that this is equivalent to a phase error of only 0.6°. If the drive signal to the amplifier is very stable and the delays in the two arms of the measurement system are accurately matched then over 60 dB cancellation can be achieved and maintained. The work required to achieve this extra cancellation is not justified since the gain in sensitivity is negligible.

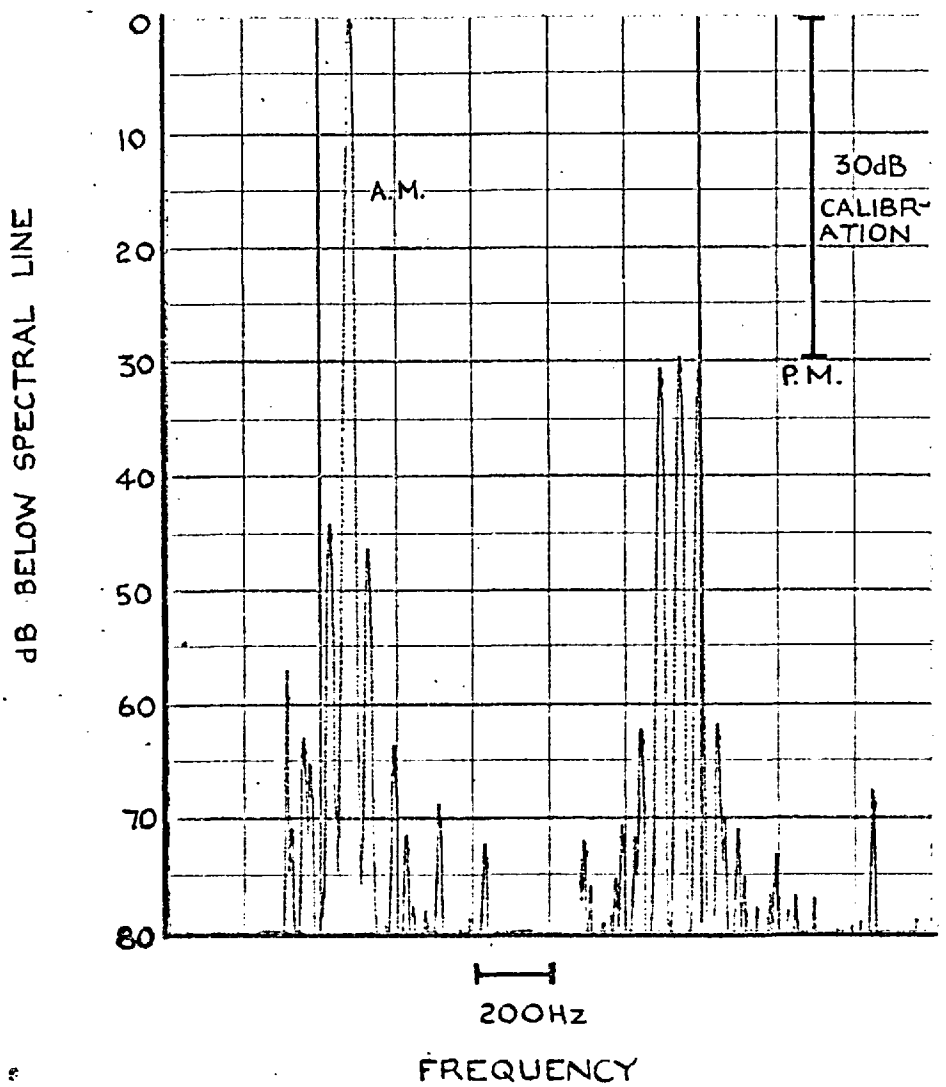


FIG. 5·2

SPECTRUM OF ONE PRF LINE SHOWING CANCELLATION OF A.M. DURING P.M. MEASUREMENTS

The major problem in making and using a system based on the principles just described is that of achieving the required sensitivity. The radar system itself required an interline noise level of 110 dB/Hz below one line of the pulse spectrum and the measuring system should have a sensitivity of at least 120 dB/Hz to obtain sensible results. At first sight it might appear that such a sensitivity could be readily achieved, however this system must work with pulsed signals which greatly increases the dynamic range required.

Consider a pulsed signal with a duty ratio d, pulse width τ and pulse repetition frequency f. The line spectrum of such a pulse train can be determined using the Fourier transform. The result of the transform is a series in which each term represents one line of the spectrum of the pulse train. This series can be shown [Reference 36] to be represented by the summation:-

$$f(t) = Ad \sum_{r=-\infty}^{\infty} \left(\frac{\sin \pi rd}{\pi rd} \right) \exp [-jrwt]$$

where A is the amplitude of the pulse.

The amplitude of the fundamental spectral component is then Ad.

The average power associated with this spectral component is thus A^2d^2.

In other words the power in the fundamental spectral line of the pulse spectrum is a factor d^2 below the peak power of one pulse. At the usual radar system duty cycles of between 0.05 and 0.001, d^2 can range from 26 dB to 60 dB. The duty cycle of the radar is therefore a very significant factor in determining the sensitivity of any noise measuring system.

The first noise measuring system to be designed used an i.f. section. An i.f. PSD was chosen because the only microwave mixer diodes available at that time were point contact diodes which have a very poor noise figure at low frequencies. By using an intermediate frequency, low noise diodes could be used in the PSD. The noise mechanisms involved are discussed in a little more detail in the next section.

A typical point contact diode microwave mixer will have a noise figure of about 10 dB and reach its 1 dB gain compression point at an input power of -10 to -20 dBm. The noise level at the output of the mixer at room temperature in a bandwidth of 1 Hz is given by:-

$$N_p = kTBN_F.$$

where N_p is the Noise Power Output in Watts,

k is Boltsmans constant.

T is the temperature in K, assumed to be 290.

B is the bandwidth in Hz.

and N_F is the noise figure of the mixer diodes.

if $N_F = 10$ (for 10 dB noise figure)

$$N_p = 4 \times 10^{-20} \text{ Watts}$$

$$= \underline{-164 \text{ dBm}}$$

If the maximum input power to the mixer is -20 dBm without distortion then the maximum dynamic range will be 144 dB under ideal conditions. The dynamic range required to measure noise 110 dB/Hz below one spectral line for a 0.05 duty ratio signal is 146 dB and for a 0.001 duty ratio it is 180 dB, allowing 10 dB extra sensitivity in both cases to ensure unambiguous measurement of the amplifier noise. The measurement of noise levels of 110 dB/Hz with a signal of duty ratio 0.05 might just be practical but measurement of a 0.001 duty ratio signal would be impossible.

This problem was overcome in the final system by two means. Firstly back diodes and schottky diodes became available for use at microwave frequencies, these have very good noise figures at low frequencies and schottky diodes can handle significantly greater power levels than point contact diodes. Using these devices it became practical to dispense with an i.f. stage and to use a microwave balanced mixer as a PSD. Secondly a cancellation circuit was devised which selectively cancelled the P.R.F. lines but not the noise. A combination of both these techniques enabled a sensitivity of 150 dB/Hz below one spectral line to be achieved with a 0.05 duty cycle signal. The corresponding sensitivity would be 116 dB/Hz for a 0.001 duty ratio signal.

Another major feature offered by an additive noise measurement system is its insensitivity to phase noise on the source driving the power amplifier. This has been demonstrated in Appendix 4. The A.M. component of the source noise is not cancelled by the action of the PSD but for the quiet oscillators used in low noise systems the A.M. component of its noise is usually very small and can be neglected by comparison with the F.M. noise. Even if the PSD were able to cancel the A.M. noise on the source the non-linearities in the power amplifier would prevent any effective cancellation. In conclusion it is possible to say that noise from the source is not a limiting factor in the measurement of amplifier noise. The results quoted in the next chapter show that this is true in practice.

5.2 Development of the Noise Measuring System

Several circuits were investigated in the course of developing the final successful system. All the circuits worked on the principles described in the previous section. The first circuit used an i.f. stage to overcome the low frequency noise associated with point contact microwave mixer crystals

and this is briefly described in the next sub-section. The final circuit used a microwave phase sensitive detector using schottky diodes which have a very much superior low frequency noise performance and better power handling capabilities than point contact diodes. This technique eliminates the i.f. stages, greatly simplifying the system. This circuit, together with the calibration system is described at the end of this section.

(a) The First Noise Measuring System

When development of the noise measuring system was started point contact diodes were the only microwave mixer diodes available. This type of diode exhibits very high levels of $^{1}/_{f}$ type noise or flicker noise. This type of noise is high at low frequency and falls off as $^{1}/_{f^n}$ where n is usually greater than one. The phenomenon is not well understood and is present to some extent in all PN junction diodes and to a smaller extent in thermionic devices. It was not practical to try and use these diodes to mix down to zero i.f. because of the very high noise figure. Consequently an i.f. of 10.7 MHz was used where the noise figure is typically about 10 dB. The phase sensitive detector could now use relatively low frequency mixer diodes with very much better low frequency noise figures. The general arrangement of this noise measurement circuit is shown in Figure 5.3.

Commercial mixers were used to mix down to the i.f. frequency of 10.7 MHz. 10.7 MHz was chosen as the i.f. frequency since a design for the i.f. amplifiers already existed and the local oscillator used in the radar system could also be used for noise measurement. The microwave couplers, variable phase shifters and variable attenuators were all standard commercial items. The phase sensitive detector was tailor made for the task and used a pair of thermionic diodes as the detector since these were

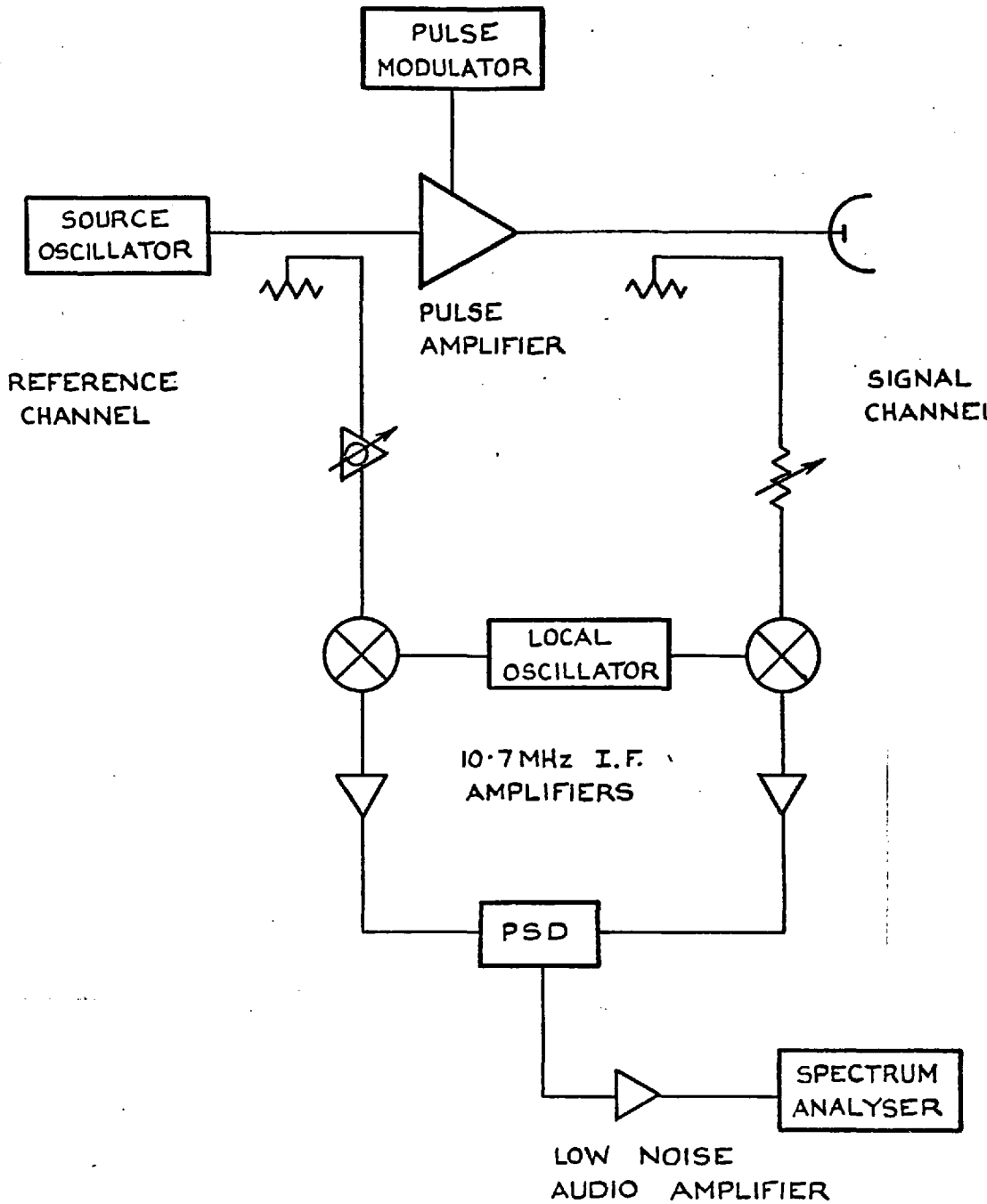


FIG. 5·3

BASIC NOISE MEASURING SYSTEM WITH I.F. PSD

thought to have a very much better low frequency noise performance than semiconductor diodes.

The spectrum analyser used to make the measurement of the noise was a Rohde and Schwarz audio frequency spectrum analyser type FNA. This instrument has a frequency range from 30 Hz to 20 kHz with a resolution of 10 Hz or 200 Hz and a dynamic range of 80-90 dB. The smallest detectable signal was 1 μV into 100 kΩ using the 10 Hz filter. The spectrum measured by the instrument is plotted on an integral X-Y recorder using a standard printed card calibrated from 0 to 80 dB in 10 dB increments. The sensitivity of the instrument was insufficient for all measurements and a low noise pre-amplifier was used to amplify the signal from the PSD to a suitable level for analysis.

This noise measurement system was used to measure the noise generated by the 5 kW TWT shortly after the transmitter was commissioned. The technique immediately proved its worth since a modulation component was discovered halfway between each pair of P.R.F. lines. This was identified as a modulation on the 10 kV d.c. to the TWT and was caused by overshoot in the stabilising amplifier in the power supply. This problem was solved by correcting the frequency compensation within the amplifier.

The noise measuring systems sensitivity was measured and found to be only 110 dB/Hz below one line of a pulsed signal with 5% duty ratio. This was adequate for measurements of the system performance but it did not allow measurement of tube noise. Another problem was caused by slow drift in frequency of the local oscillator which caused a change in the relative phasing of the two arms of the PSD. This made measurement of the P.M. component of the noise difficult since the cancellation of the A.M. component varied during the measurement. This problem was cured by carefully

equalising the path lengths of the reference and output signals. The equalisation was done using co-axial cable and it was necessary to wind this on a drum since movement of the cable effected the phase balance.

The noise which limited the sensitivity was found to originate in the PSD and not the microwave mixers. No work was done to improve the PSD because schottky barrier mixer diodes and back diodes became available, both of which offered better microwave mixer performance at low or zero intermediate frequencies. Consequently the i.f. approach was abandoned and back diodes and schottky diodes were used in a microwave PSD.

(b) The Final Noise Measurement System

The final noise measurement system used a microwave balanced mixer as a phase sensitive detector. This became possible with the introduction of schottky barrier mixer diodes which have two significant advantages over point contact diodes. They have improved low frequency noise figures and they are capable of handling about one hundred times more power before limiting. Assuming a noise figure of about 20 dB (at 1 kHz say) and a power input of +10 dBm reference signal and 0 dBm output signal, then the sensitivity would be approximately 130 dB/Hz below one line for a pulse train with 5% duty ratio. This is a considerable improvement on the i.f. system described previously. A back diode mixer offers similar advantages in noise performance but is not capable of handling such a high signal power. The corresponding sensitivity for a back diode would be about 120 dB/Hz assuming a noise figure of 16 dB and a limiting reference signal input of -5 dBm and output signal input of -15 dBm. Despite the rather poorer theoretical performance of back diodes a sample was tried in a microwave mixer. This produced a sensitivity of 115 dB/Hz, close to the theoretical figure quoted above. This result was obtained at a frequency of 1 kHz from

zero frequency, the diode noise increased significantly at lower frequencies. Since the schottky diode mixer offered very much better performance the back diode was not used.

The final mixer chosen for use as a PSD was an Aertech "Orthostar" double balanced mixer employing a star connected bridge of four schottky diodes. The operation of the mixer has been described by Mouw and Fukuchi [37]. The advantage of a star connected bridge over the normal ring configuration is the elimination of the transformer connecting the low frequency port to the diodes. Instead a direct connection can be made which improves the d.c. and low frequency performance of the mixer when it is used as a PSD. The Aertech mixer offers a noise figure of 8 dB and a power handling capability of up to +15 dBm in the reference channel.

Figure 5.4 shows the noise measuring system complete with the means of calibration devised. During the measurement of A.M. noise the P.R.F. lines are uncancelled and can be used as a reference with which to compare the noise levels and no other calibrating signal is required. If P.M. noise is being measured then the P.R.F. lines are suppressed and no reference is available. The original level of the uncancelled P.R.F. lines could be used but if small adjustments are made to the microwave amplifier or attenuators then the reference level might be changed. The calibration system shown is capable of inserting a known level of A.M. or P.M. modulation on the output signal. This appears on the output spectrum as a modulation line on either side of each P.R.F. line and spaced at the modulation frequency from the P.R.F. line.

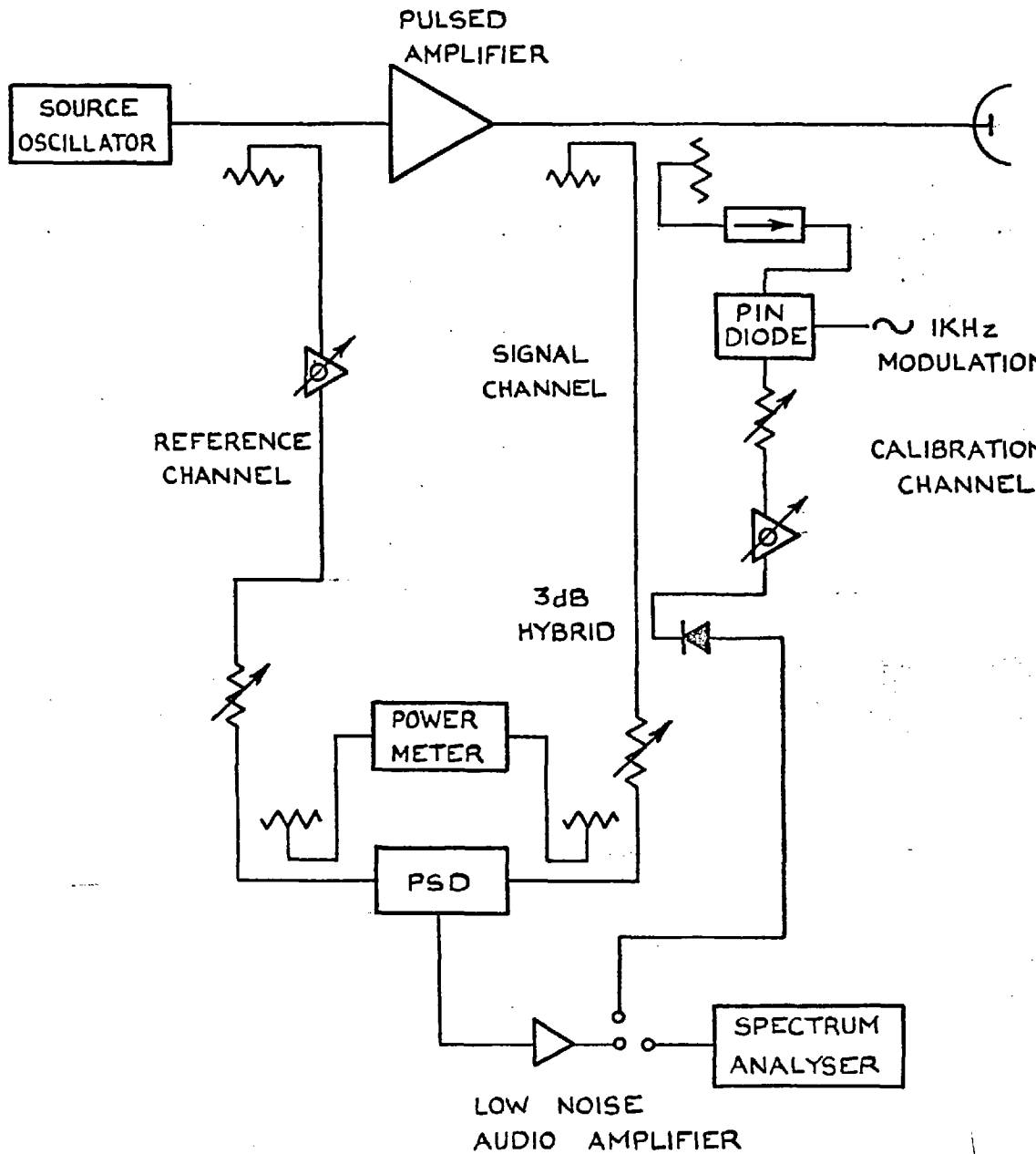


FIG. 5·4

NOISE MEASURING SYSTEM WITH CALIBRATION CHANNEL ADDED

The method used is to take a small sample (-10 dB) of the output signal and amplitude modulate it at quite a high level with a PIN diode modulator. The modulated signal is then passed through a step attenuator and a phase shifter and added to the original output signal in a 3 dB hybrid coupler. The amplitude of the resulting modulation on the output of the hybrid can be measured using a diode detector and the audio spectrum analyser. The two signals into the 3 dB hybrid must be adjusted by using the phase shifter so that they are in phase. The resultant modulation will then be A.M. which is detectable using the diode detector. After measurement the calibration signal can be converted to P.M. by inserting 90° of phase shift into the calibration arm using the phase shifter. This technique uses the principle used to distinguish between A.M. and P.M. noise in the PSD. The calibration line can be accurately altered in level by adjusting the step attenuator. The isolator shown in the diagram prevents modulated r.f. leaking back into the main channel via the sampling coupler. This would destroy the accurate phasing between the two channels which is necessary to convert the A.M. modulation into P.M. in the 3 dB hybrid. Even using an isolator, accurate calibration signals at levels lower than about 75 dB below a P.R.F. line could not be achieved. This did not prove embarrassing in practice since 50 or 60 dB calibration lines were adequate for all the measurements.

The procedure for making a measurement of the interline noise of an amplifier is as follows:-

(a) The equipment is connected as shown in Figure 5.4 and the delay in the reference and signal arms is adjusted to be as nearly equal as possible by inserting lengths of co-axial cable. This cable must be held as rigidly as possible since it can produce small phase changes if it moves about. If the two arms are not equalised then small changes in the source

frequency will change the relative phasing of the two signals at the PSD and degrade the accuracy of the measurement.

(b) The peak power entering the reference port of the PSD is adjusted to be +10 dBm which is just less than the maximum power handling capacity of the diodes.

(c) The peak power entering the signal port of the PSD is adjusted to be 0 dBm (one tenth of the reference power). Both these adjustments are done using a power meter to measure the mean power and converting the reading to peak power by dividing by the duty ratio. Adjustment to the power levels is made by using the variable attenuators.

(d) A calibration signal at a frequency of 1 kHz is applied to the output signal. The level of the calibration line is measured by using the audio spectrum analyser connected to the output of the 3 dB hybrid via a detector diode. The modulation line appears on either side of each P.R.F. line and the phase shifter in the calibration channel is adjusted to maximise the line which ensures that the modulation is pure A.M. The level of the modulation line can now be adjusted to the desired value using the step attenuator. If a P.M. calibration line is required the phase shifter is adjusted to minimise the calibration line (the detector diode is not sensitive to P.M.). The output signal is then connected to the PSD.

(e) The spectrum analyser is connected to the low frequency output port of the PSD via a low noise audio amplifier. The interline noise levels can then be measured. A.M. measurements are made by adjusting the output signal arm phase shifter to maximise the P.R.F. lines and with the calibration signal adjusted for A.M., 90° of phase shift should cancel the P.R.F. lines by 40-60 dB and enable the P.M. noise components to be measured. The calibration signal must also be re-adjusted to convert the modulation to P.M.

It is very important that any changes made to the settings of any component should produce the desired result or the measurement will be inaccurate. In particular the following checks must be made:-

(i) 10 dB extra attenuation in the output signal arm should reduce the measured spectrum by 10 dB. If it does not then the PSD, audio amplifier or spectrum analyser are overloaded.

(ii) 10 dB extra attenuation in the calibration arm should reduce the calibration signal alone by 10 dB.

(iii) 90° change in phase shift in either the calibration arm or the output signal arm should change the relevant signal from A.M. to P.M. or vice-versa. If only a partial change occurs then r.f. leakage may be upsetting the phase relationship of the signals.

The latter effect produced many problems during the measurement of the noise generated by the high power amplifier. The general level of the r.f. leakage from the waveguide run was often comparable to the power levels of the signals entering the PSD. If this occurs then it is almost impossible to achieve a stable cancellation of the A.M. components during measurement of P.M. Even movement of the operator in the vicinity of the equipment destroyed the balance. The ultimate solution to this problem was to do the measurements with the noise measuring equipment in a screened room. All the signals sampled from the output waveguide run were taken to the screened room in solid co-axial lines to minimise external pick-up. Even so it was still necessary to restrict entry to the transmitter cabin to avoid perturbation of the local leakage fields during a measurement.

The sensitivity finally achieved with this equipment using the star connected schottky barrier diode balance mixer was 126 dB/Hz below one P.R.F. line. This is quite close to the predicted figure of about 130 dB/Hz.

5.3 Improvements to the Basic Noise Measurement System

Two further modifications were made to the equipment to increase the sensitivity still further. One modification was the incorporation of a gate after the PSD to pass the signal during the transmitted pulse and attenuate the system noise between pulses. The other modification involved cancelling the signal to the PSD with an equal amplitude anti-phase sample of the drive signal to the microwave amplifier. This should cancel the P.R.F. lines of the spectrum but leave the noise unchanged. A higher level of signal could then be fed into the PSD resulting in increased sensitivity.

Figure 5.5 shows the video noise gate connected into the equipment. The video noise gate used was a simple diode bridge gated on and off from a pulse generator triggered by the transmitter. Using the gate a reduction in noise was expected determined by the duty cycle of the equipment. If the signal to the reference arm of the PSD is c.w. then the PSD diodes will generate noise continuously. If the video gate is arranged to just pass the transmitted pulse then the noise fed to the analyser will be reduced by an amount equivalent to the duty factor. If the duty cycle is 4% then the reduction in noise that could be expected would be about 14 dB.

The noise gate was incorporated into the equipment and the performance measured. The noise was suppressed by about 16 dB and the dynamic range increased by about 10 dB. The difference was due to both the insertion loss of the gate and eclipsing loss since the sampling pulse was shorter than the r.f. pulse. Optimum performance was achieved with the video gate placed after the low noise video amplifier and with moderate signal levels. At high signal levels there was some leakage through the gate which degraded the performance.

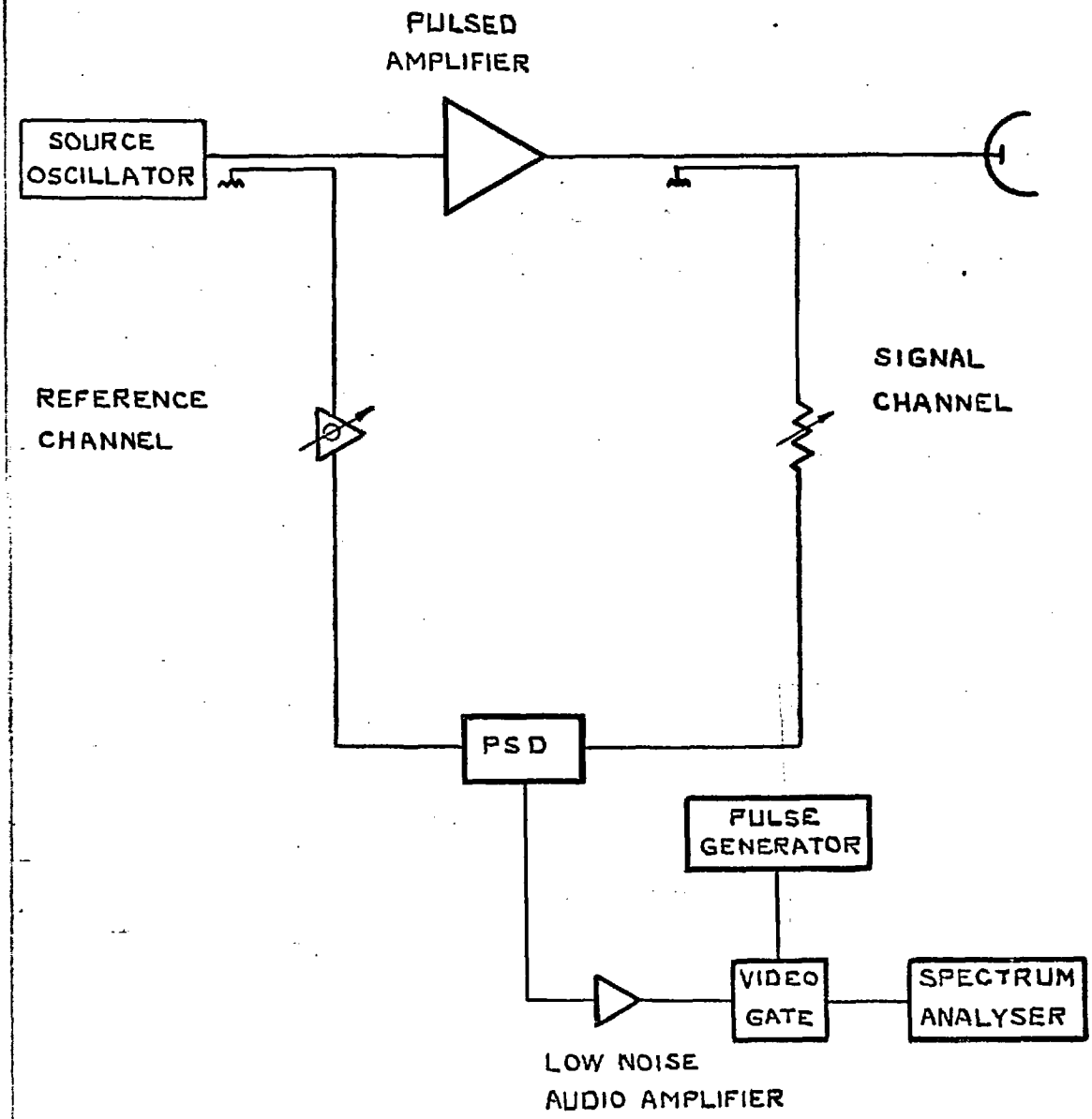


FIGURE 5·5

NOISE MEASURING SYSTEM WITH VIDEO NOISE GATE

Figure 5.6 shows the effect of the video noise gate on the noise from a detector diode fed from the c.w. reference line of the noise measurement equipment. A.M. modulation at 1 kHz has been inserted as a reference. The spectrum on the left is the noise and modulation ungated. The effect of gating is shown on the right. The noise has been suppressed by 10-15 dB with an insertion loss on the signal of 6 dB. However modulation lines close to zero frequency appeared. These were thought to be due to jitter and pick-up from the pulse generator driving the gate. They were reduced but not eliminated by careful screening and earthing of the gating circuitry.

Cancelling the amplitude modulation P.R.F. lines of the pulse spectrum offered the possibility of up to 30 dB increase in dynamic range and sensitivity. Figure 5.7 shows the additions required to the existing measurement circuit. A sample of the r.f. drive is fed forward and added to the r.f. output in anti-phase in a 3 dB hybrid coupler. It was essential to match the two path lengths to the 3 dB hybrid or poor cancellation resulted. Even with accurate matching only about 10 dB cancellation was observed on a power meter. Observation of the cancellation achieved using a detector showed that excellent cancellation occurred at the centre of the pulse but very little cancellation occurred at the leading and trailing edges of the pulse. This had been anticipated because even well matched path lengths could not compensate for the phase transients introduced by the TWT during the rise and fall of the r.f. drive. The phase transients could be directly related to the A.M. to P.M. conversion characteristics of the tube. Since these transients could not be matched out the only way a reasonable cancellation could be achieved was to gate them out with a PIN diode switch placed after the 3 dB hybrid. Using the PIN diode, as shown in Figure 5.7, in excess of 30 dB's cancellation was obtained measured with a power meter. Since the PIN diode sampling pulse is of necessity a little narrower than

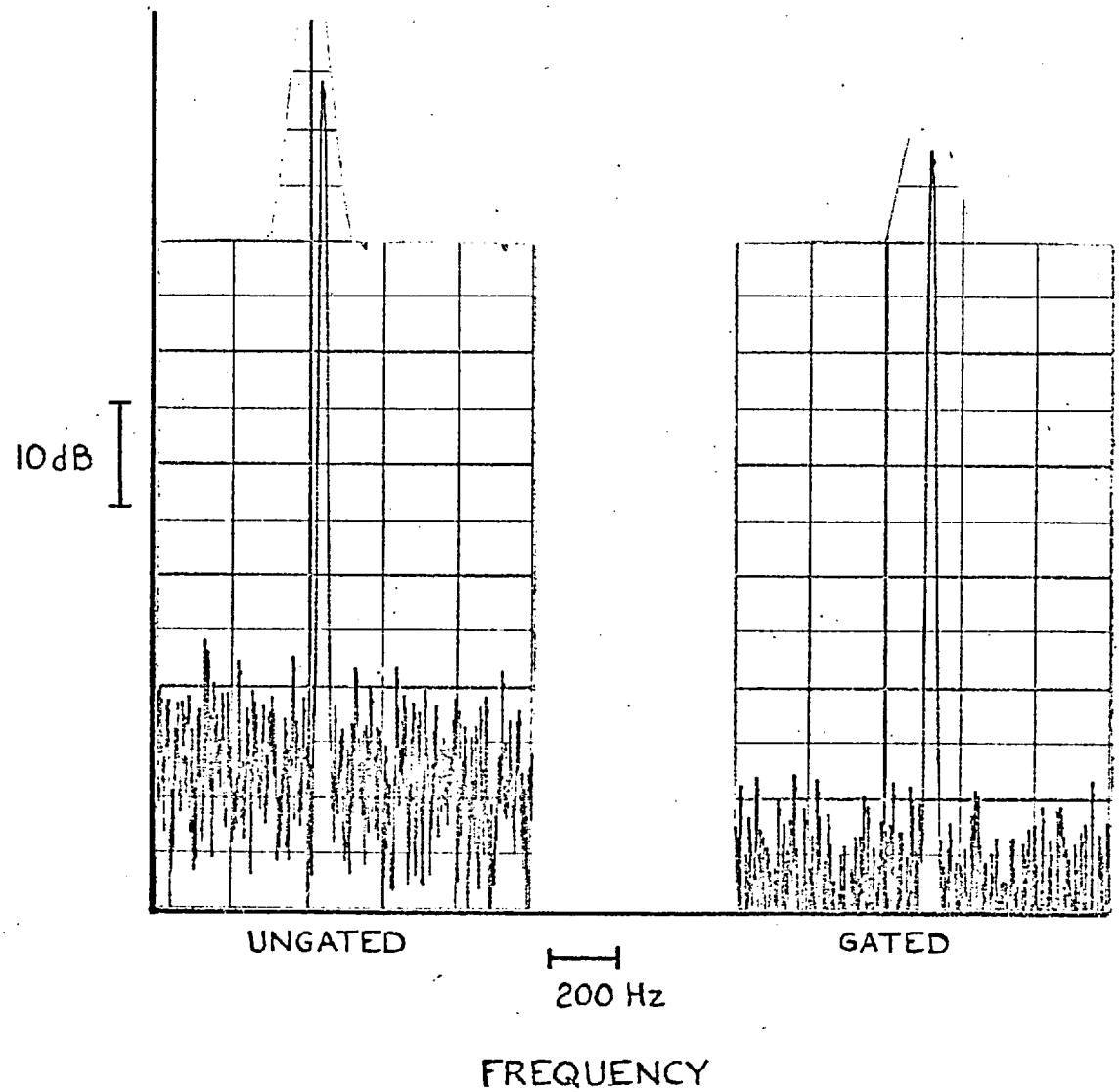


FIG. 5·6
EFFECT OF VIDEO NOISE GATE

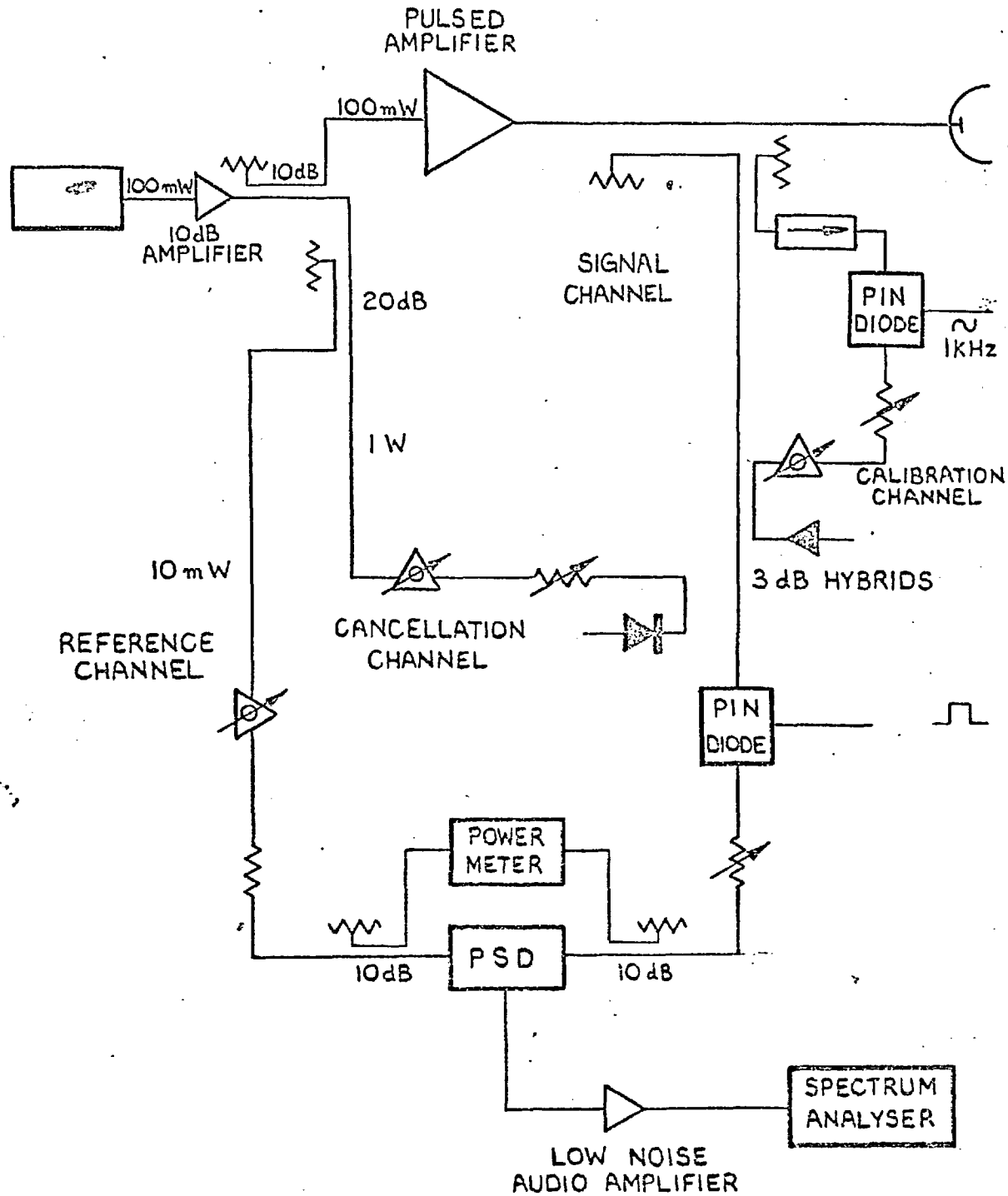


FIG. 5·7

NOISE MEASURING SYSTEM WITH CANCELLATION CHANNEL ADDED

the r.f. output pulse, some eclipsing loss will occur. However this would be unlikely to be greater than 1 or 2 dB which is insignificant when compared with the potential gain of up to 30 dB in sensitivity. A more serious drawback is the elimination of edge effects such as jitter by the PIN diode gating, additionally unwanted jitter could be introduced by the PIN diode itself. However for the examination of noise generated during the centre portion of the r.f. pulse, cancellation offered significant gains.

To make use of the full potential of the cancellation system a 10 dB increase in the available drive power was required. The maximum signal power into the PSD was 0 dBm and if a cancellation of 30 dB was assumed a signal with a power level of 1 watt must enter each input port of the 3 dB hybrid. The r.f. output signal was derived from a high power amplifier via a chain of couplers so that it was easy to obtain a 1 watt signal. The source driving the amplifier was only capable of producing 100 mW of which only 10 mW was available for both the reference arm of the PSD and the cancellation system. A transistor microwave amplifier with a gain of 10 dB was acquired and installed in the drive line to the power amplifier as shown in Figure 5.7. The 100 mW drive c.w. r.f. signal could then be amplified to approximately 1 watt. This was then divided into the three channels with 10 and 20 dB couplers. Approximately 900 mW of power was then available to cancel the r.f. output.

Great care had to be taken with the adjustment of the system prior to a measurement since if an uncancelled one watt signal were to be applied to the PSD, its diodes would be destroyed. The adjustments to the relative phase and amplitude of the two signals into the 3 dB hybrid were done with the PSD disconnected and the cancellation observed with a power meter via the 10 dB coupler shown. A calibration signal was imposed upon the r.f. output in the conventional manner but before cancellation. It was possible

to observe the modulation line monitored after the cancellation hybrid on the spectrum analyser. The amplitude of this line should be unaffected by cancelling the main signal. Since no significant variation occurred during the cancellation procedure correct operation of the cancelling mechanism was assumed.

It was important that once the signal had been cancelled that drift in the source oscillator frequency or changes in the phase length of the TWT should not occur. If the path lengths of the two arms are not exactly equal, which is difficult to achieve, then drift in the source frequency will cause a change in relative phase at the 3 dB hybrid and the cancellation will suffer. Similarly if the beam voltage on the TWT should vary its phase shift will alter and the cancellation will degrade. In practice the cancellation could be maintained at 30 dB without adjustment for long periods, providing the equipment had been allowed to warm up for over one hour. This result was expected since the radar system had been designed to be very stable in frequency and phase.

Once stable cancellation had been achieved the signal was connected into the rest of the noise measuring system and A.M. and P.M. measurements made in the manner already described. An increase in sensitivity of about 20-25 dB was obtained giving an overall sensitivity of 150 dB/Hz below one P.R.F. line of the 5% duty ratio signal.

Problems caused by r.f. leakage and earth loops were even more troublesome and difficult to eradicate. Sensible measurements could only be made with the equipment in a screened compartment with the r.f. signals fed into it in solid co-axial line. With the r.f. leakage reduced in this way d.c. blocks could be used to break earth loops. Mains frequency interference was reduced by running the low noise video amplifier from a battery. No attempt was made to use cancellation and a video noise gate together since this

would only have compounded the r.f. leakage and interference problems and the resultant gain in sensitivity would be marginal. Since a sensitivity of 150 dB/Hz is adequate to measure the noise produced by any existing type of microwave power amplifier, there was little to be gained by increasing the sensitivity further.

5.4 Summary

The noise measuring system described in the previous section has the following features:-

(a) The basic circuit has a sensitivity of 130 dB/Hz below one P.R.F. line of a 5% duty ratio pulsed r.f. signal.

(b) Separate measurements of A.M. and P.M. components of the additive noise from the microwave amplifier can be made.

(c) A simple calibration circuit has been devised which enables accurate calibration of the system during the measurement.

(d) The basic circuit is simple and uses only readily available equipment.

(e) The sensitivity can be improved 10 dB by the addition of a video noise gate.

(f) Up to 150 dB/Hz sensitivity can be obtained by employing cancellation. The improvement is obtained at the expense of increased susceptibility to r.f. leakage which entails the use of a screened room in which to make the measurements.

Details of the measurements made with the equipment on a TWT and a CFA are given in the next chapter.

CHAPTER 6

RESULTS OF NOISE MEASUREMENTS

The noise measuring system described in the previous chapter was used to measure the interline noise generated by the TWT and CFA power amplifiers used in the pulse doppler radar described in Chapter 4. The two principal objectives of these measurements were:-

(a) To determine the interline noise level produced by the radar and to reduce this noise as far as possible.

(b) To separate the noise contribution made by the amplifier tubes from the noise induced by power supplies, in order to determine the ultimate restrictions on the performance of radar systems.

The measurements quoted in this chapter are given in two sections, those on the 5 kW TWT and its power supplies and those on the 100 kW CFA, when driven by the TWT. In general the noise levels produced by the two tubes and their power supplies were as expected. The TWT had an inherently very low noise output of 110-130 dB/Hz below a spectral line although it proved difficult to stabilise its power supplies to a level that reduced their modulation components below -75 dB. The CFA had a much higher inherent noise output of 80-90 dB/Hz below one spectal line but no power supply contributions could be detected.

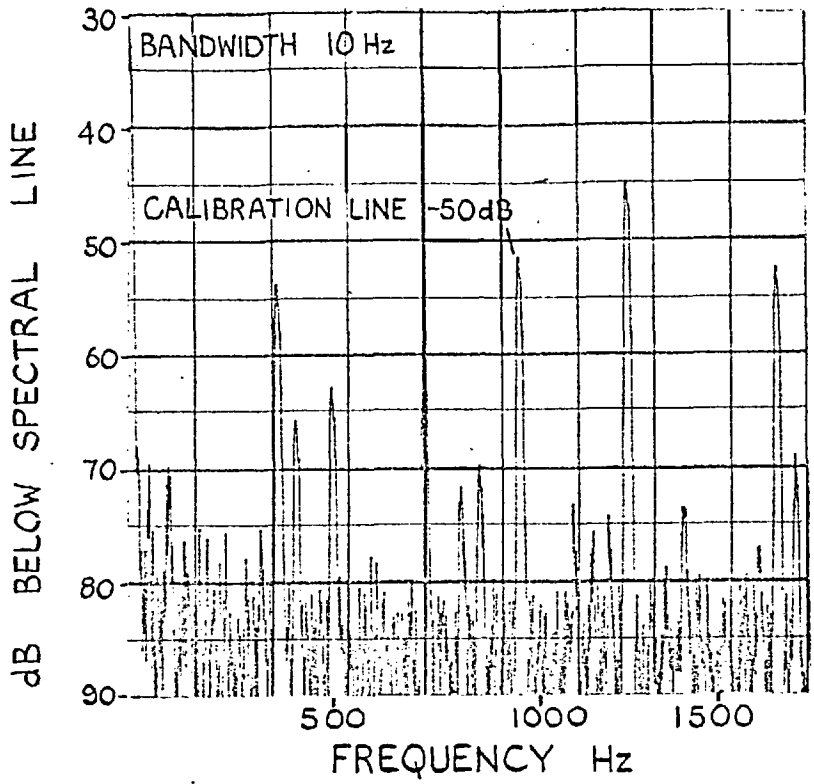
These results are described in detail overleaf.

6.1 Noise Measurements with the 5 kW TWT Transmitter

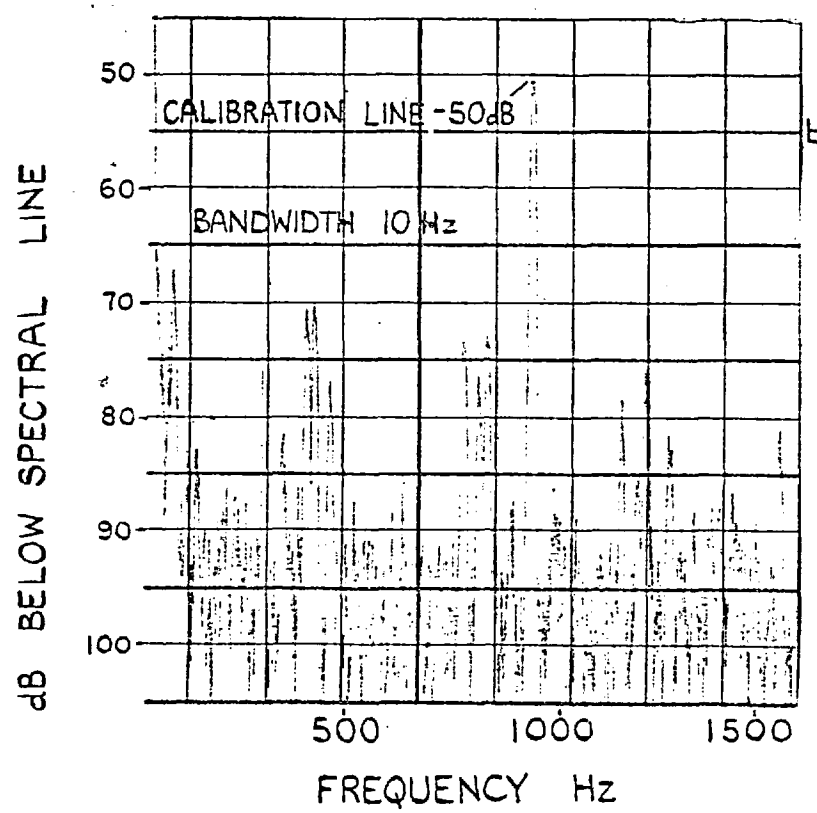
Noise measurements were made on this transmitter at an early stage in its development to check that the power supplies to the TWT were stabilised sufficiently to ensure adequate radar system performance. The very high sensitivity noise measuring system employing amplitude cancellation was not required for this measurement since the basic, simple system shown in Figure 5.4 had adequate sensitivity to measure the levels of power supply ripple modulation expected.

Figure 6.1a shows part of the P.M. interline noise spectrum obtained. The transmitter was operating at a P.R.F. of about 8 kHz and the spectrum shows the modulation lines produced by ripple on the power supplies to the TWT in the first 1.5 kHz band out from the fundamental spectral line of the pulse spectrum. A calibration line at -50 dB is shown at a modulation frequency of 1 kHz. The predominant modulation components are at multiples of the nominal mains frequency of 400 Hz. The frequency produced by the motor-generator was not tightly controlled and in this case was somewhat above 400 Hz. The mains input to the modulator was three phase and when rectified to produce the high voltage d.c. required the predominant ripple frequency was 1.2 kHz. This component can be clearly seen in the spectrum at a level of -45 dB. The pairing occurring at some of the modulation frequencies was caused by identical modulations reflected from the next spectral line.

The level of spurious modulation from the power supplies was very much higher than was desirable and a programme of noise reduction was started. This involved improvements to the frequency and transient response of the feedback amplifier controlling the series stabilising tetrode in the -10 kV h.t. supply. After each modification and adjustment the noise measuring system was used to check the effect on the interline noise. Some 20-30 dB improvement in power supply noise was



(a) BEFORE NOISE REDUCTION PROGRAMME



b) AFTER NOISE REDUCTION PROGRAMME

AT LEAST 20dB IMPROVEMENT

FIG. 6·1

INTERLINE NOISE, MODULATION INTRODUCED BY TWT POWER SUPPLIES

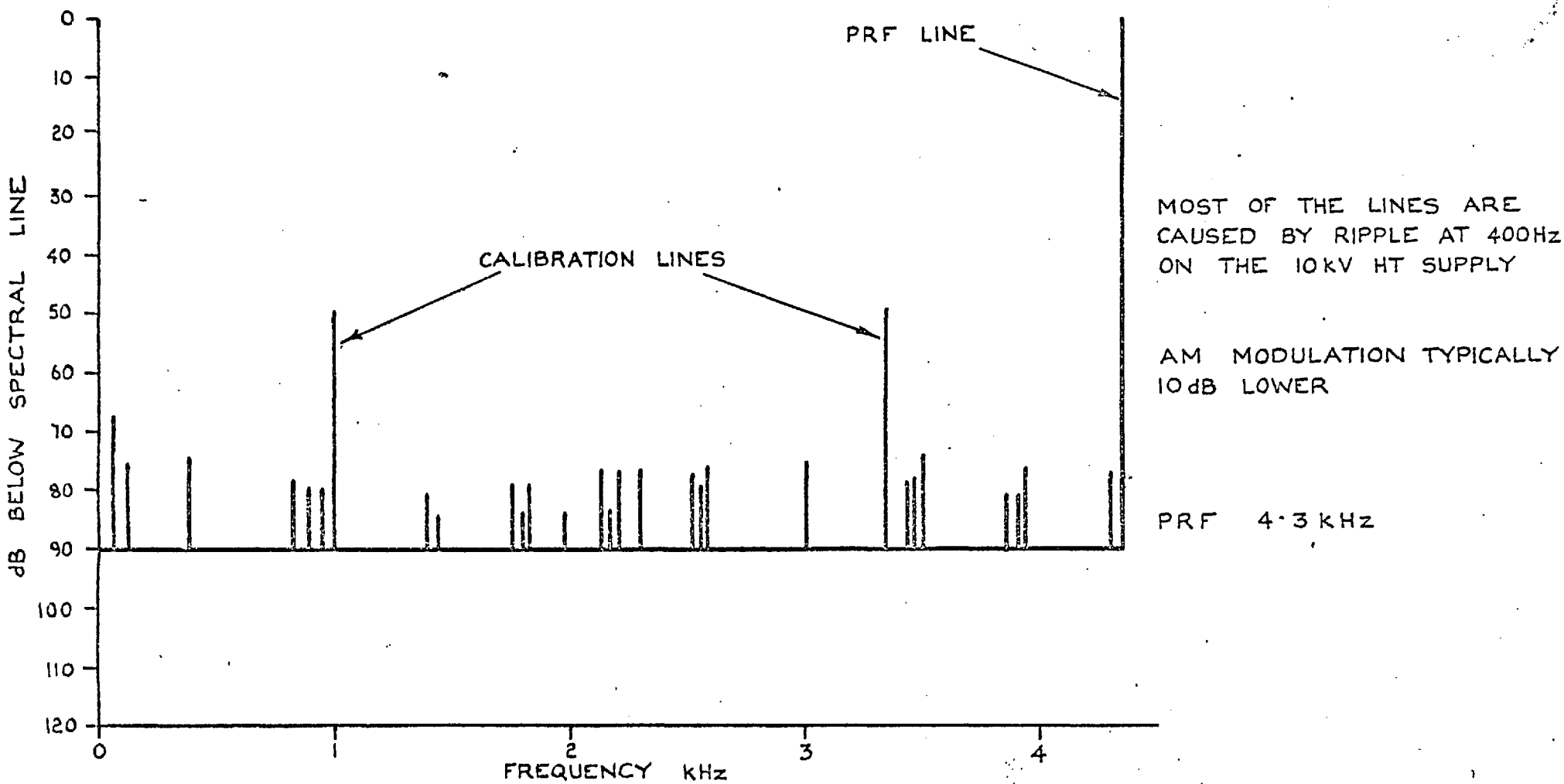
obtained as shown in Figure 6.1b which corresponded to the improvements observed on the power supply ripple voltage. The level of interline noise produced by the transmitter was then less than the noise introduced by the source oscillator and the combination was adequate for the first radar system trials.

The general noise level of -85 dB to -95 dB shown in Figure 6.1 was not produced by the TWT or power supplies but by the noise measuring system itself and represented the limiting sensitivity of the simple noise measuring system. Once the ripple on the power supply had been reduced, the dc supply was examined directly on the audio analyser to check that all the modulation lines on the r.f. spectrum were caused by ripple on the power supplies and not by vibration or jitter. The first 400 Hz modulation was measured as 100 mV r.m.s. variation in h.t. voltage which corresponds to a variation in phase through the tube of 0.03°. (The tube manufacturers quote a phase pushing figure of typically 0.3° per volt change in h.t. voltage). This phase change corresponds to a modulation line 69 dB below one spectral line. This is almost exactly the level measured for this modulation line in the P.M. spectrum of Figure 6.1b.

The level of power supply induced modulation finally achieved is shown in Figure 6.2. This figure is a representation of the spectrum between the fundamental and first P.R.F. lines. The general level of the modulation varies between 75 and 80 dB which gave satisfactory radar performance. It was necessary to re-check the interline noise levels periodically so that small re-adjustments could be made to the transmitter to maintain its performance as components aged. If the equipment was to be developed for use in an operational radar system then the stability of the power supplies for the amplifiers would have to be maintained over long periods without detailed checking, and consequently the stabiliser would have to be designed with this capability.

FIG. 6·2

PHASE MODULATION LINES CAUSED BY RIPPLE ON TWT POWER SUPPLIES

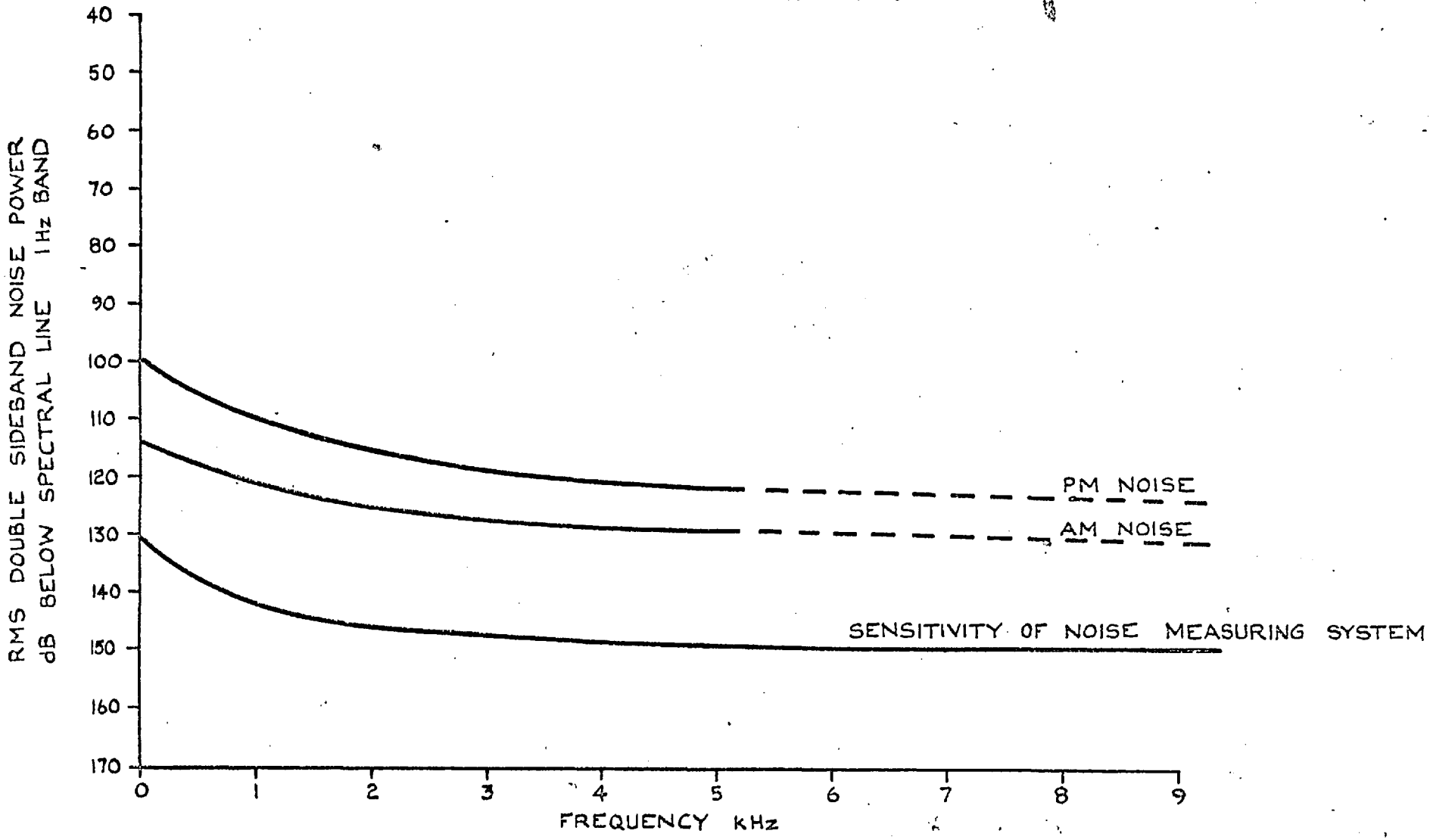


Once the transmitter was capable of satisfactory performance with the radar system, attention was directed towards the measurement of the noise produced by the TWT itself. For this measurement the high sensitivity noise measuring system using cancellation, shown in Figure 5.7, had to be used. This system needed very careful setting-up to eliminate ground loops and r.f. leakage interference. It was also necessary to make the measurement of the noise from the TWT during silent hours in the establishment to reduce unwanted interference from other radar systems and equipment on the site.

The fact that interference from other systems was a problem even inside a fairly carefully screened cabin demonstrates the high sensitivity of the noise measuring system. The problem of interference from other radar systems did not become apparent for some time since the spectrum analyser responded to the radar signal on each rotation of the radars antenna. The responses appeared as regularly spaced spikes on the spectral plot which looked very similar to ripple modulation lines. However with some experience it became possible to recognise the different characteristics of a response caused by ripple modulation and that caused by interfering radars. Accurate measurements could then be terminated if interference became apparent which might otherwise compromise the results.

Finally measurements of both the P.M. and A.M. noise from the TWT were obtained and are shown in Figure 6.3. These graphs show the variation of the r.m.s. double sideband noise power with frequency separation from the fundamental spectral line of the pulsed spectrum. The P.R.F. of the radar system at the time was 9.6 kHz and consequently the noise measured was the vector sum of the noise contributions from all the P.R.F. lines. However the noise from each line falls off quite rapidly with frequency and only contributions from the nearest two P.R.F. lines were significant.

FIG. 6·3
AM & PM NOISE GENERATED BY 5kW TWT

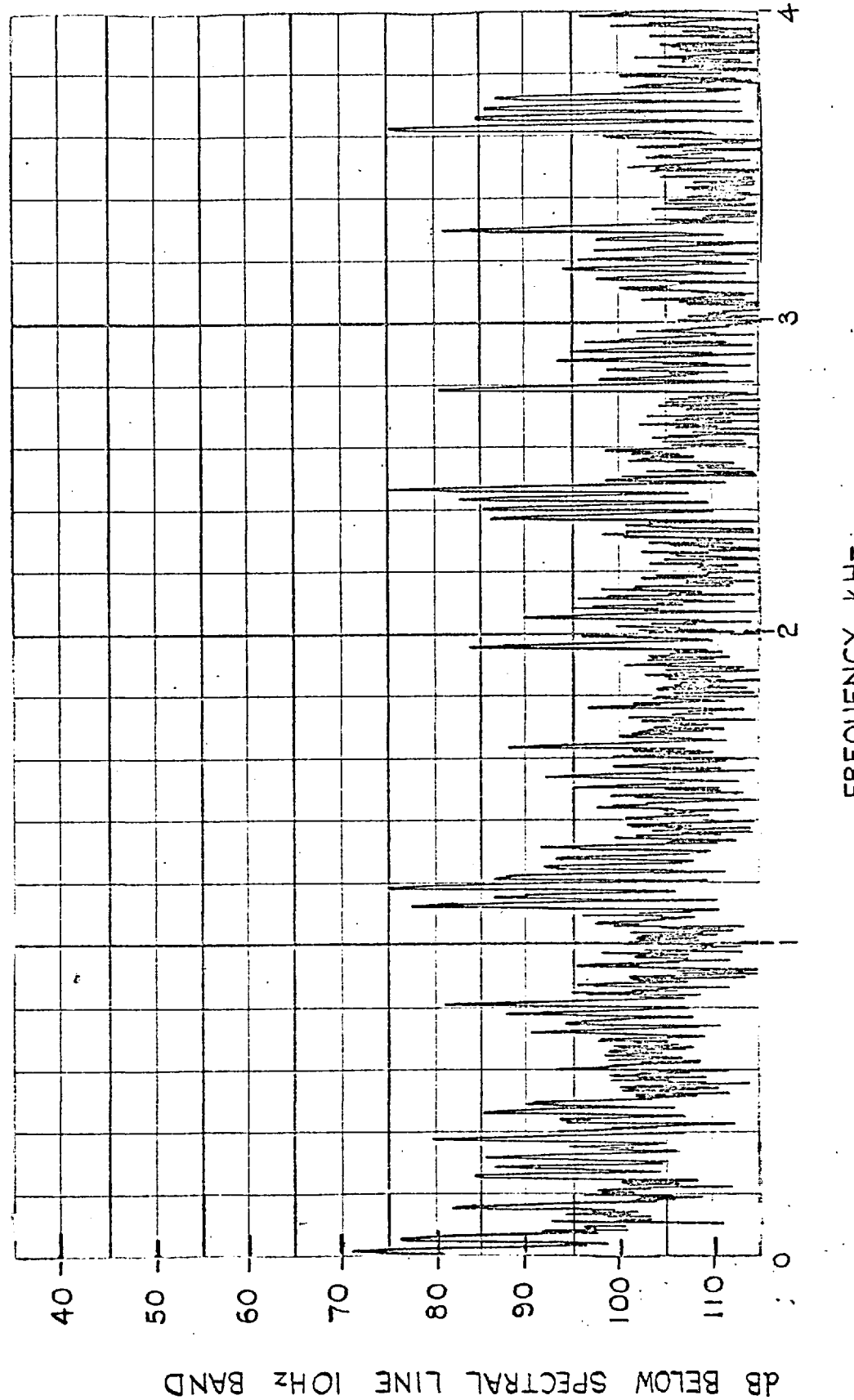


The measurement of the noise levels shown was complicated by the presence of the power supply ripple modulation already described and the results shown in Figure 6.3 had to be interpreted from the noise level existing between these ripple modulation lines. A typical phase noise measurement spectrum is shown in Figure 6.4. Here the dominant modulation lines are at 400 Hz intervals and these in turn support small 50 Hz modulation lines which are second order intermodulation products where the 50 Hz component is probably introduced via the grid circuit. Intermodulation products arise because the TWT behaves as a non-linear amplifier since it operates in saturation. Despite these modulation lines it is clearly possible to measure the general noise level, although the accuracy of the measurement suffers.

The accuracy obtained in these measurements is approximately ± 3 dB. This error is determined by the accuracy to which the calibration line can be set, by the accuracy of the spectrum analyser and by the estimation accuracy of the mean level of the noise on the spectral plot. The accuracy of the analyser is the most critical since this affects both the calibration accuracy and the measurement accuracy. The manufacturers state an error of ± 1 dB for the analyser. If one assumes that the error is the same when measuring the noise and the calibration line, then the error tends to cancel. If this assumption cannot be made then the error could be as much as ± 2 dB. It is assumed here that the error lies between the two at ± 1 dB. Errors in estimating the mean noise level were estimated at ± 2 dB giving a total measurement accuracy of ± 3 dB. Errors arising in the noise measuring system can be neglected because of the calibration technique used.

The interline noise produced by the tube itself did not vary significantly as the operating conditions were changed. Only small variations in

FIG. 6·4 TYPICAL PM NOISE PLOT OBTAINED USING TWT.



supply voltages of about ± 5% could be made without taking the operating conditions beyond the range specified by the tube manufacturer. To do so would have courted disaster since small variations in grid voltage in particular, can greatly increase the electron beam interception by the slow wave structure, which could destroy it. Since the slow wave structure interception current could not be monitored separately from the collector current, great care had to be taken in making even small variations in grid voltage.

The other variable which could be changed without risk to the tube, was the operating frequency. Unfortunately the radar system was designed for fixed frequency operation since frequency agility is not compatible with pulse doppler. However the frequency could be changed in 30 MHz increments by locking the L-band source oscillator to a different harmonic of the 30 MHz master oscillator. For other radar system reasons the frequency could only be changed to one other frequency for re-measurement of the tubes interline noise. No change in noise output was found. This result was expected since the conditions occurring within the tube would not change significantly for this relatively small change in frequency. A higher noise level could be expected at the tube band edges where the electric fields are changing more rapidly, but it was not possible to operate the radar system at the appropriate frequencies.

An attempt was made to identify any other causes of the interline noise and modulation observed, such as jitter or vibration. Vibration of the tube would be caused by moving parts such as fans or water. Operation for short periods without the cooling fans was possible but no change in the interline noise pattern was noticed when the experiment was tried. The water supply could not be interrupted for the period required to make a noise measurement but contributions from this source were not expected to be significant because of the low flow rate.

Interline noise caused by jitter would not be produced by the TWT since the r.f. drive pulse to the tube was positioned inside the envelope of the pulse applied to the grid of the tube. Therefore the rise and fall of the grid pulse to the TWT could not influence the r.f. drive or produce jitter. The jitter on the r.f. drive was extremely small since the gating pulse applied to the PIN diode gate was controlled directly from a very stable master clock. No jitter contributions could be seen on the measurements performed but power supply ripple modulations could have been masking them.

The net result of the measurements on the 5 kW TWT was that the predominant cause of interline noise was power supply ripple and that TWT noise, vibration and jitter produced smaller effects.

6.2 Noise Measurements on the 100 kW CFA Transmitter

The modulator powering the CFA was very different in principle to the TWT modulator. The 10 kV d.c. power supply was generated by a number of inverters operating at a chopping frequency equal to twice the P.R.F. This power supply was described in detail in Chapter 4. The object of using the inverters was to ensure that all the ripple produced by the power supply occurred at frequencies which were equal to, or multiples of, the P.R.F. In this way any interline noise modulation produced by this ripple would occur at the spectral lines of the pulse spectrum and not in the doppler band. The inverter frequency would have to change as the P.R.F. of the radar was changed to compute true range, or modulation lines would be produced which could degrade the clutter rejection. It was recognised that clutter rejection would be degraded immediately the P.R.F. was changed due to the transient on the power supply, and the receiver was gated off for a suitable period, corresponding to about 10 pulses.

The modulator and CFA were commissioned together. The inverter power supply worked well and readily accepted ± 10% changes in P.R.F. The first CFA did not work as expected and produced considerable levels of RFI and little output power. It was also prone to arcing and could not be operated at its correct rated voltage. This device was eventually found to be leaky and was returned to the manufacturers for repair. Fortunately the spare CFA worked well and radar trials and noise measurements were able to continue. However it was only possible to make noise measurements on one tube since reprocessing the broken CFA took over a year.

Once the second CFA was commissioned and working satisfactorily its interline noise performance was measured. Preliminary measurements showed that only the simple, basic noise measuring system would be required since the interline noise level generated by the tube was high, as had been expected. Even using the simple noise measuring system which had a relatively low sensitivity, r.f. leakage prevented any sensible measurements from being made. Eventually all the measurements were made in the adjoining receiver cabin which was screened from the transmitter cabin. All the microwave signals were fed between the cabins in solid coaxial lines which reduced r.f. leakage problems although it was still necessary to ban any movement in the transmitter cabin which would change the leakage field patterns. Satisfactory measurements could then be performed.

The 100 kW transmitter was measured in two different ways. In the first case the output of the 5 kW TWT which was used to drive the CFA was also used to provide the reference signal for the noise measuring system. In this case the noise measured would be solely that of the CFA. To test the overall transmitter performance the drive to the 5 kW TWT was used as a reference, in which case the noise measured was that produced by the entire amplifier chain.

Figure 6.5 shows the interline noise produced by the CFA itself. There is little difference between A.M. and P.M. contributions and very little change with frequency separation from the fundamental spectral line. The noise level is also very much higher than that produced by the TWT. The maximum P.R.F. which could be used with the 100 kW system was 5 kHz which is why the results are only valid out to 2.5 kHz separation from the fundamental spectral line. At no time during any of the measurements of interline noise on the CFA were any modulations due to power supply ripple detected. This proved that the inverter power supply concept worked very well in practice. Any ripple modulations must have been more than 80 dB down, which was very satisfactory. It was unfortunate that the inherent tube noise prevented the measurement of the absolete level of any power supply induced modulation.

Figure 6.6a shows part of a typical spectral plot obtained from measurement of the CFA's noise. The noise is very regular with no sign of any underlying structure.

Figure 6.6b shows the effect of using the drive to the TWT as a reference signal for the noise measuring system. The general noise level is very similar since it is produced by the CFA but now power supply ripple lines have appeared which are those generated by the TWT and its power supplies. During this measurement the TWT power supplies were not well stabilised which explains why the power supply lines are of such a high amplitude. A significant feature of the results shown in the spectrums of Figure 6.6 is the cancellation of the noise on the input to the CFA by the noise measuring system. This confirms the result obtained theoretically in Chapter 5. Cancellation of noise on the r.f. input to the amplifier under test was in excess of 20 dB.

FIG. 6-5
AM & PM NOISE GENERATED BY 100kW C F A

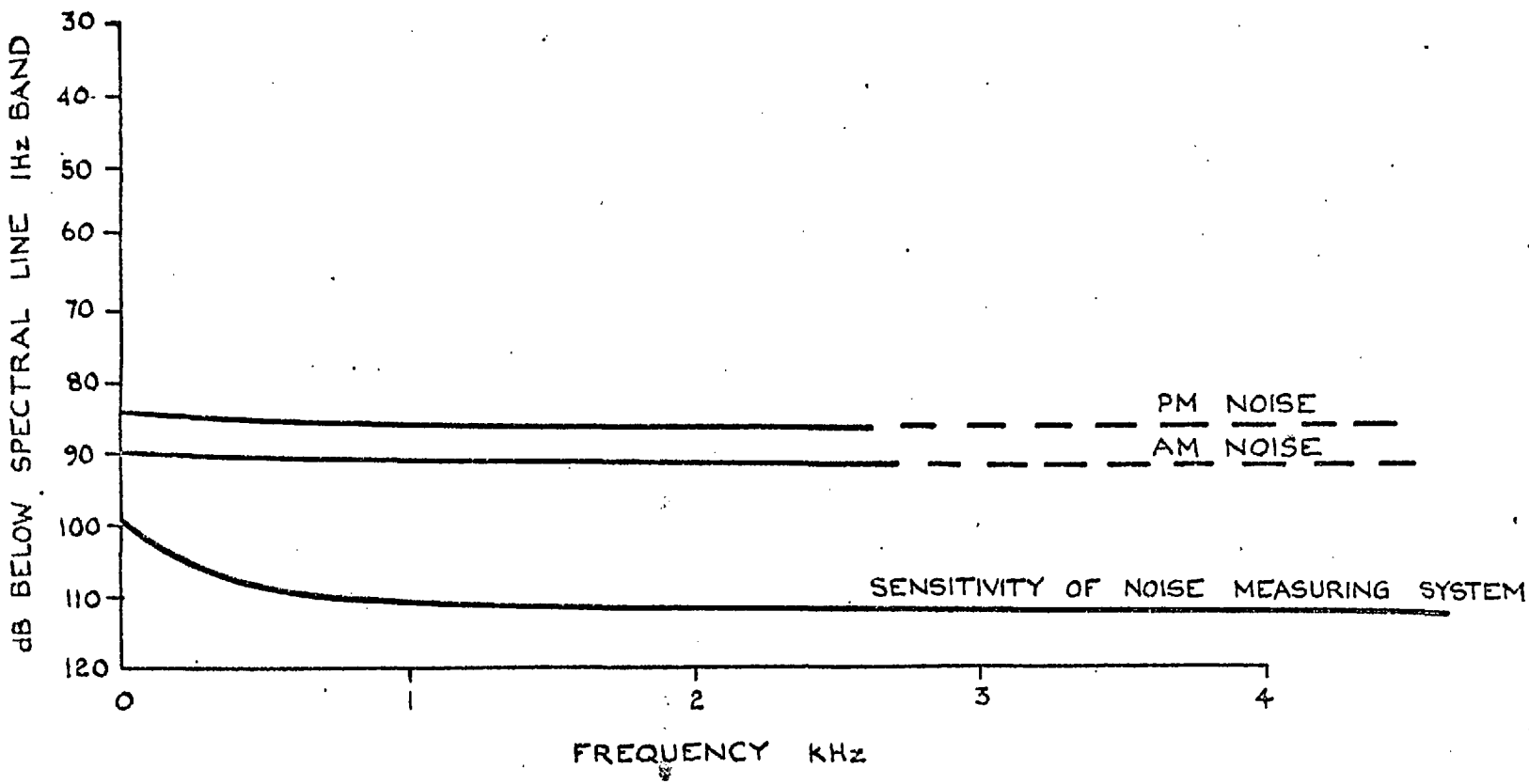
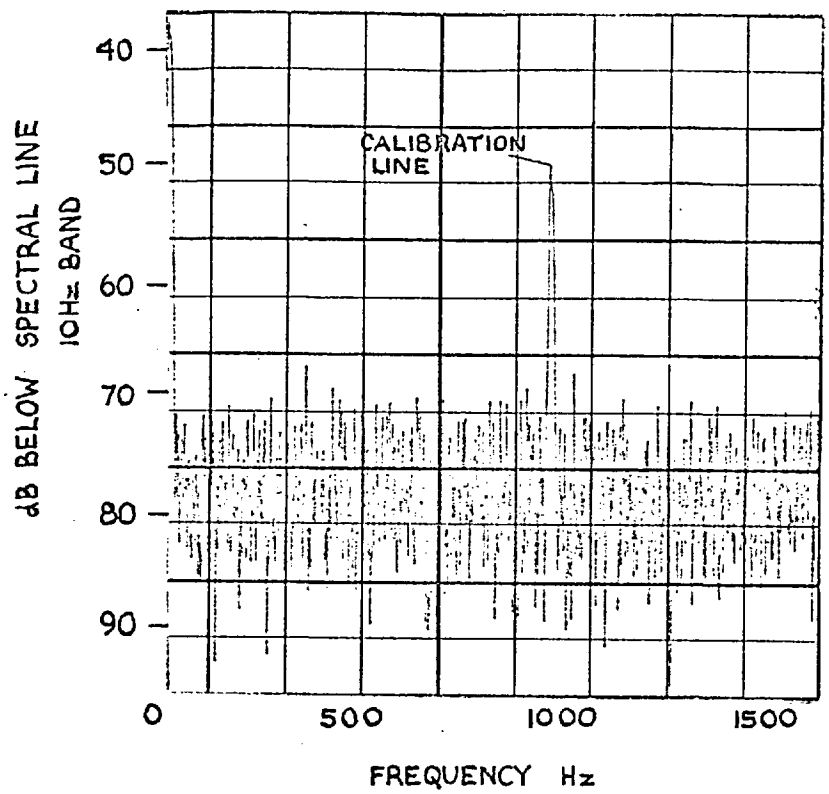
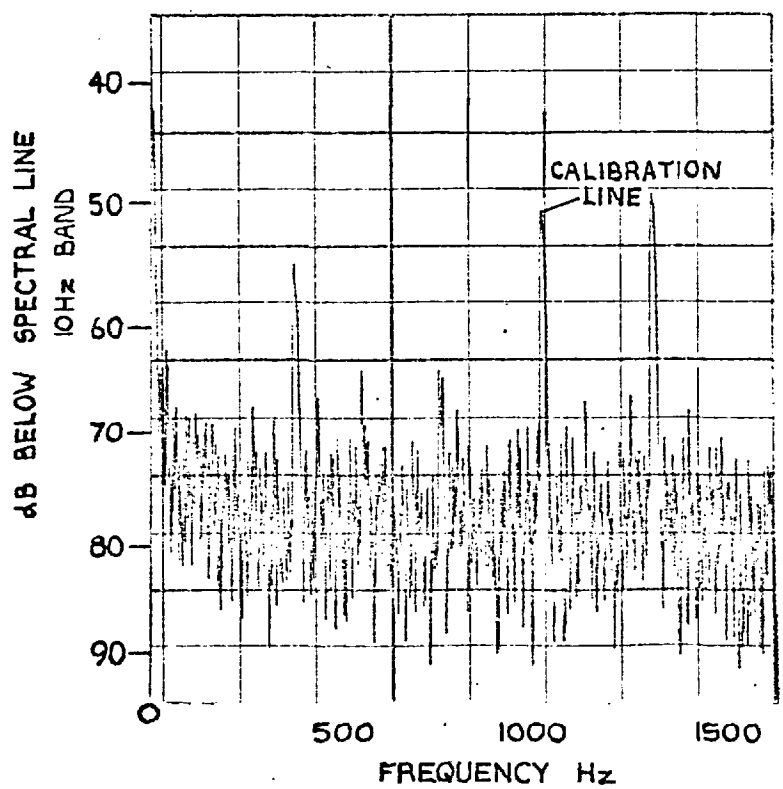


FIG. 6·6
CFA NOISE MEASURED SEPARATELY & INCLUDING
5 kW TWT CONTRIBUTION



a)
100kW CFA NOISE WITH 5kW OUTPUT USED AS A REFERENCE



b)
5kW TWT & 100kW CFA MEASURED TOGETHER

5kW POORLY STABILISED

Since the CFA was r.f. switched, jitter during start-up was more likely than with the TWT. The r.f. pulse was examined on an oscilloscope and jitter of a few nanoseconds with an apparently random characteristic was seen on the leading edge. The central portion of the r.f. output pulse was gated out and the interline noise re-measured but no change in noise level was seen. The noise contribution of the tube during the middle of the pulse was obviously greater than that produced by the jitter.

Another feature of the CFA which could generate interline noise was the method of beam quenching using a turn-off electrode. Jitter of the beam quenching pulse could in turn produce jitter of the back end of the r.f. pulse. This was examined in a similar manner to jitter on the front edge of the pulse with the same result. Apart from jitter, the CFA was capable of generating unwanted bursts of oscillation and noise during beam quenching, especially if the turn-off pulse was not correctly aligned. This effect had been observed on broadband spectrum measurements, although the noise could be reduced to less than the ordinary noise level by correct alignment of the turn-off pulse. To see what sort of effect this could have on the interline noise the turn-off pulse was deliberately delayed by 100 ns. The tube then produced a burst of oscillation at the end of the r.f. pulse. No degradation in interline noise level was observed. This was a most surprising result since the tube was producing a high level of noise and oscillation during this 100 ns interval. However broad-band spectral measurements had shown that the noise and oscillations produced were outside the band of the tube. It was probable that when mixed with the reference signal in the PSD these signals were shifted to a frequency beyond the range of the audio equipment used to measure the interline noise.

No measurements of variation of interline noise with frequency could be made for the same reasons that applied to similar measurements on the TWT. In addition the CFA produced even more RFI when an attempt was made to operate it towards the high end of its band. This resulted in constant tripping of its protecting interlocks. No time was available on the system to improve these and so operation at the high end of the band was abandoned.

In summary the interline noise on the CFA was predominantly the noise generated by the tube itself. The effects of jitter, vibration, turn-off oscillations and power supply ripple were all secondary and could not be measured.

6.3 Discussion of Results

(a) 5 kW TWT

The most significant cause of interline noise on the TWT was power supply ripple. This produced the effect which was predicted from the tubes known phase-pushing characteristics and it should be possible to design a power supply to minimise its effect. The power supply would not be the fundamental limitation on the interline noise performance of a transmitter.

The TWT did not significantly affect the jitter on the pulse because of the method of modulation used. The jitter was determined by low power circuits which can be designed with high precision. Jitter would not present a major problem with a TWT transmitter provided that the TWT was modulated in such a fashion that the electron beam is switched on and had reached equilibrium before the r.f. drive was applied. Any of the three types of modulator suitable for TWT's described in Chapter 3 would be suitable for this purpose.

The limitation on the TWT's interline noise performance was the noise produced by the tube itself. The measured noise level of the TWT tested varied between 110 and 130 dB/Hz below a spectral line depending upon the frequency separation from that line. This would be adequate to give a clutter rejection of 80-100 dB which is considered to be sufficient to meet most system requirements. If higher levels of clutter rejection were required then more work on the design of tubes would be needed to investigate the causes and to reduce interline noise generation.

The noise level of -130 dB/Hz measured can be equated to the noise that could be expected if the tube could be run c.w. In this case the noise would be -156 dB/Hz below the carrier. This noise level is then equivalent to a noise figure of 38 dB, which is a typical figure which has been measured on c.w. tubes of a similar type.

The interline noise generated by the TWT showed some of the characteristics of flicker or $1/f^{n}$ type noise at frequencies below 2 kHz. This effect was not very pronounced and the noise was generally fairly flat within the range of measurement. In this case any attempt to reduce the noise should concentrate on reducing the noise figure in the first instance. Very successful programmes of noise reduction have been performed on low power c.w. receiver TWT's and a similar approach could be adopted. The noise of these tubes has been reduced by ensuring that the beam is laminar and well formed and that the interception on the structure is low. This has generally necessitated the use of multiple focussing electrodes at different voltages in the electron gun and close attention to the beam confining magnetic field.

Such techniques have never been used in high power tubes partly because of the great difficulties in designing and fabricating a multi-electrode high power gun which can withstand the high power involved and

partly because of the complication of the power supply providing the different voltages for these focussing electrodes. Beam confinement in high power tubes requires either bulky solenoids or periodic permanent magnet (PPM) focussing which is usually smaller. Solenoid focussing provides a more uniform beam with a lower interception on the slow wave structure. PPM focussing cannot produce such a uniform beam and if a low noise tube was required, solenoid focussing would be preferred.

In view of the difficulty in attempting to reduce interception and noise in high power tubes any work of this nature would be very costly and time consuming. Since the existing devices are adequate for all current and projected needs such a programme would be superfluous at this stage.

The results achieved with the TWT are broadly similar to those obtained by Sann [26] although Sann was working entirely with low power klystron amplifiers. However the beam forming and focussing systems for klystrons are similar to TWT's and so a similar performance could be expected for low power tubes. A high power klystron amplifier has been investigated by Cooper [38] and in this case the interline noise was only about 100 dB/Hz below a spectral line. This could be caused by the very high interception levels on the output cavity of high power klystrons which suggests that TWT's, with their lower interception, would have a lower noise level. Warren [28] working with an X-band medium power TWT, has measured noise levels of better than 140 dB/Hz using a tube with solenoid focussing, which tends to support the supposition that good beam formation and focussing are important if low noise is needed.

(b) 100 kW CFA

The major cause of interline noise produced by the CFA transmitter was exactly the opposite of the TWT since the CFA's self generated noise was dominant. The A.M. and P.M. noise levels were 30-40 dB higher than the noise measured with the TWT, but no power supply components were seen. No changes in the tubes operating parameters affected the interline noise. It was significant that the jitter of the front edge of the pulse did not contribute towards the noise. This situation might be different if very short pulse lengths were used since 'edge' noise would then become a larger proportion of the total noise.

The noise produced by the CFA varied very little with frequency separation from the fundamental spectral line and the characteristics of the noise looked the same as white noise with no underlying structure. Although the noise level was so much higher than that produced by the TWT the radar system performance was degraded only slightly since power supply ripple had limited the performance of the TWT. The clutter cancellation obtained was about 65 dB which represents the best that could possibly be achieved with this CFA because of its high noise output.

Very few measurements of interline noise generated by CFA's have been reported. Schoffield [39] has measured the noise produced by an experimental injected beam CFA operating at S-Band and with a peak power output of 300 kW. The P.M. noise output in this case was about 90 dB/Hz below a spectral line. Only limited measurements were possible because the maximum P.R.F. which could be used was 400 Hz resulting in spectral lines only 400 Hz apart. It is difficult to compare this result with the work reported here because the operating mechanisms of the two tubes are so different.

It is difficult to suggest any useful approach towards reducing the noise generated by the CFA since its operating mechanism is so complex. However recent research reported by Damon et al [40, 41] on injected beam CFA's has shown that broad band noise generated by the tube could be reduced by 20-30 dB by tilting the magnetic field in the gun region by 1-2°. This may lead to a similar reduction in interline noise. Without such a reduction the use of CFA's in pulse doppler radar systems is severely limited.

The fact that no power supply ripple lines appeared in the interline noise spectrum demonstrated that the inverter technique of using a chopping frequency equal to a multiple of the P.R.F. worked well. Application of this technique to power supplies for gridded TWT's could result in a transmitter capable of very stable performance suitable for pulse doppler radar systems with excellent clutter rejection.

CONCLUSIONS

The following conclusions may be drawn from the work described in this thesis:-

1. A simple additive noise measuring system for measuring interline noise on pulsed microwave amplifiers has been derived. The sensitivity of the system was 130 dB/Hz below the fundamental spectral line of the pulse spectrum for signals with a duty ratio of 5%. This sensitivity degrades to 94 dB/Hz for signals with 0.1% duty ratio. The measurement accuracy was ± 3 dB.

2. This basic noise measuring system was improved using a cancellation circuit which gave a sensitivity of 150 dB/Hz at 5% duty and 116 dB/Hz at 0.1% duty. The measurement accuracy was held at ± 3 dB but the special calibration circuit devised was essential using the cancellation circuit.

3. Great care must be taken in making these measurements since the results can easily be prejudiced by r.f. leakage or ground loops.

4. The phase noise generated by the VA133G 5 kW peak power, PPM focussed TWT was 120-130 dB/Hz below a spectral line at 5% duty. The amplitude noise was about 10 dB lower than the phase noise.

5. The power supply for the 5 kW TWT was the major contributor to the interline noise, producing mains related modulations 70-80 dB

below a spectral line. These limited the performance of the radar system. With careful design, noise introduced by power supply components could be eliminated, leaving the tube noise as the final limiting factor.

6. Although no measurements could be made to demonstrate this hypothesis it was felt that a major contributor to the tube noise could have been interception on the slow wave structure. This was corroborated to some extent by Coopers' measurements on a klystron which had very much greater interception and a higher noise output. If interception is a contributor to the tube noise then solenoid focussing might give better beam confinement than PPM focussing and consequently a lower noise level.

7. The phase noise generated by the QKS1319 100 kW peak power CFA was 85 dB/Hz below a spectral line at 2% duty. The amplitude noise was a few dB below the phase noise.

8. The power supply for the CFA did not contribute any measurable interline noise. This demonstrates not only the CFA's insensitivity to variation of its supply voltage but also that the inverter techniques used in the power supply worked as expected.

9. The TWT has a very much better interline noise performance than the CFA and is therefore the best choice of broadband power amplifier for use in systems, such as pulse doppler radars, which require high stability.

10. An inverter power supply with the chopping frequency locked to a multiple of the P.R.F. is capable of very good stability with small size and high efficiency. This type of power supply would be a good choice for systems requiring high stability.

Suggestions for further work are limited. The sensitivity of the noise measuring equipment is more than adequate for current needs and improvements could be made simply by increasing the power available from the source. At present existing travelling wave tubes offer an interline noise performance which is good enough for all current and projected equipments and the effort and expense needed to improve their performance could not be justified.

However if the need arose the following avenues could usefully be explored:-

1. A direct comparison of PPM and solenoid focussing on the tube noise, monitoring interception on the slow wave structure.

2. Examination of the electron gun geometry to improve the focussing of the electron beam.

3. A study of the noise already on the electron beam as it enters the interaction region. A better understanding of the noise properties of high power pulsed electron guns could lead to improvements in noise performance.

4. Careful design of the collector to reduce or eliminate reflected electrons which would otherwise be intercepted by the slow wave structure. This is an effect known to have caused an increase in noise due to the extra interception and found during work on depressed collector TWT's.

5. The work reported by Damon suggests that improvements to the noise generated by injected beam CFA's can be made. Further research in this area is continuing and it is likely to bear more fruit than work on distributed emission CFA's. The injected beam CFA has its electron beam formed outside the interaction region and consequently the beam is more amenable to control.

APPENDIX 1

ANALYSIS OF THE EFFECT OF JITTER IN PULSE TIMING AND PULSE LENGTH

1. The Perfect Pulse

The pulse train transmitted by radar systems approximates to a periodic function and can be expressed in terms of a Fourier series each term of which represents a spectral component of the pulse train in the frequency plane.

This series can be shown (Reference 36) to be given by:-

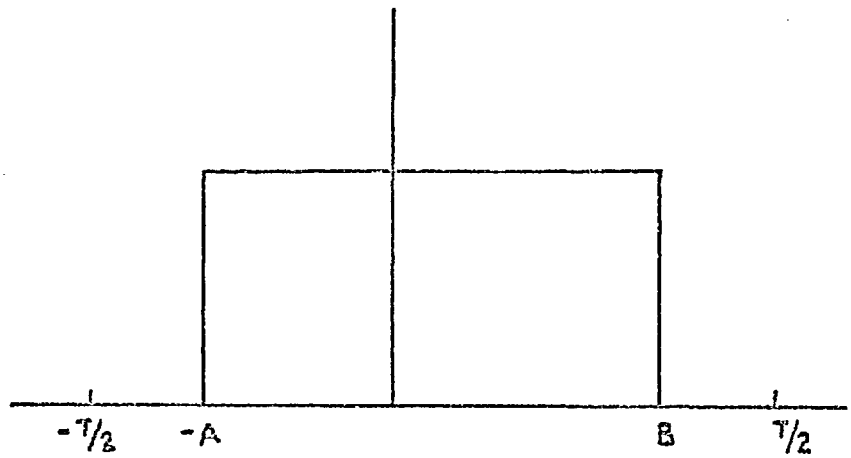
$$f(t) = \sum_{k=-\infty}^{\infty} \frac{C_K}{T} e^{-j W_k t} \qquad [A1.1]$$

where T is the period of the function and $\frac{C_K}{T}$ is the amount of the k^{th} harmonic W_k, contained in f(t).

C_k is determined by evaluating the integral

$$C_k = \int_{t_0}^{t_0 + T} f(t)\, e^{-j W_k t}\, dt \qquad [A1.2]$$

Consider a pulse train, one period of which is shown below.



The pulse width is A + B and the period T.

From Equation A1.2 it can be shown that:-

$$C_0 = \frac{A + B}{T} \qquad [A1.3]$$

and $$C_n = \frac{1}{2\pi jn} \left[e^{jnw\,A} - e^{-jnw\,B} \right] \qquad [A1.4]$$

and if d is the duty cycle $= \left(\frac{A + B}{T}\right)$

then the standard result is obtained:-

$$f(t) = \sum_{n = -\infty}^{\infty} \frac{\text{Sin } n\pi d}{n\pi} \; e^{jnwt} \qquad [A1.5]$$

This represents a spectrum of discrete lines spaced at a frequency of $1/T_0$ (the PRF) the envelope of which is a sin x/x function.

This analysis can be extended to cover the case of jitter in pulse length and pulse repetition interval.

2. Jitter in Pulse Length

The pulse represented in the figure had edges defined by -A and B. If jitter occurs then the positions of these edges will vary. For convenience let the jitter be periodic of the form

$$A + a \cos w_a t$$

$$B + b \cos w_b t$$

Equation A1.3 gives the amplitude of the fundamental line of the spectrum. This now becomes:-

$$C_o = \frac{A + B}{T} + \frac{a}{2T}\left[e^{jw_a t} + e^{-jw_a t}\right] + \frac{b}{2T}\left[e^{jw_b t} + e^{-jw_b t}\right]$$

This single spectral line is replaced by five lines - the fundamennal line and two pairs of modulation lines spaced at f_a and f_b from the fundamental line.

The amplitude at the other spectral lines is derived from Equation A1.4:-

$$C_n = \frac{1}{2\pi nj}\left[\exp[jnw(A + a \cos w_a t)] - \exp[-jnw(B + b \cos w_b t)]\right]$$

$$= \frac{1}{2\pi nj}\left[e^{jnw A} \sum_{m=-\infty}^{\infty} J_m(nwa)\, e^{jm\left(w_a t + \frac{\pi}{2}\right)} - \right.$$

$$\left. e^{-jnw B} \sum_{l=-\infty}^{\infty} J_l(nwb)\, e^{jl\left(w_a t + \frac{\pi}{2}\right)}\right]$$

Each of the terms in this equation represents an infinite series of modulation lines spaced at the respective jitter frequencies. If the jitter amplitude is small (< 1 ns) then

$$J_m(k) \doteq \frac{x^m}{2^k m!}$$

in which case the jitter lines decrease in amplitude very rapidly as m or l increases.

3. Jitter in Pulse Repetition Interval

The length of the pulse does not vary but its position in time does. In this case the jitter on the leading and trailing edges of the pulse is synchronous and can be represented thus:-

$$A + a \cos w_a t$$

$$A - a \cos w_a t$$

There are now no lines modulating the fundamental spectral line because C_o reduces to $\frac{A + B}{T}$ again.

At the other spectral lines

$$C_n = \frac{1}{n\pi} \sin(nw A) \sum_{m=-\infty}^{\infty} J_m(nw A)\, e^{jm\left(w_a t + \frac{\pi}{2}\right)}$$

and jitter lines appear as before.

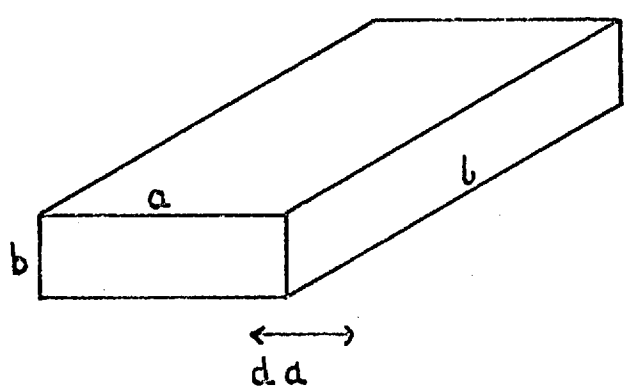
4. Random Jitter of either Edge of the Pulse

Random jitter can be considered as jitter at all frequencies and will thus produce a noise like modulation spectrum about each spectral line. However for a finite jitter amplitude random jitter could never produce a worse effect than periodic jitter at a single frequency.

APPENDIX 2

PHASE MODULATION DUE TO VIBRATION IN WAVEGUIDE COMPONENTS

1. Vibration of the broad wall dimension



Suppose the above length of waveguide has its broad wall vibrated in width by $f(A) = A \sin w_a t$.

The phase shift produced by the guide is given by:-

$$\phi = \frac{2\pi l}{\lambda g}$$

$$\frac{d\phi}{d\lambda_g} = \frac{2\pi}{\lambda_g^2}$$

For the normal TE_{10} mode of the waveguide

$$\frac{1}{\lambda_g^2} = \frac{1}{\lambda_0^2} - \frac{1}{4a2}$$

$$-\frac{2}{\lambda_g^2}\frac{d\lambda_g}{da} = \tfrac{1}{2}\left(\frac{1}{a^3}\right)$$

$$\frac{d\lambda_g}{da} = -\tfrac{1}{4}\left(\frac{\lambda_g}{a}\right)^3$$

$$\frac{d\lambda_g}{da} \cdot \frac{d\phi}{d\lambda_g} = \frac{d\phi}{da} = \frac{\pi 1 \lambda_g}{2a^3}$$

The waveguide input can be represented by $E_0 \cos w_o t$ and the output by $E_0 \cos(w_o t + \phi(t))$

$$\phi(t) = \phi_0 + d\phi$$

where ϕ_0 is the fixed phase shift down the length of the guide.

$$d\phi = \frac{\pi 1 \lambda_g}{2a^3}\, da$$

$$\text{So } E = E_0 \cos\left[w_o t + \phi_0 + \frac{\pi 1 \lambda_g}{2a^3} A \sin w_a t\right]$$

Neglecting ϕ_0 which is constant and substituting A_m for

$$\frac{\pi l \lambda_g A}{2a^3}$$

$$E = E_0 \cos[w_o t + A_m \sin w_a t]$$

For small amplitudes of vibration A_m is small and $\cos(A_m \sin w_a t) \rightarrow 1$ and $\sin(A_m \sin w_a t) \rightarrow A_m \sin w_a t$.

$$\text{So } E = E_0 \cos w_o t - E_0 A_m \sin w_a t \sin w_o t$$

$$= E_0 \cos w_o t - \frac{E_0 A_m}{2} \cos (w_o \pm w_a) t$$

Thus for small values of vibration the microwave carrier will be modulated with two sidebands of amplitude $\frac{E_0 A_m}{2}$ at frequencies of $f_o \pm f_a$.

It is now of interest to insert some typical figures into these equations to determine what levels of vibration could be tolerated. Consider a system operating at 1300 MHz in waveguide size WG6 and requiring and interline noise level of 100 dB.

The vibration sideband amplitude is given by:-

$$\frac{\pi l \lambda_g A}{4a^3}$$

Let the length of the waveguide be 1 metre

λ_g at 1300 MHz in WG6 = 0.32 m

a = 0.165 m.

For -100 dB sidebands

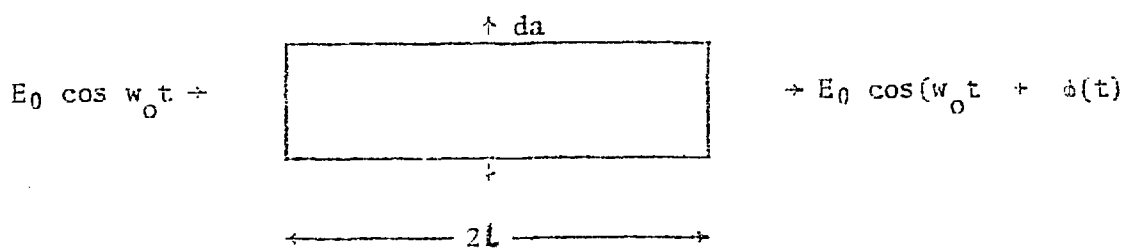
$$\frac{\pi 1 \lambda_g A}{4a^3} = 10^{-5}$$

$$A = \frac{4a^3 \, 10^{-5}}{\pi 1 \lambda_g} = \frac{4 \times (0.165)^3 \times 10^{-5}}{\pi \times 0.32} = 18 \times 10^{-8} \text{ m}$$

Thus to get acceptable levels of modulation the vibration amplitude must be less than 0.18 μm.

2. Vibration in length of a section of waveguide

Consider a length of waveguide length 2l clamped at both ends and vibrated across its axis in a periodic manner such that $f(a) = A \sin w_a t$.



The transverse movement of the waveguide will produce changes dl in the length l.

$$(l + dl)^2 = da^2 + l^2$$

$$2l\,dl = da^2 \quad (dl^2 \text{ very small})$$

$$d\phi = \frac{2\pi}{\lambda_g}\, dl$$

$$\text{So} \quad \frac{l\lambda_g}{\pi}\, d\phi = da^2$$

Signal out of waveguide will be

$$E_0 \cos(w_o t + \phi_0 + d\phi).$$

$$E_o \cos\left(w_o t + \frac{\pi}{l\lambda_g} (da)^2\right) \quad \text{ignoring fixed phase shift } \phi_0$$

da is given by A sin $w_a t$.

$$\text{So } E = E_0 \cos\left(w_o t + \frac{\pi}{l\lambda_g} A^2 \sin^2 w_a t\right)$$

$$= E_0 \left[\cos w_o t \cdot \cos\left(\frac{\pi}{l\lambda_g} A^2 \sin^2 w_a t\right) - \right.$$

$$\left. - \sin w_o t \sin\left(\frac{\pi}{l\lambda_g} A^2 \sin^2 w_a t\right)\right]$$

For small A

$$\cos\left(\frac{\pi}{1\lambda_g} A^2 \sin^2 w_a t\right) \rightarrow 1$$

$$\text{and } \sin\left(\frac{\pi\lambda^2}{1\lambda_g} \sin^2 w_a t\right) \rightarrow \frac{\pi\lambda^2}{1\lambda_g} \sin^2 w_a t$$

$$E = E_0 \left[\cos w_o t - \frac{\pi}{1\lambda_g} A^2 \sin w_o t \sin^2 w_a t\right]$$

Considering second term only this becomes.

$$\frac{E0\pi}{21\lambda_g} A^2 \sin w_o t \,[1 - \cos 2 w_a t]$$

$$= \frac{E0\pi}{21\lambda_g} A^2 \,[\sin w_o t - \tfrac{1}{2} \sin (w_o \pm 2 w_a)t]$$

So lateral vibration of a length of waveguide will produce a pair of sidebands, amplitude $\frac{E0\pi}{41\lambda_g} A^2$, at frequencies of $f_o \pm 2 f_a$.

Again it is of interest to insert typical values as before. Let the length of the waveguide be 1 metre and let the system frequency be 1300 MHz transmitted through waveguide size WG6. The interline noise level required is again -100 dB.

$$\lambda_g = 0.32 \text{ m.}$$

For -100 dB sidebands:-

$$\frac{\pi}{41\lambda_g} A^2 = 10^{-5}$$

$$A^2 = \frac{41\lambda_g}{\pi} \times 10^{-5}$$

$$\therefore A = 4.4 \text{ mm}$$

From practical considerations flexing of an entire length of waveguide is a very likely mode of vibration and fortunately the above calculation demonstrates that the modulation produced is very low for quite high levels of vibration.

APPENDIX 3

Data Sheets of the VA133G 5 kW Travelling Wave Tube and for the QKS1319 100 kW Crossed Field Amplifier.

VARIAN VA 133G

PULSED TRAVELLING WAVE AMPLIFIER

DESCRIPTION

The VA-133G is a pulsed travelling wave amplifier for use as a final amplifier in multioutput-tube radar equipment. It is an ideal pulsed driver tube for megawatt amplifiers of frequency agile, coherent radar systems. This grid pulsed tube produces a peak output of 5 kilowatts with pulses as long as 600 microseconds. The tube is cooled by liquid and forced air. It is focused by an integral, periodic, permanent magnet and is of all metal-ceramic construction.

FEATURES

Broadband-High-Power

Provides peak output pulses of at least 5 kilowatts over its 150-MHz bandwidth without adjustments.

Periodic Permanent Magnet Focusing

Needs no magnet power supply.

Long Pulse Duration

Permits peak output pulses of 600 microseconds duration at a 6% duty cycle.

High Gain

Gain of at least 47 dB minimizes drive power requirements.

GENERAL CHARACTERISTICS

Electrical

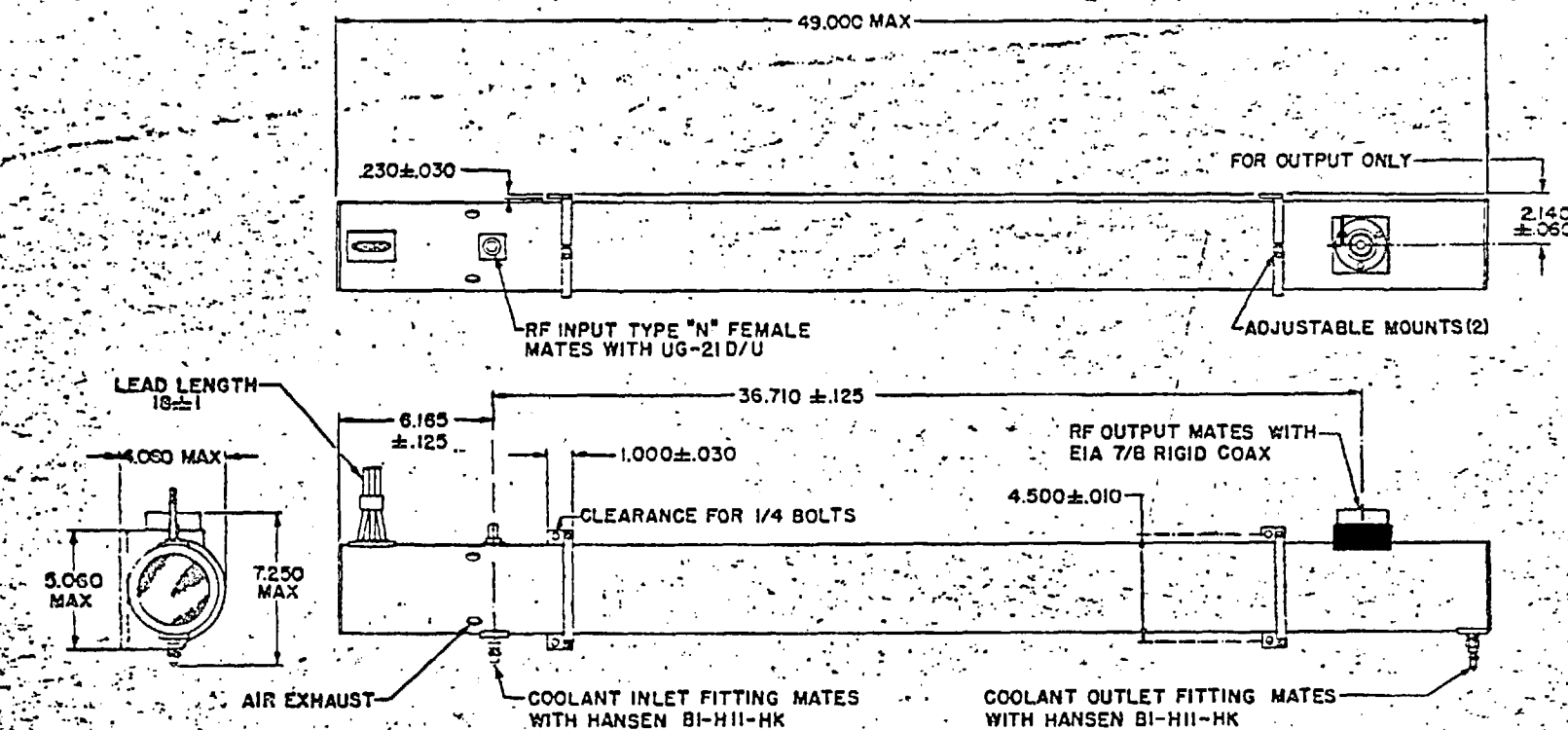
Frequency Range	1.25 to 1.40 GHz
Peak Output, minimum	5 kW
Average Output	300 W
Gain, minimum	47 dB
Capacitance, grid to all other electrodes	115 pf
Heater Voltage	12.6 V
Heater Current, typical	3.8 A
Heater Warm-Up Time	3 min

Physical

Dimensions	See Outline Drawing
Weight, approximate	65 lb
Mounting Position	Any
Cathode	Oxide coated, unipotential
Focusing	Periodic Permanent Magnet
Cooling	Liquid and Forced Air
Water Flow, minimum	0.5 gpm
Pressure Drop, max at 0.5 gpm	20 psi
Air Flow, minimum	5 cfm

OPERATING CONDITIONS AND RATINGS

	Typical Operation	Maximum Ratings	
Frequency Range	1.25 to 1.40	---	GHz
Peak Output	5	---	kW
Gain	47	---	dB
Duty Cycle, beam	---	0.06	
Pulse Duration, beam	---	600	μsec
Beam Voltage	10.0	15.0	kVd.c.
Beam Current, peak	2.5	3.0	a
Grid Voltage, peak	230	250	V
Grid Bias Voltage	-150	-500	Vd.c.
Drive Power	0.1	2	W
Heater Voltage	12.6	13.0	V
Heater Current	3.8	---	A
Heater Surge Current	---	7.0	A
Load V.S.W.R.	---	1.3:1	
Source V.S.W.R.	---	1.3:1	



COLOR CODE	
YELLOW	HEATER-CATHODE
BROWN	HEATER
GREEN	GRID

NOTE:
DIMENSIONS ARE IN INCHES.

VA-133G OUTLINE DRAWING

VA-133G
Rev. A
2/13/67

RAYTHEON QKS1319 CFA



QKS1319 CROSSED FIELD AMPLIFIER

The QKS1319 is a pulsed, forward-wave type of crossed-field amplifier capable of 100 kilowatts peak power output over the frequency range 1200 to 1400 MHz. It operates directly across a d.c. power supply and provides an instantaneous constant voltage bandwidth of 15% with 15 dB gain. Pulsing is accomplished by r.f. beam turn on and by low energy turn off via a control electrode (mu = 3). The tube permits light-weight radar design with sophisticated pulse coding and high power output at low operating voltage.

The QKS1319 features a cold secondary emitter cathode, an integral, shielded permanent magnet, and coaxial r.f. input and output couplers. It requires liquid cooling.

Reliable operation and optimum tube life can be achieved only if the radar transmitter is designed with the CFA characteristics clearly in mind. This preliminary data sheet is intended only to acquaint the reader with the basic characteristics of this tube and should not be used alone for system design. Detailed information may be obtained by contacting the Marketing Department, Microwave and Power Tube Division, Raytheon Company, Willow Street, Waltham, Massachusetts 02154.

OPERATING CHARACTERISTICS

Electrical

Frequency	1250-1350 megahertz
Bandwidth	8%
Peak Power Output	100 kilowatts
Average Power Output	3 kilowatts
Duty Cycle	.03
Pulse Duration	300 microseconds

Anode Voltage ..... 10 kilovolts
Peak Anode Current ..... 20 amperes
Heater ..... none
Driver Peak Power ..... 5 kilowatts, min
Gain ..... 13 dB
Efficiency 50%

Control Electrode Characteristics

Control Pulse Required ..... 8 kilovolts (positive, from cathode)
Pulse Current ..... 10 amperes, maximum
Pulse Duration ..... 0.5 microsecond, nominal
Electrode Capacity ..... 20 picofarads

Mechanical

Mounting Position ..... any
Dimensions ..... 8" dia x 16" (excl r.f. couplings)
Weight ..... 35 pounds
Cooling ..... 2 gpm, 15 psi water or glycol-water
Input Bushing ..... air insulated (10,000')

R.F. Couplings

Input: ..... $\frac{7}{8}$" EIA coax (50 ohm)
Output: ..... 1-5/8" EIA coax (50 ohm)
Pressurization ..... 14 psia, min

APPENDIX 4

4.1 Analysis of the Action of the Phase Sensitive Detector

The action of the PSD was demonstrated using vector representation in Chapter 5. The action can also be illustrated mathematically as follows.

Firstly consider a signal

$$\bar{S} = (\bar{V}_2 + \bar{n})e^{jwt}$$

The amplitude of this signal is given by its modulus $|S|$.

$$|S|^2 = |\bar{V}_2 + \bar{n}|^2$$

$$= V_2^2 + \bar{V}_2\bar{n}^* + \bar{V}_2^*\bar{n} + n^2$$

n^2 is small and may be neglected,

and $$|S| \simeq V_2 + \tfrac{1}{2}[\bar{V}_2\bar{n}^* + \bar{V}_2^*\bar{n}]/V_2$$

and if $\bar{S}$ were detected by an amplitude detector then the output would be the A.M. noise on $\bar{S}$,

and $$\underline{n_A = [\bar{V}_2\bar{n}^* + \bar{V}_2^*\bar{n}]/2V_2}$$

The phase of the signal is given by

$$\arg S = \tan^{-1}\left[\frac{\mathrm{Im}\ (\bar{V}_2 + \bar{n})}{\mathrm{Re}\ (\bar{V}_2 + \bar{n})}\right] \equiv \theta$$

and

$$\tan\theta = \left[\frac{\mathrm{Im}\ (\bar{V}_2 + \bar{n})}{\mathrm{Re}\ \bar{V}_2}\right] \frac{1}{\left(1 + \frac{\mathrm{Re}\,\bar{n}}{\mathrm{Re}\,\bar{V}_2}\right)}$$

$$= \left[\frac{\mathrm{Im}\ (\bar{V}_2 + \bar{n})}{\mathrm{Re}\ \bar{V}_2}\right]\left[1 - \frac{\mathrm{Re}\ \bar{n}}{\mathrm{Re}\ \bar{V}_2}\right]$$

$$\simeq \frac{\mathrm{Im}\ \bar{V}_2}{\mathrm{Re}\ \bar{V}_2} + \frac{\mathrm{Im}\ \bar{n}}{\mathrm{Re}\ \bar{V}_2} - \frac{\mathrm{Im}\ \bar{V}_2\ \mathrm{Re}\ \bar{n}}{V_2^{\,2}}$$

if $\bar{n}$ is small:

$$\equiv \tan(\phi + \delta)$$

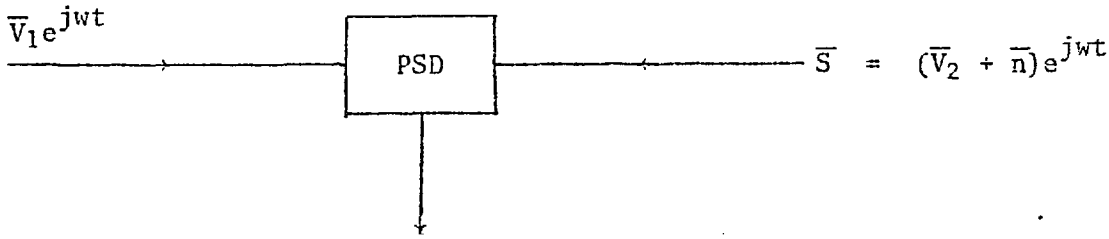
where $\tan\phi = \dfrac{\mathrm{Im}\ \bar{V}_2}{\mathrm{Re}\ \bar{V}_2}$

and for δ small:-

$$\delta = \frac{\mathrm{Re}\ \bar{V}_2\ \mathrm{Im}\ \bar{n} - \mathrm{Im}\ \bar{V}_2\ \mathrm{Re}\ \bar{n}}{V_2^{\,2}}$$

which is the phase modulation portion of the noise and would be detected as $K\delta$ if a P.M. detector was used.

Now consider an ideal PSD:-



$|V_1||S| \cos\theta$ where $\theta = \arg S - \arg V_1$

In this case $\theta = (\phi + \delta) - \psi$

where $\psi = \arg V_1$

$\phi + \delta = \arg S$

If $\psi = \phi$ then $\cos\theta \rightarrow \cos\delta \rightarrow 1$ for δ small

and PSD output $= |V_1||S|$

which is the A.M. noise contribution.

if $\psi = \phi + \frac{\pi}{2}$

$\cos\left(\delta - \frac{\pi}{2}\right) = -\sin\delta \rightarrow -\delta$ if δ is small.

So PSD output $= V_1 S \delta$

$= V_1 V_2 \delta + V_1 n_A \delta$

$= V_1 V_2 \delta \equiv K\delta$

since $n_A\delta$ is second order.

ie the PSD output now becomes the P.M. noise contribution by changing the relative phase by 90°.

By inserting 90° of phase shift the A.M. component of the signal will never be completely cancelled, but in excess of 40 dB cancellation has been observed. If the phase error is E then

$$\text{PSD output} = V_1 S \cos(\phi + E + \delta - \psi)$$

$$\text{and if } \psi = \phi + \frac{\pi}{2}$$

$$\text{PSD output} = V_1 S \cos\left(E + \delta + \frac{\pi}{2}\right)$$

$$= -V_1 S \sin(E + \delta)$$

$$= -(V_1 S E + V_1 S \delta) \quad \text{if } E + \delta \text{ small.}$$

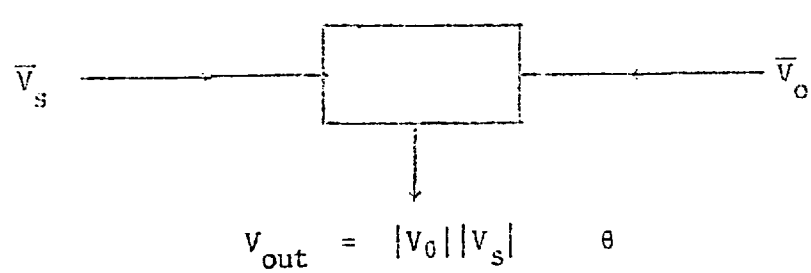
$V_1 S E$ is the cancelled portion of the A.M. component of the signal, and for 40 dB cancellation

$$|E| = 10^{-2} \simeq \frac{180 \times 10^{-2}}{\pi} \simeq 0.6°$$

So the accuracy of the phase relationship of V_1 and S must be better than 0.6° to achieve 40 dB cancellation of the A.M. modulation.

4.2 Cancellation of P.M. Noise on the Source by the PSD

Again consider the ideal PSD:-



where $V_s = A_o (1 + A) e^{jwt}$

$V_o = B_o (1 + A + A')e^{jwt}$

where A is noise on source

and A' is noise generated by the power amplifier.

$|V_s| \simeq A_o (1 + A)$

and $|V_o| \simeq B_o (1 + A + A')$

Let $\arg V_s = \gamma$ and $\arg V_o = \gamma + \phi$

$\theta = \arg V_o - \arg V_s - \alpha$

where α is phase difference inserted in the noise measuring system.

$V_{out} \simeq A_o B_o (1 + A)(1 + A + A') \cos (\phi - \alpha)$

$\simeq A_o B_o (1 + 2A + 2') \cos (\phi - \alpha)$

If $\alpha = 0$

$V_{out} \simeq A_o B_o (1 + 2A + A')$ assuming ϕ small.

This is the amplitude modulation and includes the amplitude noise on the source.

If $\alpha = \frac{\pi}{2}$

$V_{out} \simeq A_o B_o \phi$ assuming ϕ, A and A' small.

This is the P.M. noise generated by the power amplifier and the source noise has been cancelled. In general the A.M. noise generated by oscillators of the sort used in very stable systems, is very small and can be neglected by comparison with the P.M. noise produced.

REFERENCES

1. Skolnik M I, Introduction to Radar Systems, Chapter 12, McGraw-Hill 1962.
2. Hadad J D, Basic Relation Between the Frequency Stability Specification and the Application, Proc 1964 IEEE-NASA Symposium on the Definition and Measurement of Short-Term Frequency Stability, Washington DC US Govt, Printing Office, NASA SP-80, 1965, pp 11-18.
3. Leason D B and Johnson G F, Short-Term Stability for a Doppler Radar: Requirements, Measurements and Techniques, op cit, pp 3-10.
4. Goetz L P and Skillman W A, Master Oscillator Requirements for Coherent Radar Sets, op cit, pp 19-28.
5. Raduziner D M and Gillespie N R, Coherent Radar F.M. Noise Limitations, op cit, pp 29-38.
6. Caldwell Jr, J J, Satellite Range and Tracking Accuracy as a Function of Oscillator Stability, op cit, pp 39-42.
7. Sydnor R L, Short-Term Stability Requirements for Deep Space Tracking and Communications Systems, op cit, pp 43-50.
8. Shields R B, Review of the Specification and Measurement of Short-Term Stability, Microwave Journal, Vol 12, No 6, June 1969.
9. Mooney D and Ralston G, Performance in Clutter of Airborne Pulse MTI, C.W. Doppler and Pulse Doppler Radar, IRE International Convertion Record, Part 5, 1961, pp 55-62.
10. Sydnor R, Caldwell J J and Rose B E. Frequency Stability Requirements for Space Communications and Tracking Systems, Proc IEEE, Vol 54 No 2, February 1966, pp 231-236.

11. Raven R S, Requirements on Master Oscillators for Coherent Radar, op cit, pp 237-243.

12. Leeson D B and Johnson G F, Short-Term Stability for a Doppler Radar: Requirements, Measurements and Techniques, op cit, pp 244-248.

13. Bungung J J, Nesbeda P and Safran H, A Unified Analysis of Range Performance of C.W., Pulse and Pulse Doppler Radar, Proc IRE October 1959, pp 1753-1762.

14. Drage S A and Marsh S B, Equipment for Measuring Spurious Modulation of X-Band C.W. Oscillators, RRE Memorandum No 1201 November 1955.

15. Technical Report on the Theory of Operation and Sensitivity of the NME Type 123, Application Note No G5/101, James Scott (Electrical Engineers) Ltd 1962.

Technical Note on Improved High-Power NME's Type 123, Application Note No G5/102, James Scott (Electrical Engineers) Ltd, 1962.

16. Grauling Jr, C H and Healey III, D J, Instrumentation for Measurement of the Short-Term Frequency Stability of Microwave Sources, Proc IEEE, Vol 54, No 2, February 1966, pp 249-257.

17. Whitwell A L and Williams N, A New Microwave Technique for Determining Noise Spectra at Frequencies Close to the Carrier, Microwave Journal November 1959 p 27.

18. Ashley J R, Searles C B and Palka F M, The Measurement of Oscillator Noise at Microwave Frequencies, IEEE Trans on Microwave Theory and Techniques, Vol MTT 16, No 9, September 1968, pp 753-760.

19. Ondria J G, A Microwave System for Measurements of A.M. and F.M. Noise Spectra, op cit, pp 767-780.

20. Blomfield D L H, Private Communication.

21. Cooper D, The Measurement of the Spectral Distribution of Incidental Noise Modulation on Pulsed Microwave Signals: An Examination of the Possibilities of Using an Instrument Intended for Measurements on Continuous Signals and Theoretical Analysis. Marconi Co Interim Technical Memorandums Nos 2688 and 2689 November 1967. The Marconi Co Ltd, Research Laboratories, Great Baddow, Chelmsford Essex.

22. Koontz R F, Fine Grain Spectrum Analysis of Pulsed Microwave Amplifiers, IRE Trans on Microwave Theory and Techniques November 1962.

23. Burnsweig J, Hurt F and O'Brien H, Intra-Spectral Noise and Transfer Functions of Pulsed Final Power Amplifiers, Proc 1964 IEEE, Electron Devices Meeting, October 29, 1964 Washington DC.

24. Smith M J, Noise Measurements on Pulsed Electrostatically Focussed Klystrons, Proc of Conference on Microwave and Optical Generation and Amplification, Cambridge 1966.

25. Feasibility Study on the Noise Measurement of Pulsed Microwave Signals. Interim Reports Nos 1-3 and Final Report. Contract No KH/Q/178CB15(a)2. James Scott (Electrical Engineers) Ltd, 1968.

26. Sann K H, The Measurement of Near Carrier Noise in Microwave Amplifiers IEEE Trans on Microwave Theory and Techniques Vol MTT 16, No 9, September 1968, pp 761-766.

27. Straub W F, Measuring Excess Noise of Microwave Devices, Instruments and Control Systems, March 1970.

28. Warren K, Marconi Co Ltd, Private Communication.

29. Crowfoot T P, C-Band Amplitron Evaluation, Final Report, ASWE Laboratory Note No XRE-68-16 1968. Admiralty Surface Weapons Establishment, Portsdown.

30. Clark J, Further Evaluation of an X-Band Pulsed Amplitron and TWT Package, Report No TPA 534/19, Part 2, 1971, Royal Radar Establishment, Malvern.

31. Hollis E E, Matheson A I and Griffin W J, A.M. and P.M. Noise Measurements on a Cold Cathode CFA, Microwave Journal Vol 14, No 4, April 1971, pp 37-44.

32. Pierce J, Travelling Wave Tubes, Van Nostrand, 1950.

33. Gittins J F, Power Travelling Wave Tubes, English Universities Press, 1964.

34. Okress, Crossed Field Microwave Devices, Vols I and II, Academic Press, 1961.

35. Blomfield D L H, Private Communication.

36. Craig E J, Laplace and Fourier Transforms for Electrical Engineers, Chapters 8 and 9, Holt, Reinhart and Winston, 1964.

37. Mouw R B and Fukuchi S M, Broad-Band Double Balanced Mixer Modulators Parts I and II, Microwave Journal Vol 12, No 3, March 1969 and Vol 12, No 5, May 1969.

38. Cooper D, Marconi Co Ltd, Private Communication.

39. Schoffield B P, Royal Radar Establishment, Private Communication.

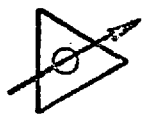
40. Damon L, Nicholls N S and Schoffield B P, The Reduction of Noise in High-Power Crossed Field Amplifiers. To be published in Electronics Letters.

41. Damon L, Nicholls N S and Schoffield B P, Noise Reduction in High Power Injected Beam Crossed Field Amplifiers by use of a Curved Magnetic Field. Proc European Microwave Conference, Brussels 1973.

APPENDIX 5

LIST OF SYMBOLS USED IN THE DIAGRAMS

Variable Phase Shifter



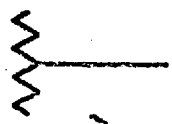
Variable Attenuator



Step Attenuator



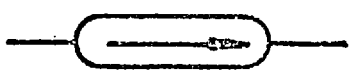
Dummy Load



Directional Coupler



Isolator



Diode Detector for Monitoring



APPENDIX 6

THE SPECIFICATION FOR THE COMPONENTS USED IN THE NOISE MEASURING SYSTEM

The components used in the different configurations of the noise measuring system described in Chapter 5 were carefully selected for the tasks they had to perform. In many cases standard components already available in the laboratory could be used but some of the more specialised components had to be purchased or made specifically for use in the equipment. In the following sections the specifications needed for each of the major components of the noise measuring system are discussed.

A6.1 THE BASIC NOISE MEASURING SYSTEM

The basic noise measuring system shown in Figure A6.1 includes sampling couplers before and after the pulsed amplifier under test, a phase shifter, level setting variable attenuators, phase sensitive detector (PSD), low noise audio amplifier and a spectrum analyser.

The flexible coaxial cable used for the r.f. connections was UR67 with Standard Type N connectors.

a. The Sampling Couplers

The power levels required by the PSD in its reference and signal arms were 10 mW and 1 mW respectively. Suitable microwave couplers were used to sample the signals at the input and output of the amplifier under test. Different types of coupler were needed for each sampling point. The input to the 5 kW t.w.t. was in UR67 flexible coaxial cable with Type N connectors and a commercial coaxial coupler was used in this position with a coupling factor

of 10 dB and a directivity of better than 20 dB. An isolator between the amplifier and this sampling coupler was essential since the VSWR of a typical amplifier was likely to be worse than 1.5:1. Reflections from this point could get into the reference arm of the noise measuring system and degrade the phase balance of the circuit. To achieve 40 dB cancellation of am in the PSD a phase accuracy of 0.5° and an amplitude accuracy of at least 1% is required. If the reflected leakage signal is in the worst phase relationship to the main signal then the maximum phase error, θ, is given by:

$$\text{Sin } \theta \simeq \frac{\text{Amplitude of reflected signal}}{\text{Amplitude of reference signal}}$$

For 0.5° error the amplitude of the reflected leakage signal must be less than 1% of the reference signal, ie 40 dB down.

If the VSWR of the amplifier is 1.5:1 the reflected signal is 14 dB down and with a coupler of directivity 20 dB the signal in the reference channel will only be 34 dB down which is insufficient. The isolator improved the VSWR to better than 1.1:1 which made the reflected power insignificant. The isolator was also required to protect both the source and the noise measuring system from arcs in the t.w.t. which reflect very high power r.f. pulses which could cause damage.

The output from the 5 kW t.w.t. was in $\frac{7}{8}$" EIA solid coaxial line and a specialised Narda Microwave Corporation coaxial 30 dB coupler was used in this position. The coupler had a directivity of 20 dB which was adequate since all measurements were made with the r.f. output coupled into a dummy load with a VSWR low enough to ensure that the reflected power was insignificant. The Narda coupler had Type N connectors on its output port and an ordinary low power coaxial coupler was used to reduce the power to approximately the level required. Final level setting was done using the variable attenuators.

For measurements at the 100 kW peak power level of the CFA a waveguide size WG6 crossguide coupler was used with a coupling factor of 30 dB and a directivity of 20 dB. This coupler was made at ASWE using standard aluminium waveguide and designed from information taken from the 1969 Microwave Handbook. WG6 crossguide couplers are now available from commercial sources.

b. Variable Attenuators and Power Meter

Variable attenuators were used in the reference and signal arms for accurately setting the power levels into the PSD. A microwave power meter was used to measure the power levels as shown in Figure A6.1, and therefore the attenuators used need not be calibrated accurately. These attenuators had an attenuation range of 1-20 dB which was adequate to cater for the

power levels used. The only desirable feature required was a low change of phase with change of attenuation, to avoid repeated resetting to achieve the phase balance of the circuit. Even fairly low grade, cheap, variable attenuators possess this feature and proved to be satisfactory.

The attenuators used in the noise measuring system were made by Microlab/FXR and the power meter was a Hewlett-Packard Model 431B.

c. Phase Shifter

The phase shifter was used to change the relative phase of the two signals into the PSD by 90° for am and pm measurements. Appendix 4 showed that to achieve 40 dB cancellation of am during pm measurements a setting accuracy of ± 0.6° was required. This could be achieved using either a crude, coaxial, trombone line stretcher or a precision calibrated coaxial phase shifter. However, it was much easier to adjust the precision phase shifter and this type of device was used for the measurements. The Narda Model 3752 phase shifter used had a range of only about 0-180° at the frequency of the measurements and a trombone line stretcher was used in series so that the final phase shifter setting for pm measurements could be adjusted to be at the middle of its range. This allowed am measurements to be made at two settings (± 90°) of the phase shifter. Correct operation of the measuring circuit could be assessed since the phase shifter was calibrated and if more or less than 90° of phase shift was required to go from pm to am settings then r.f. leakage was present which had to be eliminated.

Although the calibration of the phase shifter gave a useful check on the performance of the system it was not essential for correct operation of the circuit.

d. The Phase Sensitive Detector

The requirements for the PSD were as follows:

i) Low noise figure at low frequencies.

ii) High input power capability without burn-out or distortion, to give a high dynamic range.

iii) Good linearity.

iv) Good rejection of am noise on the reference channel since only pm noise on the source is cancelled by the operation of the noise measuring system.

v) Good isolation between ports.

As described in Chapter 5 several types of mixer for use as a PSD were examined. Point contact diode mixers were rejected at an early stage since their flicker noise was so high that an i.f. PSD would have been required. Back diode and Schottky diode mixers became available and both of these had very good low frequency noise figures. The back diode had a superior noise figure at low frequencies (15 dB at 1 kHz compared with 20 dB for the Schottky diode) but its power handling capabilities were very much lower than the Schottky diode. Overall the Schottky barrier mixer diode had a dynamic range advantage over the back diode of 10-15 dB. This was a significant advantage since the dynamic range of the PSD ultimately determined the sensitivity of the noise measuring system.

Once the type of diode best suited to the application had been chosen the mixer configuration was examined. A double balanced star connected mixer was finally chosen for the following reasons:

i) It used a bridge of 4 diodes which increased its power handling capability by 6 dB compared with a single ended mixer.

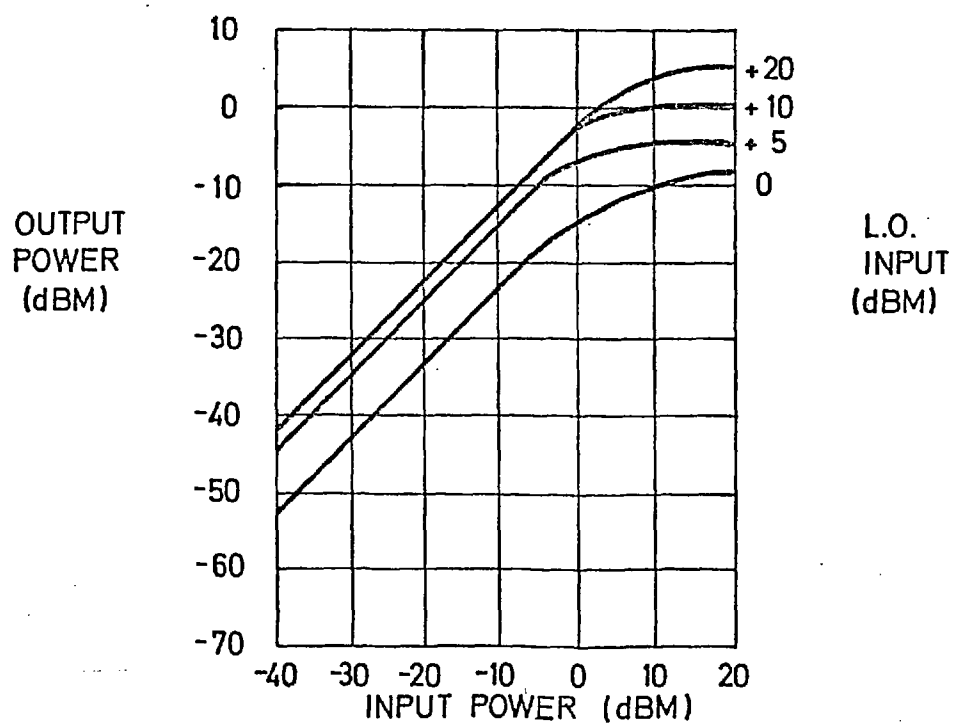
ii) The conversion loss was up to 6 dB lower than other mixer configurations.

iii) It had very good isolation between ports.

iv) The star connection of the diodes allowed direct coupling to the output port, eliminating a coupling capacitor and resulting in excellent low frequency response.

An Aertech Industries mixer was used, Model Number MX2000. This mixer is described in some detail by Mouw and Fukuchi [37].

The graph below, taken from Reference 37, shows the variation of output power with input power for various local oscillator or reference channel signal levels.



The linearity is excellent up to 0 dBm signal input power with either +10 or +20 dBm reference channel power. The lower limit would be set by the noise generated by the mixer.

e. The Low Noise Audio Amplifier

The low noise amplifier was required to boost the output from the PSD to a level sufficient to drive the spectrum analyser. The amplifier used was a Brookdeal Electronics Nanovolt Preamplifier Type 431. This amplifier was designed to give a good noise performance when coupled to low source impedances such as the PSD. It had a voltage gain of 60 dB and accepted a 1 mV input signal without distortion. A major advantage of this amplifier was its ability to operate off dry batteries thus eliminating the problem of stray pick-up by earth loops.

f. The Spectrum Analyser

The spectrum analyser used for the noise measurements had to have the following features:

i) Frequency coverage of at least 20 Hz to 20 kHz to allow measurement between several P.R.F. lines.

ii) A resolution sufficient to discriminate P.R.F. and power supply ripple lines.

iii) A dynamic range of at least 80 dB displayed at one time on a logarithmic scale.

iv) Good sensitivity.

v) Either a built-in X-Y or chart recorder or the provision of suitable outputs to drive an external recorder.

Capability for swept frequency measurements.

At the time these measurements were started the best available analyser was the Rhode and Schwarz Type FNA. This instrument had an 80 dB dynamic range displayed on a logarithmic scale and a minimum sensitivity of 1 μV. The frequency coverage extended from 30 Hz to 20 kHz with a resolution of 10 Hz to 3 dB and $\pm$ 30 Hz to 60 dB achieved using crystal filters. An integral X-Y recorder was available to plot the spectrum being measured on specially printed cards.

The analyser was easy to set up and very convenient to use. The spectra obtained were clear and relatively easy to interpret (see Figure 6.6). A longer averaging time would have been an advantage since the background noise level could then have been smoothed to its mean level more closely, making interpretation easier.

During the experimental programme a Hewlett-Packard wave analyser Type HP3590A/3594A became available. This instrument offered a more flexible performance than the Rhode and Schwarz. It had a frequency coverage of 30 Hz to 620 kHz with a 90 dB dynamic range and 10 Hz resolution. It also had facilities to use a longer averaging time than the Rhode and Schwarz although this would have significantly increased the duration of the measurements since the frequency would have to be swept more slowly.

The instrument was very much more expensive than the Rhode and Schwarz and did not have a built-in recorder. It was also more difficult to set-up and not so convenient in use although the overall results were better.

A6.2 THE CALIBRATION CIRCUIT

The calibration circuit is shown in Figure A6.2.

A sample of the output signal from the pulsed amplifier under test is coupled out via the 10 dB coupler, amplitude modulated by the PIN diode and added to the original signal in a 3 dB hybrid coupler. Provided that the modulated sample of the signal is small compared with the main signal then the addition in the hyrbid coupler will result in either am or pm calibration lines on the main signal, depending upon the phase relationship of the two signals. The principle is the same as that used by the noise measuring system to distinguish am from pm modulation.

If the two signals into the 3 dB hybrid are in phase then they will be added together directly in one output port and with a 90° phase difference in the other. This is a property of hybrid junction of this type. Therefore if the calibration channel signal is amplitude modulated then the resulting output at one port of the hybrid will be amplitude modulated and the other output will be phase modulated at the same level.

A detector diode and the spectrum analyser can be connected to the amplitude modulation output and the calibration line directly compared with a P.R.F. line to measure the exact level of calibration.

The PIN diode used was Marconi-Saunders Type Number 6053/1, and was capable of up to 30 dB attenuation. It was biased to produce about 10 dB attenuation by a $1\frac{1}{2}$ volt dry battery and potentiometer and the bias level was varied by a very small amount by a sine wave signal generator coupled to the diode through a capacitor. In this way a low level of amplitude modulation at 1 kHz was applied to the microwave signal. Provided that only low levels of modulation were used very little distortion was produced. PIN diodes used in this way produce purely amplitude modulation and very little phase modulation. However, this particular PIN diode did not have a very good VSWR and a ferrite isolator was used to prevent any of the modulated signal being reflected

back into the main signal channel. This could result in unwanted modulation on the main signal at a low level. Provided that the isolator had an isolation of better than 20 dB and a coupler with a high directivity of 30 dB was used, calibration levels as low as 75 dB below a P.R.F. line could be generated.

The relative phase of the two signals into the 3 dB hybrid was adjusted using a precision calibrated phase shifter of the type described in the previous section. Again this was used because it could be set easily and a cheaper trombone type of line stretcher would have been adequate.

The level of the calibration line was adjusted using a step attenuator with 10 dB increments for coarse adjustments and the signal generator output control for fine adjustments. The only critical requirement for the step attenuator was a low change in phase shift with changes in attenuation. However, most step attenuators currently available have excellent phase characteristics.

A6.3 THE CANCELLATION CIRCUIT

The noise measuring system with the cancellation circuit is shown in Figure A6.3. The couplers, variable attenuator and phase shifter were all selected to the same standards as similar components discussed in the previous sections of this appendix. The PIN diode switch used to gate out the rise and fall of the pulse, which could not be cancelled, was made by Hewlett-Packard, Type Number HP8403A. The instrument included driving circuits and pulse generators to modulate the PIN diode which was convenient since PIN diodes require specially shaped pulses to achieve fast rise and fall times. The PIN diode switch itself was made up of a number of series diodes giving a maximum attenuation of 80 dB in the 'off' state. Since only 30 dB cancellation of the pulse was required 30-40 dB attenuation would have been sufficient. Hewlett-Packard make an alternative PIN diode switch which gives only 35 dB attenuation which is cheaper and would be quite adequate for the task.

The 80 dB diode was only used since it was available in the laboratory. Two Marconi-Saunders PIN diodes of the type used in the calibration circuit could be used as a cheaper alternative but special driving circuits would have to be made to pulse them 'off' and 'on'.

A6.4 THE VIDEO GATE

The video gate shown in Figure A6.4 was required to attenuate the PSD noise, generated between the r.f. pulses, to increase the dynamic range of the system. It was only advantageous to use the gate if the reference signal

to the PSD was cw. If the reference signal is pulsed, which is the case if one of the later stages of a pulsed amplifier chain is being measured, then no noise is generated in the PSD between pulses.

The maximum reduction in noise level expected from the use of a video gate is proportional to the duty factor. With a duty factor of 4% up to 14 dB improvement could be expected.

The video gate circuitry used was a modified version of one of the range gates used in the pulse doppler radar described in Chapter 4. The circuit is shown in Figure A6.5. The input signal is buffered by an emitter follower and gated by a diode bridge contained within the CA3019. The diodes in the bridge are made on a common substrate and are closely matched to give a high attenuation in the off state. The diode bridge is switched by the differential amplifier CA3028A.

The video gate had an isolation of better than 30 dB in the off state with an insertion loss of 3 dB in the on state. It would accept a 1 V peak-to-peak signal with acceptable distortion and was powered by a 12 V dry battery to minimise mains hum. The gating pulse was obtained from a commercial pulse generator triggered by the transmitter pre-pulse.

The video gate was placed after the low noise audio amplifier so that any noise contributed by the amplifier would be gated out as well.

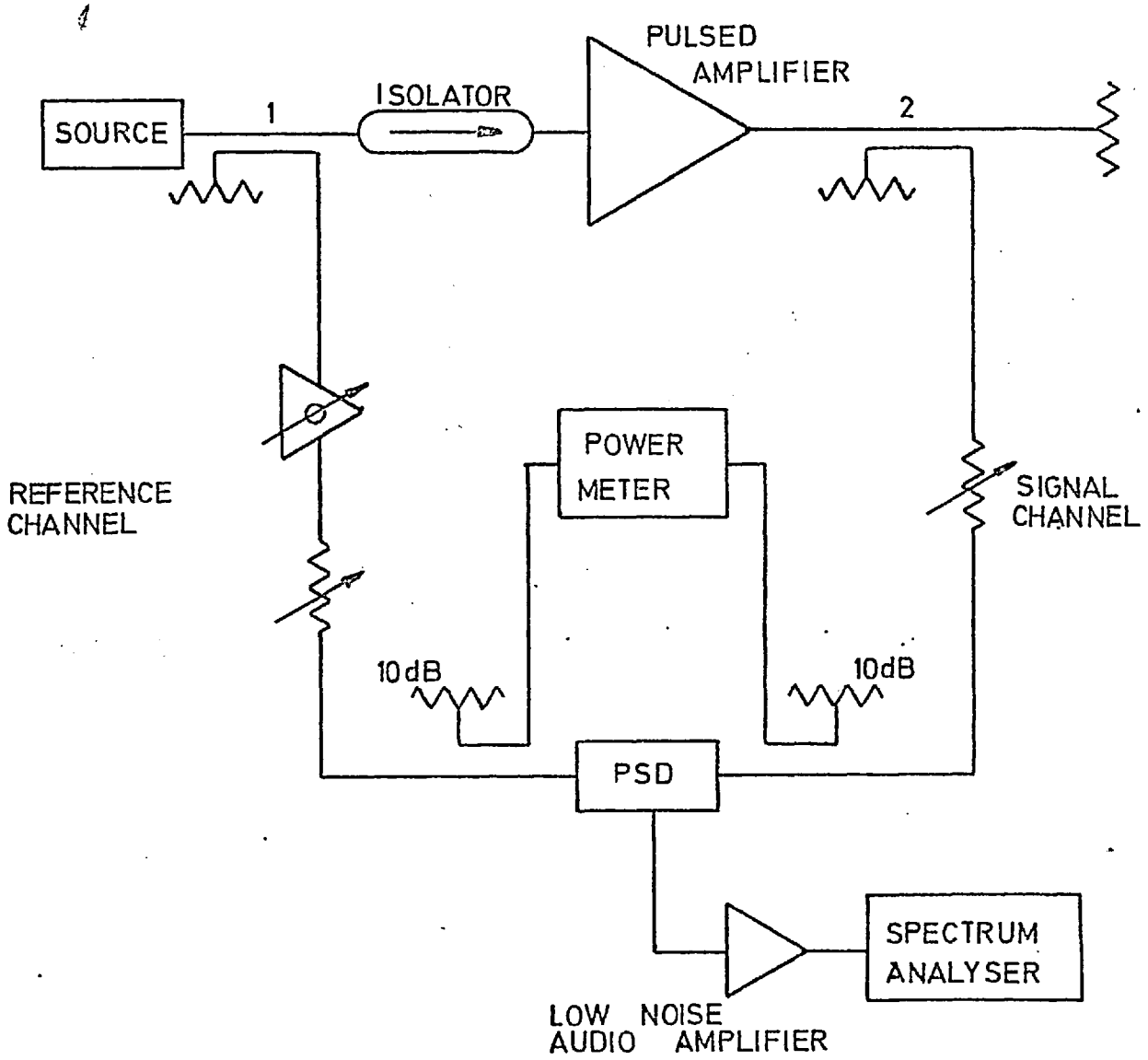


FIG. A6·1 BASIC NOISE MEASURING SYSTEM

COUPLERS 1 & 2 WERE SELECTED TO GIVE THE CORRECT POWER LEVELS REQUIRED

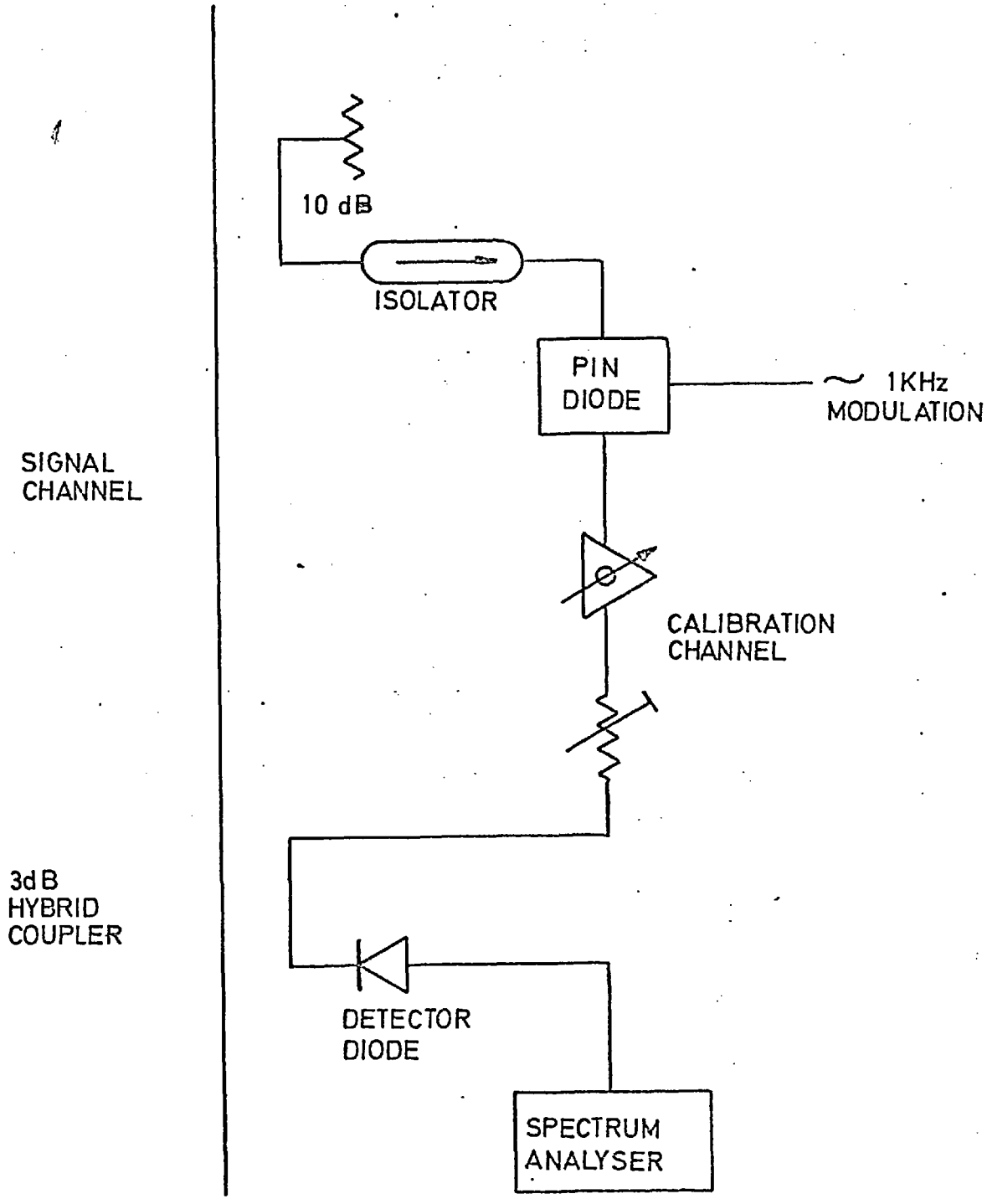


FIG. A6·2 THE CALIBRATION CIRCUIT

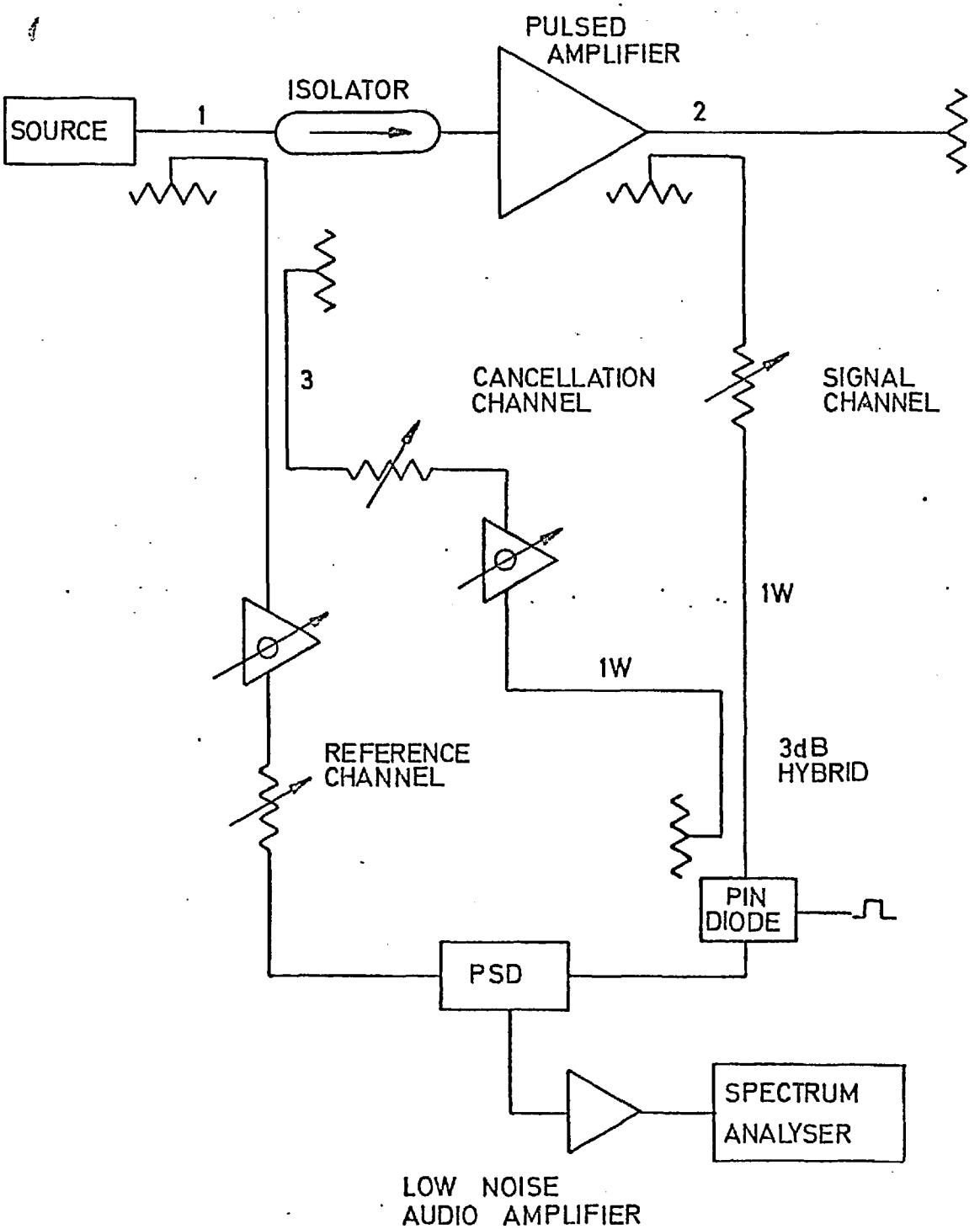


FIG. A6·3 THE CANCELLATION CIRCUIT

COUPLERS 1 2 & 3 WERE SELECTED TO GIVE THE CORRECT POWER LEVELS REQUIRED

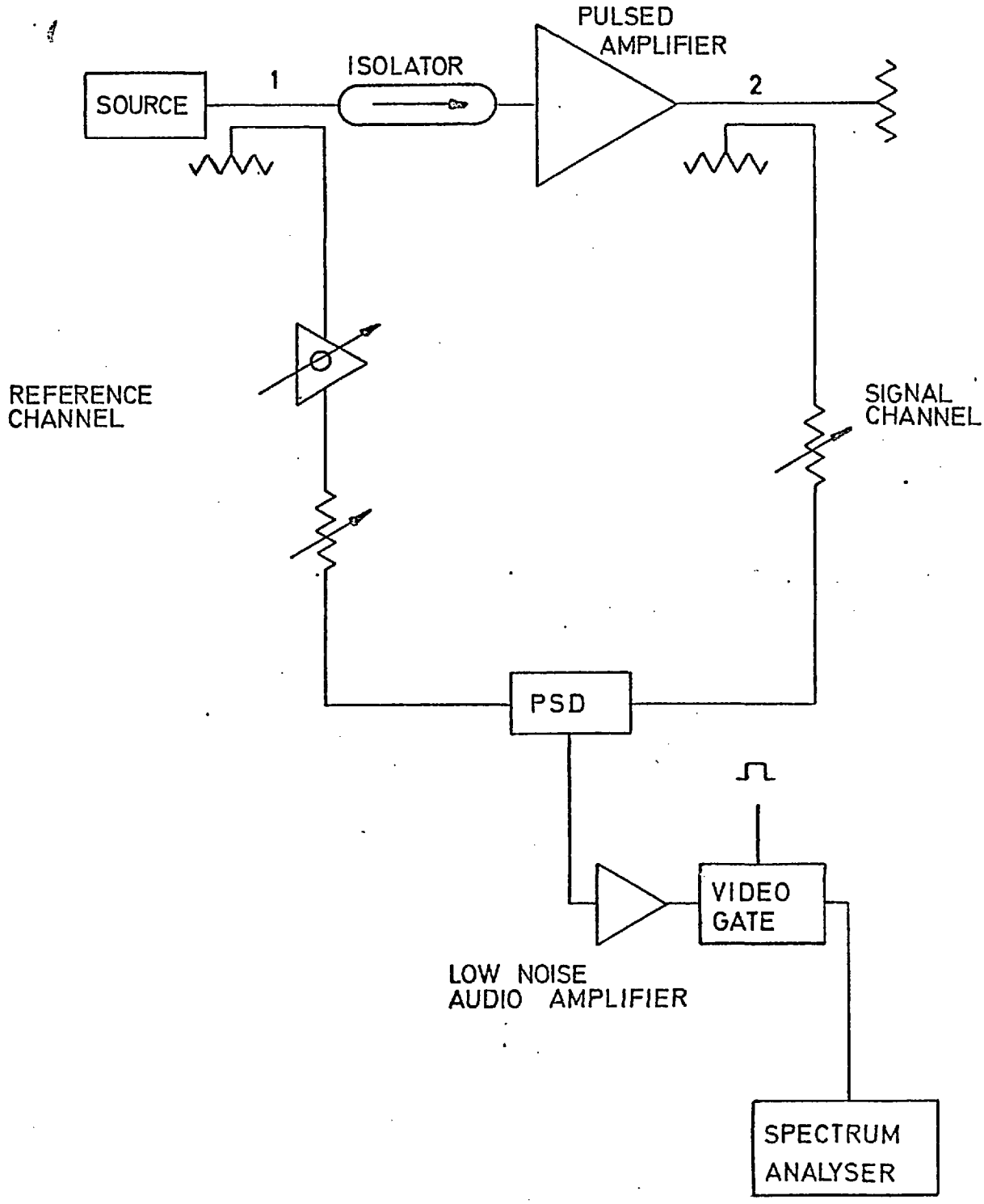


FIG. A6·4 THE VIDEO GATE

COUPLERS 1 & 2 WERE SELECTED TO GIVE THE CORRECT POWER LEVEL REQUIRED

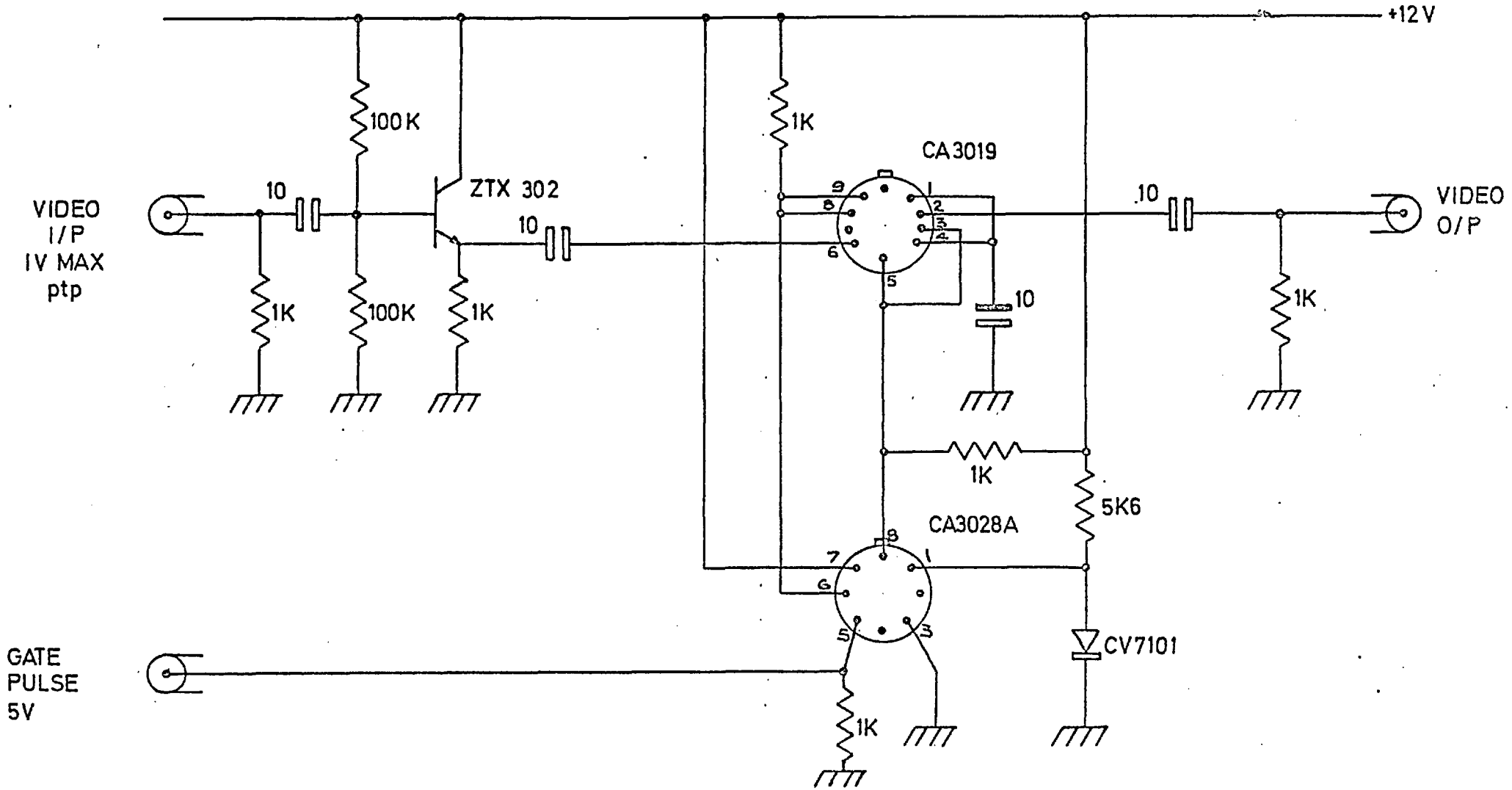


FIG. A6·5 THE VIDEO GATE